Formation of spatial structures in Rayleigh–Bénard convection

A. V. Getling

M. V. Lomonosov Scientific-Research Institute of Nuclear Physics, Moscow State University
(Submitted December 17, 1990; resubmitted May 16, 1991)
Usp. Fiz. Nauk **161**, 1–80 (September 1991)

The problem of the selection of forms and scales of convective flows in a horizontal layer of liquid heated from below is studied. The basic types of two- and three-dimensional flows, defects of roll structures, exchange of convective regimes, and different situations in which two-dimensional rolls have a preferred wave number are described. It is shown that when considered in terms of an optimal (preferred) wave number, to which a roll structure tends and which may or may not be reached depending on the overall geometry of the flow, the different experimental and theoretical results form a unified consistent picture. The basic methods used for investigation of convective structures are described.

1. INTRODUCTION

Convection associated with nonuniform heating is, without exaggeration, the most commonly occurring type of flow of gas and liquid in the universe. Convection also plays an important role in different technological setups. All this already completely explains why investigators have shown such steadfast and intent interest in convection. In the last few years, however, this interest has also been powerfully stimulated by another circumstance: convection problems are a rich source of material for the development of new ideas about the relation between order and chaos in hydrodynamics and between simplicity and complexity in the structure and behavior of hydrodynamic objects.

Convection in a two-dimensional horizontal layer of liquid heated from below—*Rayleigh–Bénard convection*[1)]—is, by and large, studied most often. This problem incorporates significant features characteristic of many phenomena of hydrodynamic instability. At the same time, in convection of this type the spatial effects are largely decoupled from the temporal effects because there is no intense average flow, and this makes it much easier to study such flows both theoretically and experimentally. Rayleigh–Bénard convection provides extensive possibilities for investigating the spontaneous appearance of ordered spatial structures and it thus raises very subtle questions about the realizability of forms and scales of flows—selection of flows which are in some sense optimal.

The stability of some particular stationary flow allowed by the equations has a direct bearing on the realizability of the flow. What is more, stability is often considered to be the main criterion of realizability: "The flows that occur in nature must not only obey the equations of hydrodynamics, but also be stable: small perturbations, if they arise, should decrease with time."[1] However this necessary condition is not sufficient. The class of stable stationary solutions of the equations of hydrodynamics is, generally speaking, much larger than the class of flows which arise spontaneously under appropriate conditions. As more and more information is accumulated it is becoming increasingly clearer that the thesis "All stable flows are realized" can be countered by "Not always and not all stable flows." Very special initial conditions may be necessary in order for a stable state to be reached, and such conditions may not exist at all. Rayleigh–Bénard convection is an excellent illustration of this.

In the theory of convection the problem of the realizability of stable flows is the central problem for many other problems, in particular, problems arising in practical applications. The average characteristics of convection (primarily the heat flux transported by the convecting liquid), which are so often needed, can in principle be derived from the equations, once the form and scale of the flow have been found and, therefore, the amplitude of the velocity can be calculated.

This review is devoted to questions concerning the formation of spatial structures in Rayleigh–Bénard convective flows, the problem of selection of the forms and scales of the structures, and the exchange of convective regimes. In the last ten years an avalanche of publications on convection has appeared, and many authors touch upon, explicitly or implicitly, the problem of structure formation. The abundance of material has made it necessary to limit this review to only those works that have a direct bearing on the subject at hand. Questions about the effect of complicating factors, which impart to the flow qualitatively new features as compared with the classic case of Rayleigh–Bénard convection, had to be omitted. As a result, for example, very interesting effects associated with large variations of the parameters over the height of the flow and therefore many situations with a more complicated vertical structure of the flow fall outside the scope of this review. Regimes in which the temperature gradients are so large that turbulence develops in the convecting liquid are also not discussed.

Attention is focused on the physical picture of the flows and the mathematics is kept to the necessary minimum.

Of the published reviews, Ref. 2 is probably closest to the present review with regard to the subject matter. References to other reviews will also be encountered in the text.

The present review is organized as follows. After the basic concepts and notation are introduced (Sec. 2), the different approaches used for studying the problem experimentally and theoretically are described (Sec. 3). Next, after a

 0038-5670/91/090737-40$01.00

classification of the basic types of structures and convection regimes has been given (Secs. 4 and 5), the different characteristic scenarios of the evolution and types of geometry of flows—often referred to as "mechanisms of selection" of scales—are studied (Sec. 6). In each case the results obtained by the different methods described in Sec. 3 are compared. In particular, the experimental data are presented in parallel with the theory. Section 7 summarizes and generalizes the material presented.

In an attempt to standardize the notation as much as possible, in many cases the notation used in the original works has been changed. These changes are mentioned only where misunderstandings are possible.

2. BASIC CONCEPTS

It is convenient to tie, in one way or another, all results concerning Rayleigh–Bénard convection to the classic formulation of the linear problem, first given by Rayleigh[3] and later in a more general form by Pellew and Southwell[4] and discussed in detail by Chandrasekhar in his monograph of Ref. 5. In recalling this problem, it is helpful to introduce the concepts and notation that will be needed below.

The problem includes the system of hydrodynamic equations in the *Boussinesq* (or *Oberbeck-Boussinesq*) *approximation*. The original (narrow) meaning of this term is as follows.[5] The density ρ of the fluid is assumed to be a function of only the temperature T (i.e., the fluid is assumed to be incompressible):

$$\rho - \rho_0 = -\rho_0\alpha(T - T_0), \tag{2.1}$$

where ρ_0 is the value of the density at some suitably chosen "average" (or, better to say, reference) temperature T_0. Then, if the volume thermal expansion coefficient α is small and variations (in the region of interest) of the material parameters of the fluid (kinematic viscosity ν, thermal diffusivity χ, and the same coefficient α) are small, for processes which are not too fast the density and these parameters can be considered to be constant in all terms but one in the equations: The density remains variable in the term where it is multiplied by the acceleration of gravity $\mathbf{g}$ (this term represents the buoyancy force that is responsible for convection). Heating due to viscous dissipation is also negligible.

Under steady-state conditions the barotropic temperature distribution (such that $[\nabla T, \mathbf{g}] = 0$, if the velocity $\mathbf{v} = 0$) should be a linear function of the vertical coordinate z: $T = T_1 - \beta z$ (in what follows it is called the *unperturbed* distribution and β is the unperturbed temperature gradient). The quantity $\theta = T - T_1 + \beta z$ is termed the temperature perturbation for arbitrary T and the deviation of the pressure p from the distribution corresponding to such a linear temperature profile is the pressure perturbation p'. In this notation the Boussinesq equations have the following form:

$$\frac{\partial \mathbf{v}}{\partial t} + (\mathbf{v}\nabla)\mathbf{v} = -\frac{\nabla p'}{\rho_0} - \mathbf{g}\alpha\theta + \nu\Delta\mathbf{v}, \tag{2.2}$$

$$\frac{\partial T}{\partial t} + \mathbf{v}\nabla T = \chi\Delta T, \tag{2.3}$$

$$\operatorname{div}\mathbf{v} = 0. \tag{2.4}$$

Cordon and Velarde[6] gave the most rigorous substantiation of the Boussinesq equation under very broad assumptions. They extended it[7] to the case when compressibility (in a thick layer) and viscous dissipation effects appear. A discussion of the conditions under which the Boussinesq approximation is applicable is contained in Ref. 8.

In what follows we shall be concerned exclusively, except where explicitly stipulated, with situations when the Boussinesq approximation is valid.

We shall study a flat horizontal layer of liquid ($0 \leqslant z \leqslant h$; the z axis of the Cartesian coordinate system x, y, z is oriented upwards, so that $\mathbf{g} = \{0, 0, -g\}$) and we shall assume the temperatures at the undeformed top and bottom surfaces of the layer to be fixed (i.e., the thermal conductivity of the boundaries of the layer is infinite):

$$\begin{aligned} T &= T_1 \quad \text{at} \quad z = 0, \\ T &= T_2 = T_1 - \Delta T \quad \text{at} \quad z = h, \end{aligned} \tag{2.5}$$

where $\Delta T = \beta h$. This determines the condition

$$\theta = 0 \tag{2.6}$$

on both boundaries. We confine our attention to the case $\beta > 0$. We assume that each surface of the layer is either rigid or free, and correspondingly we impose on the boundary either the no-slip condition

$$\mathbf{v} = 0, \tag{2.7}$$

or the condition that the vertical component of the velocity and the tangential stresses vanish:

$$v_z = 0, \quad \frac{\partial v_x}{\partial z} = \frac{\partial v_y}{\partial z} = 0 \tag{2.8}$$

(for the bottom boundary the last two conditions (2.8) are, as a rule, very artificial, but under these conditions the equations are much easier to solve; the well-known cases when the assumption of free boundaries strongly affects the properties of the solutions will be mentioned below).

Several methods of transforming to dimensionless variables in this problem are encountered in the literature. In what follows we shall employ the following, most useful method. We take the thickness h of the layer as the unit of length, the time $\tau_\nu = h^2/\chi$ of vertical diffusion of heat as the unit of time, and the temperature difference ΔT between the surfaces of the layer as the unit of temperature. Then the system (2.2)–(2.4) can be written in the following dimensionless form:

$$\frac{1}{P}\left[\frac{\partial \mathbf{v}}{\partial t} + (\mathbf{v}\nabla)\mathbf{v}\right] = -\nabla\pi + \hat{\mathbf{z}}R\theta + \Delta\mathbf{v}, \tag{2.9}$$

$$\frac{\partial\theta}{\partial t} - v_z + \mathbf{v}\nabla\theta = \Delta\theta, \tag{2.10}$$

$$\operatorname{div}\mathbf{v} = 0; \tag{2.11}$$

here

$$R = \frac{\alpha g \Delta T h^3}{\nu\chi}, \quad P = \frac{\nu}{\chi} \tag{2.12}$$

are the basic parameters characterizing the convection regime and are the Rayleigh and Prandtl numbers, respectively; π is the dimensionless form of the quantity p'/ρ_0; and, $\hat{\mathbf{z}}$ is a unit vector in the direction of the z axis. In what follows, the formulation of the problem in the form of Eqs. (2.9)–

(2.11) and Eqs. (2.6)–(2.8) will be referred to as the *standard* formulation.

Assuming $\mathbf{v}$ and θ to be infinitesimals we linearize Eq. (2.9) and (2.10) with respect to these variables, after which we operate on Eq. (2.9) with the operator $z\cdot\mathrm{curl\ curl}$ and employ Eq. (2.11). The system then reduces to two equations for v_z and θ. We eliminate θ, fix the horizontal velocity vector $\mathbf{k} = \{k_x, k_y, 0\}$, and seek v_z in the form of normal modes $\exp(\lambda t)w(z)f(\mathbf{x})$, where λ is the growth rate, $\mathbf{x} = \{x, y, 0\}$, and $f(x) = \exp(i\mathbf{k}\cdot\mathbf{x})$ or some spatially periodic solution of the two-dimensional Helmholtz equation $\Delta f + k^2 f = 0$, i.e., the linear combination

$$f(\mathbf{x}) = \sum_{j=1}^{N} c_j \exp(i\mathbf{k}_j\mathbf{x}), \tag{2.13}$$

where the vectors $\mathbf{k}_j$ differ only with respect to their orientation: $|\mathbf{k}_j| = k$. We obtain the following equation for w:

$$(\mathrm{D}^2 - k^2 - \lambda)(\mathrm{D}^2 - k^2 - \frac{1}{P}\lambda)(\mathrm{D}^2 - k^2)w = -Rk^2 w, \tag{2.14}$$

where $\mathrm{D} = \mathrm{d}/\mathrm{d}z$.

The boundary conditions (2.6)–(2.8) give, using Eq. (2.11),

$$v_z = \frac{\partial v_z}{\partial z} = 0, \quad \theta = 0 \quad \text{on a rigid boundary,} \tag{2.15}$$

$$v_z = \frac{\partial^2 v_z}{\partial z^2} = 0, \quad \theta = 0 \quad \text{on a free boundary.} \tag{2.16}$$

The transformed equations (2.9) and (2.10) for the normal modes permit reducing Eqs. (2.15) and (2.16) to a collection of conditions for the variable v_z (or w):

$$w = \mathrm{D}w = (\mathrm{D}^2 - 2k^2 - \frac{1}{P}\lambda)\mathrm{D}^2 w = 0 \quad \text{on a rigid boundary,} \tag{2.17}$$

$$w = \mathrm{D}^2 w = \mathrm{D}^4 w = 0 \quad \text{on a free boundary.} \tag{2.18}$$

Thus Eq. (2.14) together with the conditions (2.17) or (and) (2.18) form an eigenvalue problem for the growth rates λ and the eigenfunctions $w(z)$.

In the case of two free boundaries this problem can be solved simply and leads to an explicit expression for the eigenvalues λ_n corresponding to the eigenfunctions $w_n = \sin(n\pi z)$ $(n = 1, 2, \ldots)$. It is obvious directly from this expression that for any $R > 0$ both existing values of $\lambda_n(R, P, k)$ are real, and in addition one value is always negative while the other one is positive if

$$R > R_n(k) \equiv \frac{(n^2\pi^2 + k^2)^3}{k^2} \tag{2.19}$$

and negative if $R < R_n(k)$ (in what follows we shall take λ_n to be the second value). Each function $R_n(k)$ has a minimum. The line $R = R_1(k)$ in the plane (k, R) delimits the region of damping of all possible infinitesimal perturbations and the region of growth of the perturbations of the lowest mode $n = 1$ (Fig. 1). Obviously, if

$$R < R_c \equiv \min R_1(k) = R_1(k_c) = \frac{27}{4}\pi^4 = 657{,}511,$$

$$k_c = \frac{\pi}{\sqrt{2}} = 2{,}221 \tag{2.20}$$

the rest state of the liquid in the layer is stable with respect to

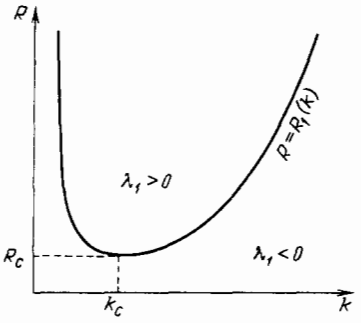

FIG. 1. The neutral stability curve of a layer of motionless liquid. States lying above the curve are unstable and states lying below the curve are stable.

infinitesimal perturbations. The quantities R_c and k_c are, respectively, the *critical Rayleigh number* and the *critical wave number*. In the *critical (neutral) regime* $R = R_c$ steady-state motion with infinitesimal amplitude and a unique wave number $k = k_c$ is possible. For $R > R_c$ (*supercritical regime*) the layer is *convectively unstable*, and disturbances whose wave numbers lie between the two roots of the equation $R = R_1(k)$, in other words, between the abscissas of the points of intersection of the straight line $R = \mathrm{const}$ and the two branches of the *neutral curve* $R = R_1(k)$, can grow. This is how the problem, to be discussed in Sec. 6, of selection of wave numbers in supercritical regimes arises.

In cases when both surfaces of the layer are rigid and when one surface is rigid while the other one is free the calculations are more difficult, but the results are qualitatively the same (the eigenfunctions are different). We note that for two rigid boundaries

$$R_c = 1707{,}762, \quad k_c = 3{,}117. \tag{2.21}$$

Near $R = R_c$ and $k = k_c$ the growth rate $\lambda_1(R, P, k)$ can be represented by the expansion

$$\lambda_1 = \tau_0^{-1}[\varepsilon - \xi_0^2(k - k_c)^2], \tag{2.22}$$

where

$$\varepsilon = \frac{R - R_c}{R_c} \tag{2.23}$$

is the *supercritical reduced Rayleigh number*, and the characteristic time and length scales

$$\tau_0 = \left(R_c \frac{\partial\lambda_1}{\partial R}\right)^{-1}_{R_c, k_c}, \quad \xi_0 = \left(\frac{1}{2R_c}\frac{\mathrm{d}^2 R_1}{\mathrm{d}k^2}\right)^{1/2}_{k_c} \tag{2.24}$$

are called, respectively, the *relaxation time* and the *coherence length*. In some (specially stipulated) cases we shall designate by ε some different, but physically analogous quantities. The scales τ_0 and ξ_0, calculated in a number of articles, in particular Refs. 9 and 10, are equal to

$$\tau_0 = \frac{1 + 1{,}954P}{38{,}44P}, \quad \xi_0 = 0{,}3847 \quad \text{for two rigid boundaries,} \tag{2.25}$$

$$\tau_0 = \frac{2(1 + P)}{3\pi^2 P}, \quad \xi_0 = \left(\frac{8}{3\pi^2}\right)^{1/2} \quad \text{for two free boundaries.} \tag{2.26}$$

An important feature of the normal modes of the linear

problem is that the eigenvalues are degenerate with respect to the different functions $f(\mathbf{x})$—the growth rates λ_n depend only on the wave number $k = |\mathbf{k}_j|$. Different functions $f(\mathbf{x})$ correspond to solutions in the form of different systems of *convective cells*—elements of the spatially periodic structure of the flow which have the property that the normal component of the velocity vanishes on their vertical boundaries.[2)] The configuration of the cell in the plane (x, y) is called a *planform*. Thus the linear problem is degenerate with respect to planforms. Together with the question of wave-number selection, the question of which planforms should actually be observed are part of the general problem of the realizability of convective flows.

Among the cells observed experimentally under different conditions, three types of cells are most characteristic. To a first approximation they can be described by the following three planform functions.

1. *Two-dimensional rolls* (Fig. 2a) have a "prototype" given by the function

$$f(\mathbf{x}) = \cos kx. \tag{2.27}$$

Since the wave vector $\mathbf{k}$ is oriented in the x direction, such rolls (parallel to the y axis) are called *x-rolls*. In this case it makes sense to call a pair of neighboring rolls, occupying an entire spatial period, a cell. In two such rolls the liquid circulates in the (x, z) plane in opposite directions.

2. *Hexagonal cells* (Fig. 2b) are described by the function

$$f(\mathbf{x}) = 2\cos\left(\frac{\sqrt{3}}{2}kx\right)\cos\left(\frac{1}{2}ky\right) + \cos ky = \cos\left[\frac{k}{2}(y+\sqrt{3}x)\right] + \cos\left[\frac{k}{2}(y-\sqrt{3}x)\right] + \cos ky. \tag{2.28}$$

They consist of a superposition of three systems of rolls with wave vectors having modulus k and making an angle of $2\pi/3$ with one another.

3. *Square cells* can be represented by the function

$$f(\mathbf{x}) = \cos\left(\frac{k}{\sqrt{2}}x\right)\cos\left(\frac{k}{\sqrt{2}}y\right) = \frac{1}{2}(\cos kx' + \cos ky') \tag{2.29}$$

(where the coordinate system x', y' is rotated by an angle $\pi/4$ relative to the system x, y; an example of such a cell is the region $-\pi/k < x' < \pi/k$, $-\pi/k < y' < \pi/k$).

Everything said in this section pertains to the idealized case of an infinite layer. We shall see below that the presence of sidewalls, bounding a finite region of the layer, can strongly affect the development of convection in this region. The important parameter then becomes the *aspect ratio*

$$\Gamma = \frac{L}{h}, \tag{2.30}$$

where L is the characteristic horizontal size of the region (for circular reservoirs L is traditionally the radius).[3)] In what follows the role of this quantity will be discussed repeatedly. We shall be interested primarily in large values of Γ.

The horizontal extent L determines the characteristic time of horizontal diffusion of heat $\tau_h = L^2/\chi = \Gamma^2\tau_v$, with which the times of large-scale processes could be related.

3. EXPERIMENTAL APPARATUS

3.1. Experiment

We shall describe here, without going into technical details, the most important and general features of the setup of experiments designed to study convection in a horizontal layer.

The typical experimental arrangement is shown in Fig. 3. The layer of working liquid is bounded above and below by the plates of heat exchangers. These plates maintain the prescribed temperatures of the boundaries of the layer. The higher the thermal conductivity of the plates the more accurately the temperature can be maintained constant. For this reason, in those cases when the boundaries need not be transparent (most often for the bottom heat exchanger), a massive copper or aluminum plate is, as a rule, employed. One surface of the plate is in contact with the working liquid and the opposite surface of the plate is heated with a wire or film electric heater, the heating being regulated with an automatic electronic device, or a horizontal plane-parallel cavity, through which thermostatted water is pumped, is made in the body of the heat exchanger. If, however, the heat ex-

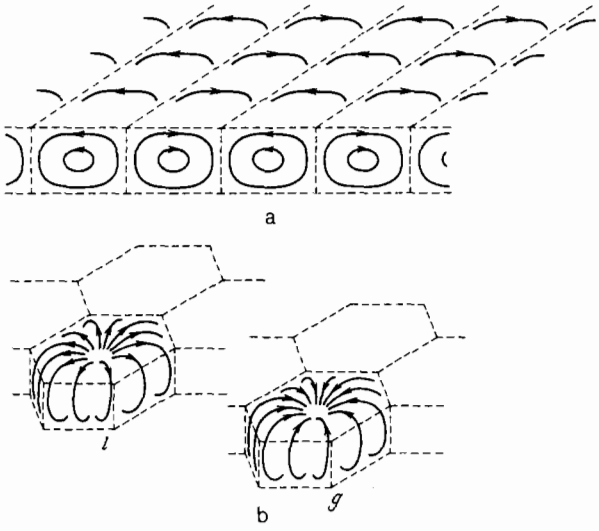

FIG. 2. Schematic diagram of convective cells. a) Two-dimensional rolls. b) Hexagonal cells of l and g types.

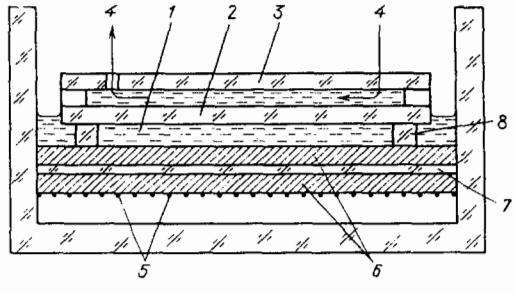

FIG. 3. Typical layout of the experimental apparatus.[11] *1*) Working liquid; *2, 3*) glass and plexiglass plates of the top heat exchanger; *4*) thermostatted water; *5*) heater; *6*) copper plates of the lower heat exchanger; *7*) glass plate (for reducing the sensitivity of the temperature of the bottom surface of the convective layer to fluctuations of the heating); *8*) calibrated insert fixing the thickness of the layer (four such inserts are located in the corners of the working region).

changer must be transparent, then it is usually made from a plate of mirror glass (which is in contact with the working liquid) and is positioned parallel to the other transparent plate; the spacing between them forms a channel for the thermostatted water. If the aim is to reproduce as closely as possible the ideal thermal boundary conditions (2.6), then the thermal conductivity of glass may be inadequate. For this reason, a sapphire single crystal is sometimes employed instead of glass, but then the horizontal dimensions of the layer must be limited to several centimeters: larger sapphire plates cannot be made.

The top heat exchanger is often detachable and its horizontal dimensions are smaller than those of the bottom heat exchanger, so that the top exchanger is often surrounded by a gap, where the working liquid has a free surface and the thickness of the liquid layer cannot be controlled. The complicated temperature distribution and the thermocapillary effect (see Sec. 4.1) give rise to disordered three-dimensional convective flows in this layer. In order to prevent these flows from affecting the convection in the working region (beneath the top heat exchanger) many experimenters surround this region with additional sidewalls by inserting a special frame. Other experimenters[11,12] intentionally do not do this, because according to their observations the gap prevents the sidewalls from strongly affecting the structure of the flow in the working region.

Sometimes the geometry of the experimental apparatus is qualitatively different: The cavity containing the working liquid is a long narrow channel, whose width is equal to or less than the height (see, for example, Ref. 13). When the liquid is heated from below short segments of convective rolls, whose ends "rest against" the long walls of the channel, are formed in the cavity (this effect will be discussed in Sec. 4.2). As a result effects associated with three-dimensional deformations of the rolls are eliminated, and it is especially convenient to study the dynamics of the wave numbers of such a simple roll flow.. But, of course, the results of such experiments can correspond to the case of a horizontal layer only qualitatively and not quantitatively.

The choice of working liquids encompasses a wide range of Prandtl numbers: diverse silicone oils ($P \sim 10$–10^4), glycerine ($\sim 10^3$), ethyl alcohol (14–17), methanol (7), water (from 7 at room temperature to 2.5 at 70 °C), and liquid helium (0.5–4.5).[4)] Experiments are also performed with air (0.71).

Convective flows are usually visualized by the shadow method, based on the temperature dependence of the index of refraction of light. Cold downward flows focus light and appear light-colored when projected on a screen, while warm upward flows scatter light and appear dark. Visualization with the help of special additives is also employed. Laser Doppler anemometry (for example, Ref. 14), optical interferometry,[15] and other methods are also employed for studying the structure of flows.

The stability of some particular prescribed type of flow is studied in a special series of experimental investigations. These are *experiments with controlled initial conditions*. The first experiment in this series was apparently performed by Chen and Whitehead,[16] and the experimental arrangement proposed by them has been used with only insignificant modifications in a number of the latest investigations. The procedure is as follows. A layer of subcritical working liquid is illuminated, through the transparent top heat exchanger, with light from a powerful lamp. First the light passes through a periodic grating consisting of strips of opaque material which are separated by transparent gaps. Due to this a roll convective flow whose wavelength is fixed externally and is equal to the period of the grating is formed. The temperature difference between the top and bottom boundaries of the layer is gradually increased up to the required supercritical value, after which the lamp is switched off and spontaneous evolution of the flow starts. In some studies the behavior of flows whose structure is more complicated than a uniform roll flow was investigated by this method. For example, a so-called bimodal flow (Sec. 6.2) was studied in Ref. 17, systems of rolls with a dislocation (Secs. 4.3 and 6.7) were studied in Ref. 18, and hexagonal and square cells were studied in Ref. 19. Gratings of an appropriate form were employed in order to produce such initial velocity fields.

3.2. Theoretical approaches

3.2.1. Small-amplitude (reduced supercritical Rayleigh number) expansion. In order to investigate supercritical regimes it is necessary to solve nonlinear equations. The perturbation method, based on expansion of the Boussinesq equations in a small parameter characterizing the amplitude of the convective motion and the degree of supercriticality, has been widely employed in the theory of Rayleigh–Bénard convection since the works of Gor'kov[20] and Malkus and Veronis.[21] Usually expansions of the form

$$\mathbf{v} = \varepsilon^{1/2}(\mathbf{v}^{(0)} + \varepsilon^{1/2}\mathbf{v}^{(1)} + \varepsilon\mathbf{v}^{(2)} + \ldots), \tag{3.1}$$

$$R = R_c + \varepsilon^{1/2}R^{(1)} + \varepsilon R^{(2)} + \ldots \tag{3.2}$$

and analogously for θ and p' are studied (in the original paper of Ref. 21 and in a number of other papers the quantity $\varepsilon^{1/2}$ is denoted as ε). This approach has been discussed many times in monographs (see, for example, Gershuni and Zhukhovitskiĭ[8]) and reviews (for example, Busse[22,23]).

We shall be interested in using such expansions primarily as a means for constructing the amplitude and phase equations, which are now widely employed for studying the dynamics of convection and which we shall discuss in Sec. 3.2.2 below.

In Ref. 24 an expansion is made not in ε but rather in the parameter $\eta = [(R - R_c)/R]^{1/2}$. This makes it possible to cover a wide range of values of R, since $\eta < 1$ for any finite value of R.

The perturbation method of Schluter, Lortz, and Busse,[25] based on the expansions (3.1) and (3.2), is most widely employed. The conditions of solvability of the inhomogeneous equations obtained at successive steps of the expansion of the starting system give successive approximations of the steady-state solution, and in addition $\mathbf{v}^{(0)}$ has the structure of the solution of the linearized problem; it turns out that if the surface tension is neglected, then $R^{(1)} = 0$ always and under symmetric boundary conditions at the top and bottom surfaces (and in the case of two-dimensional rolls, in the absence of such symmetry also) $R^{(n)} = 0$ for all odd n.

3.2.2. Two-dimensional models of three-dimensional convection. As soon as the problem of theoretical study of convective structures more complicated than uniform spa-

tially periodic structures arose, investigators started to search for ways to simplify the description of such flows. This question is especially acute when three-dimensional flows must be described: To this day the most versatile approach—numerical modeling—requires such large amounts of computer time in the three-dimensional case that an investigation with the least bit of detail is often precluded. This pertains primarily to calculations for cavities which have large aspect ratios and in which complicated nonuniform structures—*textures* (see Sec. 4.3)—arise.

The first aim of constructing simplified models is to reduce the number of spatial measurements by eliminating from the analysis the vertical dependence of the variables. This is possible because this dependence often has a "standard" form which varies little over a wide range of parameters. Calculations can be performed much more efficiently when three-dimensional flows are described by functions of two (horizontal) spatial coordinates and two-dimensional flows are described by functions of one spatial coordinate.

But it is also possible to reduce the number of independent variables. When the flow is close to being a steady-state one and evolves slowly, it can be assumed that the velocity components and the temperature are related by the same expressions as in the steady-state regime.

All recently proposed descriptions of the dynamics of convective structures by means of one (possibly, complex) function of two coordinates are based either explicitly or implicitly on the above two ideas.

1) *Amplitude equations.* It turned out that the *Newell–Whitehead–Segel* (NWS) *amplitude equation* is an effective tool for investigating the structures of weakly supercritical flows and has stimulated the formulation of very diverse problems.

Newell and Whitehead,[26] studying regimes with $(R - R_c)/R_c = \varepsilon$ (here the designation of the small parameter is different from that of Ref. 26) in a layer with free boundaries, employed a "modified neutral solution" of the roll type

$$v_z = \varepsilon^{1/2}(A(X, Y, T)e^{i\mathbf{k}_c\mathbf{x}} + \text{c.c.})\sin \pi z + O(\varepsilon), \qquad (3.3)$$

where $|\mathbf{k}_c| = k_c$ and A is a slowly varying complex amplitude or the envelope function (the other variables have analogous expressions, associated with Eq. (3.3), as in the steady-state weakly supercritical regime), to describe a wave packet with an admissible, for given ε, band of wave numbers of width $O(\varepsilon^{1/2})$. Here X and Y are slow spatial variables and T is the slow time. Thus the continuous spectrum of wave numbers is embedded in the slow space-time modulation of the amplitude, and the change of the phase factor is determined by the "central" wave number of the packet, equal to the critical wave number.

Suppose that the flow is a somewhat deformed system of x-rolls with wave number k_c. Then, in order that all wave vectors $\mathbf{k} = \{k_c + \alpha_x, \alpha_y\}$ present in the wave packet satisfy the requirement $|\mathbf{k}| = k_c + O(\varepsilon^{1/2})$, it is necessary to set $\alpha_x = O(\varepsilon^{1/2})$ and $\alpha_y = O(\varepsilon^{1/4})$. Accordingly, it is natural to choose as the slow variables

$$X = \varepsilon^{1/2}x, \quad Y = \varepsilon^{1/4}y, \quad T = \varepsilon t. \qquad (3.4)$$

Substituting Eq. (3.3) into the starting equations gives in the lowest nontrivial order the condition of solvability of the boundary-value problem—the NWS amplitude equation, which after an additional change of scale of the variables by an $O(1)$ factor assumes the form

$$\partial_T A = A + (\partial_X - i\partial_Y^2)^2 A - |A|^2 A, \qquad (3.5)$$

Here $A = O(1)$. For convenience we also write Eq. (3.5) both in terms of the starting physical variables, making the substitution $\varepsilon^{1/2}A \to A$:

$$\tau_0 \partial_t A = \varepsilon A + \xi_0^2\left(\partial_x - \frac{i}{2k_c}\partial_y^2\right)^2 A - g|A|^2 A, \qquad (3.6)$$

where τ_0 and ξ_0 correspond to Eqs. (2.24) and (2.26), while $g = 1/3\pi^2$, and in the form

$$\partial_t A = \varepsilon A + (\partial_x - i\partial_y^2)^2 A - |A|^2 A, \qquad (3.7)$$

where x, y, t, and A differ from the corresponding starting variables by $O(1)$ factors.

In Ref. 26 Newell and Whitehead derived, in addition, a system of amplitude equations which describes the interaction of several wave packets of the indicated type, whose "central" wave vectors (whose modulus is equal to k_c) make certain angles with one another.

Sometimes amplitude equations of higher order approximations are studied. An example is given in Ref. 27 (see Secs. 6.4.1).

In Ref. 28 Segel employed an entirely analogous approach to derive Eq. (3.6) (also for a layer with free boundaries).

In the case of a layer with rigid boundaries the NWS equation has the same form, only the values of τ_0, ξ_0, and g are different.[29]

In Ref. 30 an amplitude equation was derived for an axisymmetric system of annular rolls for a layer with free horizontal boundaries.

A variant of the amplitude equation was derived under broader assumptions by Cross in Ref. 31 and Kuznetsov and Spektor in Ref. 32. The boundaries of the layer can be either free or rigid. In Ref. 32, in addition, the *thermocapillary effect* (temperature-dependent surface tension) and deformability of the free boundaries were also included in the analysis. The authors do not employ the modified (modulated) neutral solution, but rather they work with the Fourier transform A_k in the variables x and y of the lowest (in the variable z) harmonics of each physical variable ($|\mathbf{k}|$ is close to k_c). The equation is derived by projecting the starting system onto the lowest characteristic function of the linear problem with the growth rate (2.22) and has the form

$$\tau_0 \partial_t A_{\mathbf{k}} = [\varepsilon - \xi_0^2(k - k_c)^2]A_{\mathbf{k}} - \int g(\hat{\mathbf{k}}\hat{\mathbf{k}}')A_{\mathbf{k}'}^* A_{\mathbf{k}''}A_{\mathbf{k}'''}\delta(\mathbf{k} + \mathbf{k}' - \mathbf{k}'' - \mathbf{k}''')d\mathbf{k}'d\mathbf{k}''d\mathbf{k}'''; \qquad (3.8)$$

here $\hat{\mathbf{k}}$ and $\hat{\mathbf{k}}'$ are unit vectors in the directions of $\mathbf{k}$ and $\mathbf{k}'$, respectively; g, as also do τ_0 and ξ_0, depends on the boundary conditions. If the free surface undergoes a finite deformation and (or) the thermocapillary effect is present, then the right side of Eq. (3.8) acquires an additional term which, to within a constant factor, is equal to[32]

$$\int A_{\mathbf{k}'}^* A_{\mathbf{k}''}\delta(\mathbf{k} + \mathbf{k}' - \mathbf{k}'')d\mathbf{k}'d\mathbf{k}''. \qquad (3.9)$$

This term can stabilize near $R = R_c$ hexagonal cells (with a hard excitation regime); see Sec. 4.1.

In Refs. 33 and 34 Siggia and Zippelius noted that in the case of a layer with free boundaries the equations admit the existence of a large-scale (depending only on the slow variables) horizontal flow $B(X, Y, T)$ (*average drift*) that is uniform in the direction of the z axis. Such flows are associated with a vertical component Ω_z of the vorticity $\vec{\Omega} = \operatorname{curl} \mathbf{v}$. The vorticity Ω_z is generated by the term $P^{-1}(\mathbf{v}\cdot\nabla)\mathbf{v}$ in the Navier-Stokes equation (2.9). Of the nonlinear terms in the starting system, however, the NWS equation takes into account only $(\mathbf{v}\cdot\nabla)\theta$ and it cannot describe the appearance of Ω_z and B. For this reason it is incomplete. It is only in the limit $P\to\infty$, when the convective term $P^{-1}(\mathbf{v}\cdot\nabla)\mathbf{v}$ becomes insignificant compared with $(\mathbf{v}\cdot\nabla)\theta$, that the large-scale flow is suppressed and the NWS equation no longer has its drawback [this also pertains to Eq. (3.8)].

Introducing the slow variables according to Eq. (3.4) and neglecting the horizontal motion, governed by the initial conditions, as well as the motion that can be eliminated by introducing rigid sidewalls, Zippelius and Siggia obtained in Ref. 34, instead of Eq. (3.6), in the lowest nontrivial order the system

$$[\xi_0^2(\partial_x - \frac{i}{2k_c}\partial_y^2)^2 + \varepsilon - \tau_0\partial_t]A = g|A|^2A + ik_c\tau_0 B_x A, \quad (3.10)$$

$$(\partial_t - P\Delta)\Omega_z = 2\partial_y[A^*(\partial_x - \frac{i}{2k_c}\partial_y^2)A + \text{c.c.}], \quad (3.11)$$

$$\partial_y\Omega_z = -\Delta B_x, \quad (3.12)$$

where $\Delta = \partial_x^2 + \partial_y^2$. The analog of Eq. (3.5) is the system

$$\partial_T A = A + (\partial_X - i\partial_Y^2)^2 A - |A|^2 A - iB_X A, \quad (3.13)$$

$$\gamma\partial_T\Omega_z = (\partial_Y^2 + \delta\partial_X^2)\Omega_z + b\partial_Y[A^*(\partial_X - i\partial_Y^2)A + \text{c.c.}], \quad (3.14)$$

$$\partial_Y\Omega_z = -(\partial_Y^2 + \delta\partial_X^2)B_X, \quad (3.15)$$

where

$$b = 2\frac{1+P}{P}, \quad \gamma = \frac{\sqrt{3}\,\varepsilon}{1+P}, \quad \delta = \frac{\sqrt{\varepsilon}}{2k_c\xi_0}. \quad (3.16)$$

As $P\to\infty$, obviously, $\Omega_z\to 0$ and $B_x\to 0$.

If the boundaries of the layer are rigid, then the horizontal velocity B cannot be constant along z and generation of the vorticity Ω_z should appear in higher order in ε. For this case Siggia and Zippelius[34] derived the amplitude equations in a nonrigorous manner, based on a phenomenological model. If Ω_z and B_x are replaced by their values $\overline{\Omega}_z$ and $\overline{B}_x$ averaged over z, then (with a corresponding choice of scales) Eqs. (3.13) and (3.15) remain unchanged, and Eq. (3.14) is replaced by

$$\overline{\Omega}_z = c_1\sqrt{\varepsilon}\, b\partial_Y[A^*(\partial_X - i\partial_Y^2)A + \text{c.c.}], \quad (3.17)$$

where $c_1 = O(1)$ is a constant and b depends on P in a manner different from that in Eq. (3.16).

We note that in the case of purely two-dimensional flow geometry the standard NWS equation (in this case one-dimensional) is also applicable for finite values of P, since drift does not arise.

Different variants of the boundary conditions for the amplitude function satisfying the NWS equation are studied in Refs. 28, 30, 35, 36, and 37. They were derived by joining the amplitudes, slowly varying in space far from a sidewall, with the corresponding much more rapidly varying function describing the boundary layer.

Thus in Ref. 36 Brown and Stewartson studied a rectangular cavity with free horizontal surfaces and rigid, thermally poorly conducting, sidewalls. They gave an amplitude description of the flow, which is a superposition of two systems of rolls—one parallel and the other perpendicular to one of the sidewalls. For the particular case of thermally insulating walls and a single system of rolls the boundary conditions have the form

$$A = 0 \text{ on all walls}, \quad (3.18)$$

$$\hat{\mathbf{n}}\nabla A = 0 \text{ on the walls, oriented perpendicular to the rolls} \quad (3.19)$$

($\hat{\mathbf{n}}$ is a unit vector normal to the wall). The authors note that the derivation of the second boundary condition presented in Ref. 28 (for different thermal boundary conditions) contains an error.

In Ref. 37 Cross studied a system of rolls making an arbitrary angle with the sidewall (not too close to the normal) for a layer with free horizontal surfaces and a wall with finite thermal conductivity. He showed that, generally speaking, a system of small-amplitude "conjugate" rolls, arranged relatively to the normal to the wall symmetrically with respect to the main rolls, will arise near the wall. The boundary conditions for the amplitude of the main system have the form

$$A = 0, \quad \hat{\mathbf{n}}\nabla A = O(\varepsilon^{1/2}), \quad (3.20)$$

where according to Eqs. (3.3) and (3.5) $A = O(1)$. The corrections introduced by taking into account Ω_z do not affect the result. It should be kept in mind that the fundamental possibility of the existence of systems of rolls making different angles with the boundary still does not mean that all orientations are physically equally legitimate (or are equally realizable); see Sec. 4.2.

2) *Manneville's "microscopic" equations.* Since the applicability of the amplitude equations is limited to fields that do not differ too much from a uniform roll structure, there arose the question of searching for ways to describe convection that are free of this constraint but are also still simple enough.

In order to describe the dynamics of textures taking into account large-scale drift Manneville[38] proposed a two-dimensional model of convection for a layer with free boundaries and small ε. The Boussinesq equations are simplified by a procedure based on the Galerkin expansion for the z-dependence of the variables. The final representation contains only harmonics with $n = 0$—drift flow $\mathbf{u}(x, y, t)$—and $n = 1$—in the form of the amplitude $w(x, y, t)$ of the vertical velocity. It is assumed that the second harmonics follow adiabatically the changes in the first harmonics and that, with respect to w, $\Delta = -k_c^2 + O(\varepsilon^{1/2})$, $\partial_t = O(\varepsilon)$. The system of equations has the form

$$\tau_0\partial_t w = \left[\varepsilon - \frac{\xi_0^2}{4k_c^2}(\Delta + k_c^2)^2\right]w - g w\left[(\nabla w)^2 + k_c^2 w^2\right] - \tau_0(u_x\partial_x w + u_y\partial_y w), \quad (3.21)$$

$$(\partial_t - P\Delta)\Delta\zeta = \frac{1}{k_c^2}(\partial_y w\,\partial_x\Delta w - \partial_x w\,\partial_y\Delta w), \quad (3.22)$$

$$u_x = \partial_y \zeta, \quad u_y = -\partial_x \zeta, \tag{3.23}$$

where ζ is the stream function of horizontal drift $\mathbf{u}$, τ_0 and ξ_0 are given by the formulas (2.26), and $g = 1/6\pi^4$. At the boundary of the two-dimensional region, where $\mathbf{v} = 0$, the variables w and ζ must satisfy the boundary conditions

$$w = \hat{\mathbf{n}}\nabla w = 0, \quad \zeta = \hat{\mathbf{n}}\nabla\zeta = 0. \tag{3.24}$$

In Ref. 38 Manneville discusses qualitatively the fact that the system (3.21)–(3.23) must change if the horizontal boundaries of the layer are rigid and drift is not uniform along z but rather similar to the Poiseuille flow.

In contrast to the amplitude equations, the model described above is based on an explicit "microscopic" description of the structure of the physical fields in the fast spatial coordinates and imposes fewer constraints on the detailed geometry of the flow. For a system of weakly deformed rolls *the amplitude equations (3.10)–(3.12) in which drift is taken* into account can be derived from Eqs. (3.21)–(3.23).

3) *Model equations.* Diverse model equations, which cannot be derived from the hydrodynamic equations, have also been proposed for the "microscopic" description of convective structures. They determine a function $w(x, y, t)$ which is the vertical component of the velocity or the perturbation of the temperature in the midplane $z = 1/2$ of the convective layer. A model is considered to be applicable if the behavior of the solutions of the model equation agrees with the known solutions of the full hydrodynamic system.

The most popular model is the equation

$$\tau_0 \partial_t w = \left[\varepsilon - \frac{\xi_0^2}{4k_c^2}(\Delta + k_c^2)^2\right] w - gw^3, \tag{3.25}$$

where w is a real function, sometimes called the *order parameter*,[5] ε is the analog of the reduced Rayleigh number, and τ_0, ξ_0, and g have the same meaning as in Eq. (3.6). This equation was proposed (in a variational formulation and with an additional term taking into account the fluctuations) in Ref. 39 and has been termed the *Swift–Hohenberg* (SH) *equation (model).* It is most often written in the form

$$\partial_t w = [\varepsilon - (\Delta + 1)^2] w - w^3, \tag{3.26}$$

which can be obtained from Eq. (3.25) by making an appropriate change of scale of the variables (after which $k_c = 1$) and redefining ε.

The SH equation is invariant under translation and rotation. For $\varepsilon < 0$ there exists the stable solution $w \equiv 0$. This solution becomes unstable at the critical value $\varepsilon = 0$ if the disturbance has a wave number $k = k_c$. Super-critical cases ($\varepsilon > 0$) are characterized by the presence of steady-state spatially periodic solutions whose wave numbers lie in the interval $(k_c - \varepsilon^{1/2}, k_c + \varepsilon^{1/2})$. In addition, the SH equation can be used to construct an amplitude equation (by the same method as the NWS equation). The amplitude equation has the same form as the NWS equation.[40] Since first used in Ref. 41, the SH equation has been used systematically in investigations of the selection problem.

In Refs. 42 and 43 the equation

$$\partial_t w = [\varepsilon - (\partial_x^2 + 1)^2] w - w\partial_x w \tag{3.27}$$

is studied, together with the SH equation, within the framework of a one-dimensional problem.

A generalization of the SH model is the family of equations[44]

$$\partial_t w = [\varepsilon - (\Delta + 1)^2] w - aw^3 - bw(\nabla w)^2 + cw^2 \Delta w, \tag{3.28}$$

where a, b, and c are free parameters, which are adjusted so as to give the best fit of the properties of the solutions to the behavior of real convective flows (see Sec. 6.3). We note that in the absence of drift Manneville's equation (3.21) reduces to Eq. (3.28) with $a = b = 1$ and $c = 0$.

Another family of model equations[44]

$$\partial_t w = [\varepsilon - (\Delta + 1)^2] w + d(\Delta w)(\nabla w)^2 + (3 - d)(\partial_i w)(\partial_j w)\partial_i \partial_j w \tag{3.29}$$

provides a generalization of the (Herzberg-)Sivashinskiĭ equation,[45] which is derived by expanding in powers of the parameter determining the slow variables the convection equations for a layer bounded by plates having poor thermal conductivity and corresponds to the case $d = 1$.

The model equations (3.25)–(3.29) do not take into account in any way the effect of drift, which in real convection, as we saw, is related with Ω_z. In order to describe drift effects Greenside and Cross proposed in Ref. 44 a modification of Eqs. (3.28) and (3.29), adding a convective term, i.e., making the substitution

$$\partial_t w \to \partial_t w + (\mathbf{U}\nabla) w, \tag{3.30}$$

where

$$\mathbf{U} = \mathrm{curl}(\zeta \hat{\mathbf{z}}) \tag{3.31}$$

is the drift velocity, determined by the stream function ζ, which is found from the equation

$$\Delta\zeta = \gamma [\nabla \Delta w, \nabla w] \hat{\mathbf{z}} \tag{3.32}$$

(here γ is some nonnegative coupling constant and $-\Delta\zeta$ is the vorticity Ω_z).

The boundary conditions for the order parameter w are usually stated in the form[46]

$$w = \hat{\mathbf{n}}\nabla w = 0 \tag{3.33}$$

at the boundaries of the two-dimensional region. They reproduce the conditions (3.18) and (3.19) for the amplitude function as well as, in lowest order, Eq. (3.20). In Refs. 44 and 47 the conditions

$$\zeta = \hat{\mathbf{n}}\nabla\zeta = 0 \tag{3.34}$$

were proposed for large-scale flow.

4) *Lyapunov functional.* The NWS equation (3.7) can be represented in the variational form

$$\partial_t A = -\frac{\delta F}{\delta A^*}, \tag{3.35}$$

where

$$F = \int \left[\frac{1}{2}\varepsilon^2 - \varepsilon |A|^2 + \frac{1}{2}|A|^4 + |(\partial_x - i\partial_y^2) A|^2\right] dx dy \tag{3.36}$$

is the Lyapunov functional (the integration in Eq. (3.36) extends over the entire region of flow), and $\delta F/\delta A^*$ is a variational (functional) derivative. The constant $\varepsilon^2/2$ is includ-

ed in the integrand so that $F = 0$ is obtained in the case when the solution of the equation is constant as a function of both the time and the coordinates, i.e., when $|A|^2 = \varepsilon$.

The amplitude equation was derived under the assumption that the deformation of the system of parallel straight rolls is small. In the case of rigid sidewalls this condition will be satisfied in the case of a rectangular region, when the rolls are oriented mainly in the same as the direction as the pair of sidewalls. For such a rectangular geometry, using the expression (3.36), Eq. (3.7), and the boundary conditions (3.18) and (3.19), it is not difficult to obtain

$$\frac{dF}{dt} = -2\int \left|\frac{\partial A}{\partial t}\right|^2 dxdy. \tag{3.37}$$

This means that F decreases for any process dynamics determined by the NWS equation. For this reason, the functional F is often called the *potential* (or the *free energy*[5]), and it is said that the NWS equation describes the *variational* or *potential* or *relaxational* dynamics.

Another example of potential dynamics is the behavior of the system described by the SH equation (3.26). This equation can be derived in the form

$$\partial_t w = -\frac{\delta F}{\delta w} \tag{3.38}$$

based on the potential

$$F = \int \left\{\frac{1}{2}\varepsilon^2 - \frac{1}{2}\varepsilon w^2 + \frac{1}{4}w^4 + \frac{1}{2}[(\Delta + 1)w]^2\right\} dxdy. \tag{3.39}$$

The boundary conditions (3.33), for example, ensure that F decreases monotonically.

When the vertical component of the vorticity and the average drift are taken into account the amplitude function is described by Eqs. (3.10)–(3.12). The dynamics is then not variational and it becomes variational only in the limit $P \to \infty$. If, however, the boundaries of the layer are rigid, then the low-order amplitude equations correspond to potential behavior of the system for finite P also, since according to Eq. (3.17) Ω_z appears in a higher order.

The model equation (3.27) is not variational. In the family (3.28) only the equations for which $b = -c$ are potential equations, while in the family (3.29) only the Herzberg–Sivashinskiĭ equation is a potential equation ($d = 1$). Thus Manneville's equation is not a potential equation, even neglecting drift. Drift, included with the help of the relations (3.30)–(3.32), destroys the potential character of any model. The point is that drift advection can result in the appearance of periodic regimes, while variational dynamics is monotonic.

5) *Phase equation.* The amplitude equation represents the flow as being the result of amplitude modulation of periodic systems of parallel rolls. The phase equation, on the other hand, represents them by the same structures but modulated in phase. This method was first used by Pomeau and Manneville in Ref. 41.

The formal derivation of the phase equation is as follows. Let $U_0(x, z)$ be a solution of the equations of the problem and let U_0 be periodic in x and correspond to a system of stationary two-dimensional x-rolls. Then, since the problem is translationally invariant, $U_0(x + \varphi, z)$ (where φ is a constant phase shift) is also a solution. For small φ

$$U_0(x + \varphi, z) = U_0(x, z) + \varphi\partial_x U_0(x, z). \tag{3.40}$$

If slow variations of φ in space and time are admitted, then $U_0(x + \varphi(x, y, t), z)$ will no longer be a solution. In this case, however, a solution of the starting (non-steady-state) problem can be sought in the form

$$U(x, y, z, t) = U_0(x, z) + \varphi(x, y, t)\partial_x U_0(x, z) + U_1 + U_2 + ..., \tag{3.41}$$

where $U_1 = O(\nabla\varphi)$, $U_2 = O(\nabla\nabla\varphi)$, etc. The equations of phase dynamics are found in the form of conditions of solvability of the linear systems of equations obtained at the successive steps of the expansion.

The phase description is obviously limited to cases when the amplitude of the rolls remains practically unchanged in the presence of deformations. This is what makes this equation different from the amplitude equation that operates with a complex envelope function and thus takes into account variations of both the amplitude and the phase.

In Ref. 41 Pomeau and Manneville employed as the starting equation for constructing the expansion (3.41) the model SH equation and they obtained, in the lowest nontrivial order of this expansion for small ε, the equation of phase diffusion in the form

$$\partial_t\varphi = D_\parallel\partial_x^2\varphi + D_\perp\partial_y^2\varphi, \tag{3.42}$$

where $D_\parallel$ and $D_\perp$ are expressed in terms of ε, k_c, and $q = k - k_c$.

In Refs. 48 and 49 Manneville and Piquemal made a gradient expansion for the complete system of Boussinesq equations. They investigated the cases of both rigid and free boundaries, but they studied only transverse or zigzag disturbances of the starting system of x-rolls (i.e., perturbations whose wave vector is oriented in the y direction). Taking into account large-scale drift (which, as we have already mentioned, is constant along the z direction in the case of free boundaries) shows that this drift is determined by the curvature of the rolls and is oriented in a manner so as to straighten the curved rolls. In the case of a layer with rigid boundaries this does not destroy the diffusion character of the relaxation of the zigzag disturbances, so that Manneville and Piquemal took the drift into account in the effective coefficient $D_\perp$ (its value is greater than in the case when drift is neglected):

$$D_\perp^{\text{eff}} = \frac{\xi_0^2}{\tau_0}\left(\frac{k - k_c}{k_c} + \frac{N(P)}{R_2(P)}\frac{R - R_c}{R_c}\right), \tag{3.43}$$

where ξ_0 and τ_0 correspond to Eqs. (2.24) and (2.25), $N(P) = 0.166 + 23.04P^{-1} + 6.196P^{-2}$, and $R_2(P) = 10.76 - 0.073P^{-1} + 0.128P^{-2}$. If, however, the boundaries of the layer are free, the process is not diffusional, but rather oscillatory (oscillatory instability will be discussed in Sec. 6.3). In Refs. 48 and 49 $D_\perp^{\text{eff}}$ is denoted as $D_\perp$.

The phase equation can be derived by making an amplitude expansion of the NWS.[29,50,51]

6) *The Cross–Newell equation.* In Refs. 52 and 53 Newell and Cross introduced a more general approach to the description of the phase dynamics. The first noteworthy feature of this approach is that the supercritical reduced Ray-

leigh number need not be small: The inverse aspect ratio is employed as the small parameter. In addition, the flow geometry does not reduce to weakly deformed, straight, parallel rolls and can be very diverse. The deviation of the phase from kx need not be small. It is only necessary that the dimensions and orientation of the rolls as well as the amplitude of the velocity in them change slowly in space and time. The method is analogous to the nonlinear WKB method.[54]

The authors derived their own equation, starting from two variants of the model description of convection (though the method of derivation is quite general):

$$\text{I. } [\partial_t - (\Delta - 1)](\Delta - 1)^2 w + (R - ww^* - \nu ww^*\Delta)\Delta w = 0, \tag{3.44}$$

$$\text{II. } \partial_t w + (\Delta + 1)^2 w - Rw + w^2 w^* = 0. \tag{3.45}$$

In each equation $w(x, y, t)$ is a complex scalar field and R is the analog of Rayleigh's number. The linear part of the model I is identical to the linearized equation obtained for the vertical component of the velocity in the Boussinesq approximation with $P = \infty$, if the layer has free surfaces and, correspondingly, the dependence of w on the vertical coordinate has the form $\sin(\pi z)$. The model II differs from the SH model (3.26) only by the fact that w is complex.

Both models have a family of spatially periodic stationary solutions of the form

$$w(x, y) = Ae^{i\theta}, \quad \theta = \mathbf{k}\cdot\mathbf{x}, \tag{3.46}$$

and in addition k and A are related with one another by the eikonal equation

$$\text{I. } R - A^2(1 - \nu k^2) = \frac{(k^2 + 1)^3}{k^2}, \tag{3.47}$$

$$\text{II. } R - A^2 = (k^2 - 1)^2, \tag{3.48}$$

which reflects the rotational degeneracy of the solutions, since it does not take into account the orientation of the vector $\mathbf{k}$.

When studying a real convective flow that is more complicated than a system of straight parallel rolls and that carries an imprint of the initial and boundary conditions it is natural to try to describe the structure of this flow by a locally periodic solution with the local wave vector $\mathbf{k}$, continuously and slowly varying in the horizontal plane. We introduce the slow variables

$$X = \eta^2 x, \quad Y = \eta^2 y, \quad T = \eta^4 t, \tag{3.49}$$

where the small parameter η^2 is the ratio of the characteristic width of a roll (or thickness of the layer) to the horizontal size of the reservoir (the inverse aspect ratio). We define the *local wave vector* as the gradient of the phase:

$$\mathbf{k}(X, Y, T) \equiv \{m, n\} = \nabla_{\mathbf{x}}\theta = \nabla_{\mathbf{X}}\Theta, \tag{3.50}$$

where $\nabla_{\mathbf{x}} = \{\partial_x, \partial_y\}$, $\nabla_{\mathbf{X}} = \{\partial_X, \partial_Y\}$, and the fast phase θ is related with the slow phase Θ by the relation

$$\theta(x, y, t) = \frac{1}{\eta^2}\Theta(X, Y, T). \tag{3.51}$$

We seek the solution of Eqs. (3.44) and (3.45) in the form

$$w(x, y, t) = w^{(0)}(\theta; X, Y, T) + \sum_p \eta^{2p} w^{(p)}(\theta; X, Y, T), \tag{3.52}$$

where

$$w^{(0)}(\theta; X, Y, T) = f(\theta; A, k) = Ae^{i\theta}, \tag{3.53}$$

and A and k, which are no longer constants but rather functions of the slow variables X, Y, and T, are once again related by the expressions (3.47) and (3.48). Substituting Eq. (3.52) into Eqs. (3.44) and (3.45), solving the resulting ordinary differential equations for $w^{(0)}$, $w^{(1)}$, ..., and requiring that each $w^{(p)}$ $(p \geqslant 1)$ be a periodic function of θ with period 2π, we find nontrivial conditions of solvability—successive approximations to the equation of the dynamics of the phase variable $\Theta(X, Y, T)$. (If R is close to R_c, the amplitude A cannot be regarded as an algebraic function of the local wave number and is described by a partial differential equation.)

The *Cross–Newell* (CN) *phase equation* has a very general form that does not depend on the details of the model. In particular, this structure of the equation is also characteristic for an expansion based on the Boussinesq equations in the limit $P \to \infty$. The variational nature of the starting model also does not affect the form of the equation: The model II is a variational model whereas the model I is not (but the presence of an average drift flow is important; see the discussion below). The CN equation can be written in the form

$$\tau(k)\partial_T\Theta = -\nabla_{\mathbf{X}}\cdot(\mathbf{k}B(k)), \tag{3.54}$$

and for the models studied, respectively,

$$\text{I. } \tau(k) = A^2k^2(1 - \nu k^2)(k^2 + 1)^2,$$

$$B(k) = A^2\frac{dA^2}{dk^2}k^4(1 - \nu k^2)^2, \tag{3.55}$$

$$\text{II. } \tau(k) = A^2, \quad B(k) = A^2\frac{dA^2}{dk^2}, \tag{3.56}$$

and A^2 as a function of k^2 is determined by the asymptotic expansions of the eikonal equations (3.47) and (3.48)

$$\text{I. } R - A^2(1 - \nu k^2) = R_0 + \nu^2 R_2 + \nu^4 R_4 + \ldots, \tag{3.57}$$

$$\text{II. } R - A^2 = R_0 + \nu^2 R_2 + \ldots \tag{3.58}$$

where $R_0 = (k^2 + 1)^3/k^2, (k^2 - 1)^2$ for the two models, respectively, $R_2 = 0$, R_4 contains terms of the form $\partial_T A/A$, $\partial_X^2 A/A$, etc. In the paper Eq. (3.54) is written in one other form, convenient for investigating stability:

$$\tau(k)\partial_T\Theta + \left(B + \frac{m^2}{k}\frac{dB}{dk}\right)\partial_X^2\Theta + \frac{2mn}{k}\frac{dB}{dk}\partial_X\partial_Y\Theta + \left(B + \frac{n^2}{k}\frac{dB}{dk}\right)\partial_Y^2\Theta = 0. \tag{3.59}$$

In order to be able to investigate regions where fragments of differently oriented roll structures meet (grain boundaries—see Sec. 4.3) and therefore the variables vary more rapidly in space than in the fragments, the authors also derived a phase equation of a higher order approximation than (3.54).

In order to include average drift in the analysis corrections must be introduced into the phase equation. In Ref. 53 Cross and Newell altered it as follows on the basis of phenomenological considerations:

$$\partial_T\Theta = -\frac{1}{\tau(k)}\nabla_{\mathbf{X}}\cdot(\mathbf{k}B(k)) - \mathbf{U}\cdot\mathbf{k}, \tag{3.60}$$

where

$$\mathbf{U} = [\nabla_{\mathbf{X}}, \zeta\hat{\mathbf{z}}], \tag{3.61}$$

$$\Delta\zeta = \gamma[\nabla_{\mathbf{X}}, \{\mathbf{k}(\nabla_{\mathbf{X}}\cdot(\mathbf{k}A^2))\}]\cdot\hat{\mathbf{z}}, \tag{3.62}$$

and γ is a coupling constant. In order to justify this choice they studied a modification, necessary for taking drift into account, of the general formal scheme of derivation of the phase equation and they presented this derivation in application to the complete system of Boussinesq equations for a layer with rigid boundaries, but with the additional assumption that the supercritical reduced Rayleigh number is small.

Finally, very recently Newell *et al.*,[210] following the above approach, expanded in powers of η^2 the complete system of Boussinesq equations with arbitrary R and P for a layer with rigid boundaries. The equations of phase diffusion and average drift were derived from the conditions of solvability in the orders η^2 and η^4, respectively. The equations arising in the order η^2 can be reduced, by means of a Galerkin expansion, to a singular system of algebraic equations. A special method that is insensitive to errors was required in order to solve this system. Ultimately, the equations for the phase Θ and the horizontal velocity V, averaged over the vertical coordinate with some weight, acquire the form

$$\partial_T\Theta = -\frac{1}{\tau(k)}\nabla_{\mathbf{X}}\cdot(\mathbf{k}B(k)) - \rho(k)\mathbf{V}\cdot\mathbf{k}, \tag{3.63}$$

$$\hat{\mathbf{z}}\cdot\left[\nabla_{\mathbf{X}}, \hat{\mathbf{k}}\alpha([\hat{\mathbf{k}}, \nabla_{\mathbf{X}}\zeta]\cdot\hat{\mathbf{z}})\right] - \nabla_{\mathbf{X}}\cdot(\hat{\mathbf{k}}\beta\hat{\mathbf{k}}\cdot\nabla_{\mathbf{X}}\zeta)$$
$$= \hat{\mathbf{z}}\cdot\left[\nabla_{\mathbf{X}}, \left\{\frac{1}{P}\mathbf{k}\nabla_{\mathbf{X}}\cdot(\mathbf{k}A^2) - \frac{\hat{\mathbf{k}}}{\tau_\alpha}\nabla_{\mathbf{X}}\cdot(\mathbf{k}B_\alpha)\right\}\right]$$
$$- \nabla_{\mathbf{X}}\cdot\left(\hat{\mathbf{k}}\left[\nabla_{\mathbf{X}}, \mathbf{k}B_\beta\right]\cdot\hat{\mathbf{z}}\right), \tag{3.64}$$

where

$$\mathbf{V} = [\nabla_{\mathbf{X}}, \zeta\hat{\mathbf{z}}], \tag{3.65}$$

$\hat{\mathbf{k}} = \mathbf{k}/k$, and B, B_α, B_β, τ, τ_α, ρ, α, β, and A^2 are explicitly computed functions of k. The quantity $\rho\mathbf{V}$, the analog of U in Eq. (3.60), plays the role of an effective phase-transporting average drift (in addition, generally speaking, $\mathrm{div}(\rho\mathbf{V}) \neq 0$). The equation (3.64) would reduce to Eq. (3.62), if the horizontal velocity averaged with respect to the variable θ over an interval of length 2π had a parabolic (Poiseuille) distribution as a function of z (then the terms with B_α and B_β would drop out, and in addition $\alpha = \beta = \text{const}$). In reality, however, this is not the case.

If $P = \infty$ and the coordinate axis X is oriented parallel to the local vector k, then the phase-diffusion equation has the same form as the Pomeau and Manneville equation Eq. (3.42):

$$\partial_T\Theta = D_{\|}(k)\partial_X^2\Theta + D_\perp(k)\partial_Y^2\Theta, \tag{3.66}$$

where

$$D_{\|} = -\frac{1}{\tau(k)}\frac{\mathrm{d}}{\mathrm{d}k}(kB), \quad D_\perp = -\frac{1}{\tau(k)}B(k). \tag{3.67}$$

Now, however, $\mathbf{k} = \nabla_{\mathbf{X}}\Theta$ is not a small perturbation of a fixed wave vector.

The relations

$$\mathbf{k}\hat{\mathbf{n}} = \mathbf{V}\hat{\mathbf{n}} = 0 \tag{3.68}$$

can be used as the boundary conditions on the side walls over wide limits,[210] and when thermal forcing at the boundary is significant (see the end of Sec. 4.2) the first condition (3.68) is replaced by

$$[\mathbf{k}\hat{\mathbf{n}}] = 0. \tag{3.69}$$

3.2.3. Numerical modeling. A detailed discussion of methods for numerically solving the equations of convection (finite-difference and spectral) falls outside the scope of this review. An idea of the finite-difference methods can be obtained from the monograph of Ref. 55. The basic ideas of spectral methods, which compete successfully with the finite-difference methods in geometrically simple problems (to which the subject of our discussion pertains) and which have a number of important advantages, are examined in detail in Ref. 56.

We note here some fundamental elements in the formulation of problems related to the problems studied in this review.

In numerical calculations the difficulty of an investigation is less dependent on the choice of boundary conditions than in the case of analytic calculations, so that it is much simpler to study the "realistic" case of a layer with rigid boundaries, though the computational algorithms based on spectral (Galerkin) methods still appear to be simpler in the case of free boundary conditions.

When modeling an infinite layer, most investigators impose at the side boundaries of the region of computation the condition that all computed fields be periodic, so that the region is one spatial period in an infinite periodic pattern. Some authors investigate the effect of the sidewalls and perform calculations for a cavity of finite horizontal dimensions (for example, Refs. 57 and 58). A formulation of the problem in which the effect of any side boundaries on the flow being modeled is completely eliminated has also been studied.[59,60]

Calculations based on a two-dimensional geometry make up a significant fraction of numerical investigations of convection in general and the selection problem in particular (for example, Refs. 61 and 62). This seems to be completely natural, since in a large range of values of the parameters convection has a quasi-two-dimensional roll-type character (see Secs. 4 and 5). Many important questions can be elucidated along this path, and the two-dimensional numerical experiments are still of interest (for example, the recent new work in Ref. 57 is very interesting).

Calculations of three-dimensional convection were first performed at the beginning of the 1970s, first for regions with small aspect ratios.[63,64] In the last few years such calculations have also been performed for regions with large horizontal extent—for example, in Ref. 58 the dimensions of the region are $11.5\times16\times1$.

Thorough investigations of the dynamics of three-dimensional convective structure by means of a numerical experiment are nonetheless very time-consuming. The two-dimensional models which have been developed to describe three-dimensional convection make it possible (within the restrictions of the models themselves) to form, using comparatively economical means, an idea of the complex spatial dynamics of the process. For this reason, many studies in which numerical modeling of three-dimensional convection

is performed on the basis of two-dimensional model equations have already appeared (Refs. 65–70, 47 and others).

4. BASIC TYPES OF STRUCTURES OF CONVECTIVE FLOWS

4.1. Two-dimensional rolls and three-dimensional cells

In Sec. 2 it was noted that different planforms in the linear problem of convection in an infinite layer are degenerate. This degeneracy remains even in the case of steady-state nonlinear supercritical regimes: For a given value of R there exist infinitely many solutions with fixed k which differ only by their planforms.[21] There thus arises the question of selecting realizable planforms.

On the basis of the experiments of Bénard,[71] who observed a flow pattern having honeycomb symmetry (each cell is a hexagonal prism in which liquid flows upward at the center and downward at the periphery; see Fig. 2b), there emerged the opinion that steady-state laminar convection in a horizontal layer occurs mainly in the form of hexagonal cells[6] (*Bénard cells*). Subsequent investigations revealed that the flow pattern in the case when the top surface of the layer is free (as in Bénard's case) is radically different from the flow pattern in the case when the layer is covered with a solid lid at the top. When such a plate is present, in a quite wide range of values of R the steady-state flow has the form of a system of rolls (Fig. 2a), if P is not too small; this assertion will be made more precise in Sec. 5. Neglecting the irregularities or structural defects, which are usually present, the velocity field of such convection is approximately two-dimensional (see, for example, Refs. 72, 74, and 75). Here "flow" refers to the "main" flow, which is not complicated by secondary flows developing as a result of flow instability (which for sufficiently large R is unavoidable), and it is assumed that the factors that would cause the conditions of the experiment to deviate appreciably from those of the standard problem (Sec. 2) are not present; these factors will be discussed below.

Bénard himself already proposed that the temperature dependence of the surface tension plays an important role in the convection that he observed. This was later confirmed, and according to the modern interpretation the existence of hexagonal cells in Bénard's experiments was governed by the quite strong thermocapillary effect. If, however, there is no free surface and only the usual (*thermogravitational*) convection occurs, the roll pattern is the preferred structure. (Of course, the idealized boundary conditions usually employed in the theory for a "free" boundary (2.8) do not make hexagons preferred, since these conditions do not take the surface tension into account.) We note that the incorrect assertion that under standard conditions the thermogravitational mechanism can by itself generate hexagonal cells is still encountered in the literature.

Starting from the assumption that quasi-two-dimensional rolls are the main form of steady-state convection, we list the most important factors which have been investigated and which could make three-dimensional cells preferred.

4.1.1. Thermocapillary effect. Block[76] was the first to give a conclusive experimental demonstration of the role of surface tension in the formation of hexagonal cells. In particular, he was able to observe cells for $R < R_c$ (and even $R < 0$), when the thermogravitational mechanism does not operate.

To this day, not too many investigations of thermocapillary convection or Bénard–Marangoni convection have been carried out. We omit the details and recommend to the reader the corresponding sections of the reviews of Refs. 77 and 78 and the introductory part of Ref. 79 as a brief introduction to this field.

Significant experimental results were obtained in Refs. 79, 80, and 81. An interesting comparison of the experimental data on and the theory of the selection of planforms under the combined action of two instabilities—the standard convective (Rayleigh) and thermocapillary (Bénard–Marangoni)—was made in Ref. 82. In Ref. 81 it was found experimentally that, when these two mechanisms interact, as ΔT increases after Bénard cells have appeared the characteristic size of the cells at first decreases and then starts to increase. Since under conditions of thermogravitational convection the scale of the flow characteristically increases with ΔT (see Sec. 6.1), it is concluded that for sufficiently large values of ΔT the Rayleigh mechanism predominates. Zero g experiments on thermocapillary convection—when the Rayleigh mechanism is not operating—have been performed on board spacecraft.[83]

The first theoretical investigations concerned the linear analysis of stability (Ref. 84, where gravity was assumed to be absent, and Ref. 85, where a combination of the two mechanisms was studied). The planforms of thermocapillary convection were studied within the framework of nonlinear problems in Ref. 86 (where, according to Ref. 32, the quantitative results need to be made more accurate), Ref. 32 (see Sec. 3.2.2), and Refs. 87 and 88.

4.1.2. Temperature dependence of the viscosity. Back in the 1930s Graham[89] discovered, while observing polygonal convective cells in a layer of air, that under steady-state conditions the air descends in the central parts of the cells—the opposite of what happens in liquids (see Fig. 2; cells with ascending motion at the center are sometimes called l-type cells and cells with descending motion at the center are called g-type cells, corresponding to the words liquid and gas; meteorologists call cells of the l type *closed* and cells of the g type *open*). Graham hypothesized that the direction of circulation depends on the sign of the derivative $\partial\nu/\partial T$: for liquids it is usually negative and for gases it is positive. This hypothesis was confirmed experimentally by Tippelskirch[90] for liquid sulfur, for which $\partial\nu/\partial T < 0$ for $T < 153$ °C and $\partial\nu/\partial T > 0$ for $153\ C < T < 200$ °C. Convective cells in these two temperature ranges are indeed of the l and g type, respectively.

One can see that circulation occurs in a direction such that the viscous stresses are weaker at the center of the cell, where they are maximum by virtue of the geometry of the flow.

Palm[91] studied slightly supercritical convection in a liquid whose viscosity depends on the temperature as

$$\nu = \nu_0 + \gamma \cos \mu(T - T_1), \tag{4.1}$$

and it is assumed that $(\gamma/\nu_0)^2 \ll 1$. The admission of such a dependence is, evidently, a departure from the Boussinesq approximation. Analyzing the interaction of the different modes with the lowest wave number, equal to the critical wave number (the critical wave number has an $O(\gamma^2/\nu_0^2)$ correction as compared with the case $\nu = \text{const}$), and using the fact that the supercritical reduced Rayleigh number and

the parameter γ are small, Palm separated from these modes the two most significant modes which give a planform function of the form

$$f(\mathbf{x}, t) = Y(t)\cos\left(\frac{\sqrt{3}}{2} k_c x\right)\cos\left(\frac{1}{2} k_c y\right) + Z(t)\cos k_c y \quad (4.2)$$

[compare Eq. (2.28)]. Analysis of the nonlinear ordinary differential equations describing the time dependence of the amplitudes Y and Z shows that the stationary state of the system in the limit $t \to \infty$ is characterized by the relation $Y = 2Z$, i.e., it corresponds to hexagonal cells. In agreement with the experimentally found law, the direction of circulation in the cell is determined by the sign of the coefficient γ.

A detailed investigation[92,93] of the system of equations, corrected by Palm, for Y and Z showed that near $R = R_c$ for sufficiently large values of γ the hexagonal cells are the only stable form of convective flow, and in addition the conclusion that the direction of circulation depends on the sign of γ remains correct. These cells are also possible for subcritical values of R, if the amplitude of the initial perturbation is sufficiently large (hard excitation). As found in Ref. 94, where a wider range of interacting modes was included in the analysis, as R increases, the two-dimensional rolls become stable, and then the hexagons become unstable.[7)] Finally, an analogous result was obtained, using a technique of this type, in Ref. 95, where not only the viscosity but also other material parameters of the medium were assumed to be temperature dependent and deformations of the free surfaces of the layer were also allowed.

In Refs. 91–95 the horizontal boundaries of the layer were assumed to be free. Calculations of the range of Rayleigh numbers where the hexagonal cells are stable for other boundary conditions are presented in Ref. 96.

Schlüter, Lortz, and Busse[25] investigated, by expanding the Boussinesq equations (with $\nu = \text{const}$) with respect to the small amplitude $\varepsilon^{1/2}$ of the flow, in the linear approximation the stability of the geometrically diverse steady-state solutions of the weakly nonlinear problem with respect to a wide class of infinitesimal perturbations. The results of this and the above-mentioned publications form a unified picture demonstrating the role of the temperature dependence of the viscosity. According to Ref. 25, in the case $\nu = \text{const}$ all three-dimensional flows are unstable, and there exists only one class of stable two-dimensional roll flows (the stability of the rolls will be studied in Sec. 6.3). This result is valid for layers with free or rigid boundaries.

The method developed in Ref. 25 was applied to a liquid whose viscosity depends weakly on the temperature (the other material parameters, generally speaking, also are weakly temperature dependent; this is discussed below).[97,98] Figure 4 shows a diagram of the stability of rolls and hexagonal cells obtained for different types of boundary conditions, and Fig. 5 shows the dependence of the amplitudes of flows of both types on R. In this case β is a (small) coefficient in the leading order (linear) term of the dependence $\nu(T)$.

Subsequent experimental investigations confirmed the general features of the theoretically predicted regularities.

Liquids whose viscosity behaves differently can exhibit different convective structures under similar experimental conditions.[99] In experiments with silicone oil, whose viscosity is virtually constant, either convective rolls (in a layer with a lid at the top) or hexagons (in a layer open at the top, where the thermocapilllary effect operates) were observed. In the case of Aroclor, whose viscosity is strongly temperature dependent, hexagons also appeared in a closed layer, if the layer was sufficiently thin and, correspondingly, the temperature gradient was sufficiently large.

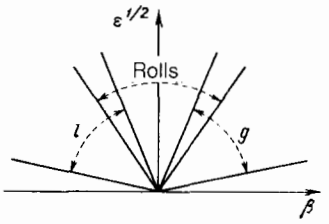

FIG. 4. The regions of stability of rolls and hexagonal cells of the l and g types.[22,98] $\varepsilon^{1/2}$ is the amplitude of the flow and β characterizes the vertical nonuniformity of the layer (see text).

In Ref. 100 controlled initial disturbances of the roll geometry were produced and the k and R dependence of the stability of the induced rolls was investigated for different values of the ratio ν_{max}/ν_{min} of the maximum and minimum viscosity in the layer (R was calculated from the value of $\nu(T_0)$ of the viscosity at the temperature $T_0 = (T_1 + T_2)/2$; this definition is used in most papers). For the working liquids employed (glycerine and polybutene oil) the quantity ν_{max}/ν_{min} reached approximately 20. It was found that for sufficiently small values of R and large values of ν_{max}/ν_{min} in the process of evolution the rolls transform into hexagonal cells (if after this R is increased, then the reverse transition occurs all the more easily the more regular the system of hexagons was).

Much larger ratios ν_{max}/ν_{min} (up to 3400) were reached using water-free glycerine in experiments with uncontrolled initial conditions.[101,102] It was found that the transition from hexagons to rolls as R increases is observed only if the parameter $\eta = \ln(\nu_{max}/\nu_{min})$ does not exceed, roughly speaking, 2. In this case the interval of Rayleigh numbers where the hexagons are stable becomes wider as η increases and agrees with the theoretical results of Refs. 97 and 98. For large values of η, however, as R increases the hexagons transform not into rolls but rather into a system of irregular tetra-, penta-, and hexagons, and now the interval of stability of the hexagons, on the contrary, shrinks as η

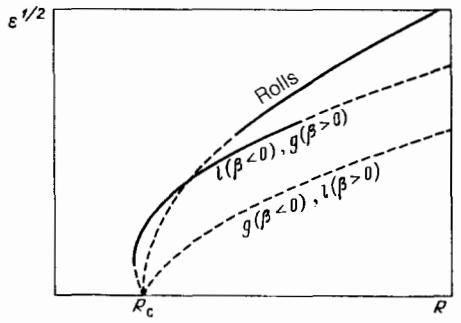

FIG. 5. The amplitudes of the rolls and the hexagonal cells of l and g types as functions of the Rayleigh number R.[22,98] $\varepsilon^{1/2}$ and β have the same meaning as in Fig. 4. The solid lines pertain to stable flows and the dashed lines pertain to unstable flows.

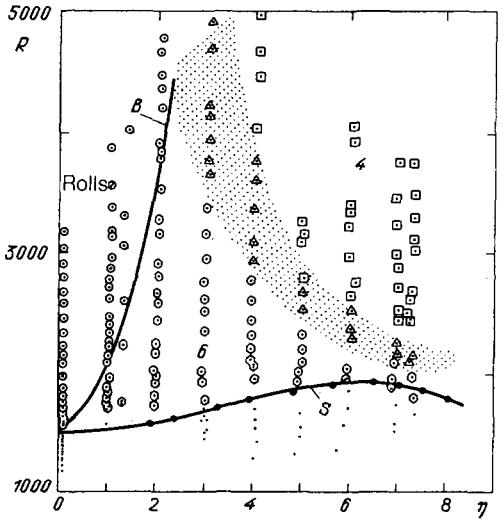

FIG. 6. The regions of stability of rolls, hexagonal (6) and square (4) cells in liquids with temperature dependent viscosity;[102] $\eta = \ln(\nu_{max}/\nu_{min})$; the Rayleigh number R is calculated with respect to $\nu(T_0)$; S is the dependence of the critical Rayleigh number on η for a layer with boundaries of finite thermal conductivity according to Ref. 101; B are the theoretical values of the maximum value of R at which the hexagonal cells must be stable.[97] Irregular tetra-, penta-, and hexagons are observed in the shaded transitional region. The dots correspond to the absence of convective motions.

increases. As R increases further the irregular patterns of polygons in turn transform into a system of square cells if $\eta \gtrsim 4$. These experimental data are presented in Fig. 6.

In Ref. 19 the stability of squares and hexagons with $R \leqslant 63{,}000$ (R was calculated as in Ref. 100) and $\nu_{max}/\nu_{min} \leqslant 10^3$ was investigated in experiments with golden syrup under controlled initial conditions. For both planforms delimited regions of stability in the (k, R) plane, analogous to "Busse balloons" for rolls (see Sec. 6.3), were found. As ν_{max}/ν_{min} increases these regions shift in the direction of higher values of k. Subcritical convection was observed in the form of squares and not hexagons (the author's calculations of R_c are based on the dependence $\nu(T)$ of the type realized in the experiment). Different instabilities and many types of transitions between flows of different structure are described in the paper.

Theoretical investigation of the possibility of the existence of square cells started with a study of their stability.[103,104] As in a series of papers on the stability of rolls (Sec. 6.3), the main flow was calculated by Galerkin's method and the stability of the flow was analyzed in the linear approximation. The boundaries of the layer were assumed to be rigid. It was found that in the case of uniform viscosity the square cells are unstable.[103] For the case of a linear temperature dependence of the dynamic viscosity μ the stability of such cells for given R depends on the ratio $r = \mu_{max}/\mu_{min}$.[104] Confining their attention only to the case when the wave number of the flow is equal to k_c and the disturbances have the same symmetry and the same wave number as the main flow, the authors found that as r increases the squares become stable first, after which the rolls become unstable.

The possibility of square cells was later investigated by Jenkins[105] who solved the problem of the evolution of a flow with the planform function

$$f(\mathbf{x}) = A(t)\cos k_c x + B(t)\cos k_c y \qquad (4.3)$$

[compare Eq. (2.29)] with small supercritical reduced Rayleigh numbers, rigid boundaries, and two variants of the function $\mu(T)$—linear and exponential. He also studied the effect of finite thermal conductivity of the boundaries (this is discussed below). For a linear function $\mu(T)$ the results agree qualitatively with Ref. 104, but the transitions were found to occur at different critical values of the parameter r (the author asserts that the disagreement is caused by the fact that the method of Ref. 104 is applicable only for small values of r). For an exponential function $\mu(T)$ the critical values r_1, r_2, and r_3, bounding the following regimes, were found: for $r < r_1$ the flow exhibits a roll structure; for $r_1 < r < r_2$ square cells exist in supercritical regimes; for $r_2 < r < r_3$ subcritical convection in the form of squares is possible; and, for $r > r_3$ both rolls and squares can exist under subcritical conditions.

In Ref. 106 Stuart stated his opinion that the solution with the planform function (2.29) is unphysical, since it does not incorporate all the characteristic features of the actually observed convective cells. However numerical modeling of refraction of light in shadow visualization with automatic readout of the results in the form of model "shadow patterns" with the help of a laser printer[107] showed that a flow of the form (2.29) gives a pattern that is very close to the observed pattern. It is interesting that this pattern is not at all similar to a checkerboard, as could be assumed on the basis of the relative arrangement of the warm upward flow and cold downward flow. In the process of shadow visualization simple vertical averaging of the temperatures does not occur (for this reason the pattern can change significantly when the sign of the convective velocity changes). Something like a negative image of "square-lined" paper—dark-colored squares with light-colored boundaries—is obtained instead of a checkerboard pattern.

4.1.3. Temperature dependence of other material parameters of the medium. The variation with the temperature of other characteristics of a material in principle plays the same role as variation of the viscosity. In the papers mentioned,[97,98] departure from the Boussinesq approximation was permitted in the following form: the thermal expansion coefficient was written as

$$\alpha = \alpha_0\left[1 + \frac{\gamma_1}{\Delta T}(T - T_0) + \ldots\right], \qquad (4.4)$$

where $T_0 = (T_1 + T_2)/2$, and the kinematic viscosity, thermal conductivity, and heat capacity at constant pressure were written analogously (with the corresponding coefficients γ_2, γ_3, and γ_4); in addition, the terms nonlinear in $T - T_0$ are higher order infinitesimals than the linear terms. Analysis of the stability of the rolls and hexagonal cells showed that the parameter β, which is a linear combination of all γ_i in dependences of the form (4.4), plays the determining role. The stability diagrams (see Fig. 4) and the diagram of the R dependence of the amplitudes (see Fig. 5) thus reflect the effect of the nonuniformity of each quantity mentioned.

An analogous conclusion concerning the character of the transition from hexagons to rolls as R increases (with the possibility of finite-amplitude perturbation of the hexagonal cells in the subcritical regime) was drawn in Ref. 95, where this effect was obtained as a consequence of the temperature dependence of the viscosity, thermal conductivity, and ther-

mal expansion coefficient. The approach employed in Ref. 95 was similar to that used in Refs. 91, 92, and 94.

The experiments of Ref. 108 show that the temperature dependence of the physical properties of a liquid is manifested in the structure of the flows all the more sharply as the thickness of the layer decreases and ΔT increases.

The effect of the temperature dependence $\alpha(T)$ on the convection pattern was observed in Ref. 109 in experiments with water at temperatures close to 4 °C (when α varies from zero to finite values). Laser Doppler anemometry showed that near the critical regime the spatial distribution of the vertical velocity has a form typical for a system of hexagonal cells. As ΔT increases hysteretic transition to roll convection occurs.

Experiments with liquid helium,[110] whose density also has a maximum value (at a temperature of 2.178 K), indicate indirectly the same effect. Since the flow of liquid helium cannot be visualized, the behavior of the heat flux through the layer as a function of the Rayleigh number was investigated. The two breaks in the curve of this dependence were interpreted as transitions from a motionless state to hexagons and from hexagons to rolls. In both cases the dependence exhibits hysteresis.

Remark. The above-studied cases of preference for three-dimensional cells are unified by a common feature: in the layer there is an appreciable asymmetry of the physical properties relative to the midplane $z = 1/2$. If, however, the layer is symmetric, then two-dimensional rolls arise. This is not difficult to understand: the transition from some system of rolls to a mirror reflection of this system relative to the midplane is equivalent [at least, in the approximation corresponding to the lowest harmonic with the planform (2.27)] to uniform translation of the entire pattern in the direction of the vector **k**. Three-dimensional cells do not have this property. It is not surprising that rolls are typical for those cases when the top and bottom parts of the layer are indistinguishable. In addition, the existence of hexagonal cells of l and g types agrees with the presence of nonuniformity of the viscosity: the direction of circulation is such that the viscosity is minimum in the region of highest rates of deformation—at the center of a cell. It can be expected that three-dimensional cells will also be preferred in the following two cases.

4.1.4. Asymmetry of boundary conditions. In particular, in Ref. 97 it was found that for a layer with rigid bottom boundary and free top boundary cells of l type should be preferred. Here, obviously, the point is that the velocity field is not mirror symmetric.

4.1.5. Curvature of the unperturbed temperature profile can also facilitate the appearance of hexagonal cells.[111] Such a curvature is made possible, for example, by internal sources of heat. We note that non-steady-state heating, which can result in the appearance of hexagons (see below), also induces curvature of the temperature profile, which under these conditions can be regarded as being unperturbed.

4.1.6. Finite thermal conductivity of horizontal boundaries. Square cells can arise as a result of significant departures from the conditions (2.5), which are realizable only if the thermal conductivity of the horizontal boundaries of the layer is infinite.

If the parameter ζ, which is equal to the ratio of the thermal conductivity of the plates bounding the layer to the thermal conductivity of the liquid, is small, then when it is taken into account in the expansion according to the scheme of Ref. 25 analysis of the stability of different steady-state solutions with $k = k_c$ leads to the following result, obtained for $P = \infty$ and infinitely thick plates.[112] Only those solutions for which $N = 2$ [see Eq. (2.13)] and the angles between the vectors $\mathbf{k}_1$ and $\mathbf{k}_2$ lie between 60° and 120° are physically realizable. Square cells are distinguished among them by the fact that they give maximum heat transfer. In addition, the most rapidly growing disturbances of unstable roll flows tend to transform the rolls into a system of squares. These results, as the authors showed, should remain substantially the same for finite P and finite thickness of the plates.

It was shown subsequently in Ref. 113 that square cells are most stable at finite amplitude also. On the basis of the fact that the horizontal scale of flows with small values of ζ should be much larger than the thickness of a layer, an expansion analogous to that employed in shallow-water theory was employed. The thickness of the boundary plates was assumed to be finite. The stability of flows with different planforms was investigated with the help of a variational principle derived in the paper.

The investigation of the equations of evolution of the planform function (4.3), which were derived by expanding in the small amplitudes (compare the previously mentioned papers of Refs. 91–96 and 105), made it possible to find[114] the critical value of the parameter ζ at which a transition from rolls to squares occurs. It depends on the ratio of the thickness of the plates to the thickness of the liquid layer and on P. For very small values of P (for example, values characteristic for mercury: $P = 0.025$) the critical value of ζ is very small and squares are possible only if the plates are virtually completely thermally insulating. If P is large, then squares arise even when the thermal conductivity of the plates is equal to that of the liquid.

Finally, further investigation by the method of Ref. 25 of the linear stability of stationary flows near $R = R_c$ with $k = k_c$, thick boundary plates, and generally speaking different (not small) values of the parameter ζ for the bottom and top boundaries of the layer (ζ_b and ζ_t, respectively), showed[115] that the rolls are unstable when the squares are stable and vice versa, and all three-dimensional solutions with $N > 2$ (including hexagonal) are always unstable. The stability diagram in the space (ζ_t, ζ_b, P) is presented in Fig. 7.

Square cells were observed near the threshold of convective instability ($\varepsilon < 0.024$) in an experiment with silicone oil ($P = 70$) with $\zeta = 7$ (glass plates).[116] A circular reservoir with $\Gamma = 20$ was employed. In the region $0.024 < \varepsilon < 0.057$ the amplitudes of two mutually perpendicular systems of rolls underwent periodic oscillations in antiphase with one another; as ε increased one system started to predominate, until (for sufficiently large ε) a single stationary system of rolls was established (neglecting the two regions near the outer walls, where the structure remained more complicated).

The experiment was subsequently altered:[117] Plexiglass was used for the boundaries and water was used as the working liquid, since $\zeta = 0.4$ and $P \approx 7$. A quite prolonged process of settling of the flow structure resulted in a system of square cells, which, in contrast to the preceding experiment, was observed in a wide range of values of ε without any indica-

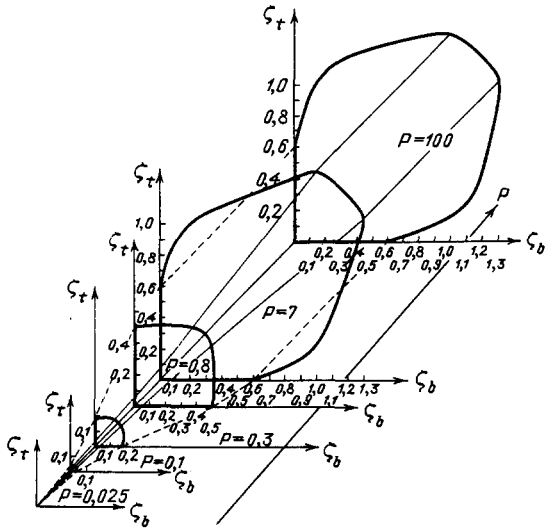

FIG. 7. Diagram of stability of square cells and rolls in the space (ζ_t, ζ_b, P).[115] Inside the region delimited by the thick curve in each plane P = const the squares are stable and outside the region the rolls are stable.

tions of destabilization. The authors believe that in the first case the silicone oil behaved as a mixture and the observed pattern is governed by the Soret effect.

The finite thermal conductivity of the boundaries was taken into account in order to compare the theoretical results with experiment and with the already mentioned article of Ref. 105, devoted to the investigation of the role of the temperature dependence $\nu(T)$.

According to calculation, subcritical convection in the form of squares should be observed for larger values of ν_{max}/ν_{min} than in the experiment of Ref. 19. The reason for this discrepancy was not determined in this work.

4.1.7. Deformation of a free surface. Thus far it was assumed everywhere that the boundaries of the layer are not deformed, even if they are free in the sense that there are no tangential stresses. Taking into account the deformability of the free surfaces (one or both) gives effects of the same type as departure from the Boussinesq approximation[95] (see above). This result was obtained neglecting surface tension, but the effect of deformation is appreciable only in very thin layers, when the effect of surface tension is also significant.

An analogous result was obtained in Ref. 32 (see Sec. 3.2.2). The authors found that deformation effects are significant if the following criterion is satisfied: $\partial \ln \rho/\partial \ln \mu \sim 1$ (μ is the dynamic viscosity). For most liquids this derivative is small and approaches unity near the inversion point, where $\partial\mu/\partial T = 0$. In particular, for sulfur inversion appears at $T = 153$ °C.

4.1.8. Non-steady-state heating. Krishnamurti[118] studied the case when the temperature of both surfaces of the layer changes slowly and linearly in time, so that Rayleigh's number remains constant and the undisturbed temperature profile in dimensionless variables has the form

$$T = \eta t - \frac{\Delta T}{h} z + \frac{\eta}{2\chi} z(z-h), \tag{4.5}$$

where η = const and χ is the thermal diffusivity of the liquid. Performing an expansion in the small parameters—the convection amplitude and the rate of heating (cooling) η and investigating the stability of rolls and hexagons (as in Ref. 25), Krishnamurti showed that the effect of non-steady-state heating is entirely analogous to that of a temperature dependence of the physical properties of a substance.[97,98] In particular, the stability diagram has the form shown in Fig. 4, if β is the parameter η. In the case of heating ($\eta > 0$) hexagons of the g type can be stable while in the case of cooling ($\eta < 0$) hexagons of the l type can be stable. An experiment in which hexagons were actually observed under conditions of non-steady-state heating and the direction of circulation in the cells agreed with the theory is described in Ref. 119. Analogous results were obtained with numerical modeling of three-dimensional flows under the conditions of the same problem, but the cells were not precisely hexagonal.[120]

An effect of this type could be caused by the periodic temporal modulation of the difference of the temperatures of the bottom and top surfaces of the layer. If this difference varies as $\Delta T(1 + \delta \cos \omega t)$, where ΔT is the average value, then expansion of the Boussinesq equations in the small amplitude of the flow and the small amplitude δ of modulation and subsequent stability analysis show that near the threshold of instability (including a narrow interval of subcritical values of R) hexagonal cells are stable.[121] For sufficiently high supercritical Rayleigh numbers the roll flow becomes stable, and for even larger values of R the hexagons become unstable. The width of the interval of values of R in which the hexagons are stable is $O(\delta^4)$ and decreases with ω.

Investigation of the system of equations for the amplitudes of several of the lowest harmonics of the Galerkin expansion of the convective disturbances ("generalized Lorenz model") confirmed[122] the qualitative results of Ref. 121, but the authors concluded that hexagons cannot be observed for small values of δ, since their interval of stability is very small and the conditions of the experiment cannot be controlled with the needed accuracy. In order to be able to observe hexagons much larger modulation amplitudes than indicated in Ref. 121 are needed.

The theoretically predicted consequences of periodic modulation of heating were observed in the experiment of Ref. 123. Regions where hexagons and rolls are stable and both types of flows coexist were singled out. The boundaries of the regions and the direction of circulation in the cells agree with the theory.

We call attention also to the experiment described in Ref. 40. The behavior of a convective heat flux through the layer of liquid helium under conditions when R varied with time either in a step-like fashion or linearly was investigated. The interpretation of the data on the basis of the amplitude equations showed that the convection at the moment of appearance was not of the roll type, but rather a transitional regime was present; the authors tentatively associate this transitional regime with a system of hexagonal cells.

4.1.9. The presence of a suspension, generally speaking, can strongly alter the mechanical properties of a liquid. For information, we call attention to the fact that, according to the experiment of Ref. 75, when the concentration of a polydispersed solid additive used for visualization is high, polygonal cells are observed in those cases when rolls appear under conditions of low concentration.

4.1.10. Secondary flows. Roll convection is observed only in a definite range of Rayleigh numbers (see Sec. 5).

Beyond the upper limit of this range rolls are unstable and the developing secondary flows make the velocity field three-dimensional.

4.2. Quasi-two-dimensional roll structures

As we saw above, in the absence of complicating factors a roll structure is the basic type of steady-state convection. In this section we study the properties of such flows in greater detail.

Even if the roll structure in a full-scale experiment is very regular and free of defects, the rolls nonetheless are never completely straight and the flow in them is never completely two-dimensional. This happens, at the very least, because of the fact that in reality the flow is always bounded by sidewalls, which can have a large effect on the structure of the flow.

On the basis of the linear problem of stability of the steady state Davis,[124] using the Galerkin method, showed that the presence of sidewalls removes the degeneracy of the eigenfunctions: In a rectangular reservoir with rigid horizontal and vertical boundaries the critical Rayleigh number is smaller than for rolls which are parallel to the short side of the reservoir. Precisely such rolls are predicted on the basis of the NWS amplitude equation[28] and its extension for the superposition of systems of mutually perpendicular rolls.[36] The conclusion that such rolls are preferred was confirmed by the experiment of Ref. 125, which was performed for different ratios of the sides of the rectangular reservoir and different aspect ratios and agreed with Ref. 124. The linear theory describes quite well[126] regimes with a different number of rolls, which were observed in Ref. 25 with different chamber geometry. In Ref. 126 it was predicted that in a nearly square reservoir systems of mutually perpendicular rolls can arise near the threshold of instability.

For an infinitely long channel with free horizontal boundaries and rigid sidewalls and aspect ratio A the linear problem gives[127] as the preferred mode rolls that are oriented across the channel, if $A < 0.1$ or $A > 1$. For intermediate values of A the overall features of the pattern are the same, but the velocity component transverse to the channel is quite large. In Ref. 128 the structure of convection in a channel with rigid walls is investigated in detail by Galerkin's method.

Rolls oriented perpendicular to the long walls of a channel were observed experimentally, for example, in Ref. 129, in a finite but long ($\Gamma = 18$) channel.

A laboratory model of an infinitely long straight channel is an annular channel between coaxial cylindrical walls. If it is not too wide, then the rolls are oriented radially, perpendicular to the walls.[130]

Extensive experimental data have shown that the indicated orientation of the rolls is a particular case of a more general tendency: Near a wall rolls tend to be perpendicular to the wall. This tendency is especially noticeable (since it affects the form of the rolls) when complicated structures with defects (textures) are observed as well as in circular reservoirs (Fig. 8).

Using the SH model equation, Pomeau and Zaleski[43] showed that in the boundary layers near a sidewall a system of rolls which are parallel to this wall must be unstable: Secondary flow in the form of rolls perpendicular to the wall and the initial rolls develops (cross-roll instability; see Sec. 6.3).

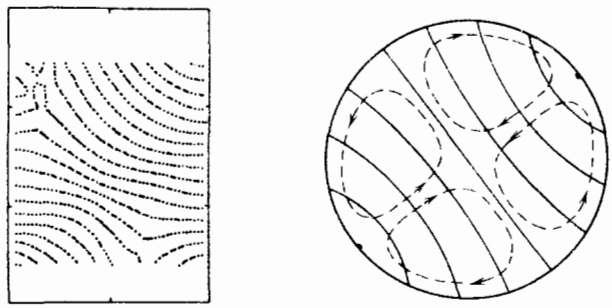

FIG. 8. Experimentally observed structures of roll flows (the boundaries of the rolls are indicated). a) Texture in a rectangular reservoir, $R = 4R_c$, $P = 2.5$;[14] regions adjoining the short walls of the chamber are not visible. b) Schematic image of curved rolls in a circular reservoir, $R = 1.14R_c$, $P = 0.7$ (according to the photograph from Ref. 131); the dashed lines depict large-scale flow obtained in Ref. 156. In both figures the tendency of rolls to approach the sidewalls at right angles can be clearly seen.

This effect was observed experimentally in, for example, Ref. 132 (in a circular reservoir) and Ref. 18 (in a rectangular reservoir—see Secs. 6.5.3); see also Fig. 9.

Cross[46] investigated the effect of a sidewall with the help of the NWS amplitude equation with boundary conditions which are identical to Eq. (3.20) in lowest order. He found that the Lyapunov functional for the system of rolls in the boundary layer is minimum when the rolls make with the wall an angle $\pi/2$ with accuracy up to $O(\varepsilon^{1/4})$.

This result was later refined by Zaleski *et al.*[133] They performed numerical calculations of the Lyapunov functional for the NWS equation in a boundary layer and they obtained an optimal (minimizing the functional) angle between the rolls and the normal to the wall different from zero and of the order of $\varepsilon^{1/4}$. Here the value of the angle is taken outside the boundary layer, quite far away from the wall; at the wall itself this angle is equal to zero in accordance with the boundary conditions. For this reason, it can be imagined that in a reservoir whose width is greater than twice the thickness of the boundary layer and whose length is appreciably larger than the width, the rolls must resemble the letter S, approaching the long sidewalls along the normal and making an angle with this normal in the central part.[133] Greenside *et al.*[65,66] (Fig. 9) obtained such S-shape structures in numerical modeling of the textures based on the SH equation and Le Gal[134] observed them experimentally (in

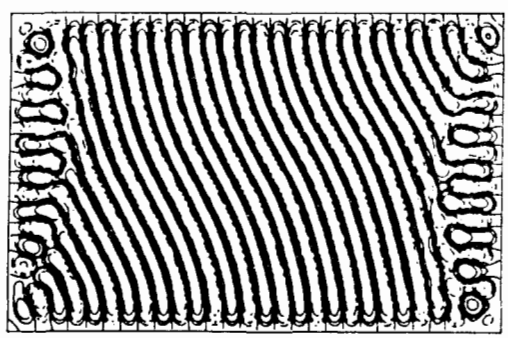

FIG. 9. S-Shaped rolls obtained by numerical modeling in Ref. 66. The cross-roll instability develops near the short boundaries of the region. A very similar pattern was observed in the experiment of Ref. 134.

addition, the observed pattern was almost identical to that shown in Fig. 9). We note that the fact that the optimal angle minimizes the Lyapunov functional does not mean in this case that this is the only realizable angle (see Sec. 6.4). Ultimately, the overall geometry of the flow, which is determined, in particular, by the shape and horizontal dimensions of the chamber and the conditions on the sidewalls, is important for some particular structure to be realized. The situation here is analogous to the question of the realizability of the optimal wave number of a system of two-dimensional rolls; this will be discussed in Sec. 6.5.

For very small supercritical reduced Rayleigh numbers the angle made by a roll with a sidewall can differ appreciably from a right angle. Thus in the experiment of Ref. 131 with $\varepsilon = 0.05$ all rolls in a circular reservoir were practically straight and parallel. It is possible that here the neglected factors, which destroy the ideal boundary conditions (3.20), become important.

The tendency for convective rolls to become aligned near sidewalls perpendicularly to the walls is now a well-known experimental fact. But, three important stipulations must be made here.

First, what has been said above does not pertain to those cases when the thermal regime of the sidewalls itself imposes a definite character on flows in the region near the wall. Suppose, for example, that the temperature at the wall is always higher than the undisturbed temperature in the layer at the same height (this happens when the heat conducting wall has better thermal contact with the bottom boundary of the layer than the top boundary of the layer, or it is heated from the outside). Then a stable upward flow will exist near the wall, and the rolls in the region near the boundary will be oriented parallel to the wall. Situations of this type with forcing at the boundary (wall) will be examined in Sec. 6.5.1. They are often deliberately produced experimentally; see Sec. 6.7.

It is understandable that the thermal effect of the sidewalls under identical boundary conditions is all the smaller the closer the thermal conductivity of their material is to that of the liquid. This is especially noticeable under conditions of non-steady-state heating:[135] walls made of 5% polyacrylamide gel, whose thermal conductivity is very well matched to that of the working liquid (water), had virtually no effect on the evolution of the flow; the structure of the flow was not correlated with the geometry of the reservoir and was not repeated from one experiment to another (though the rolls approach the sidewall at close to right angles). Polyethylene walls, however, had a forcing action on the flow, and the flow developed away from the walls into the chamber, while the structure of the flow reflected the geometry of the reservoir.

Second, the roll structure can be significantly affected even by insignificant nonuniformities of heating from below and (or) cooling from above. For example, in the well-known experiments of Refs. 136 and 137 an axisymmetric system of annular rolls in a circular reservoir arose as a result of the presence of a radial temperature gradient in the top heat exchanger, since the cooling water flowed into the central part of the heat exchanger and was pumped out near the outer edge.

Third, the effect of the walls can be significantly reduced, if there exists along these walls a zone where the layer of liquid is not covered at the top with a solid cover and its top surface is free (see Sec. 3.1 and Fig. 3). This zone plays the role of a buffer, since there arise in it three-dimensional flows with a complicated structure which easily match arbitrarily oriented rolls, arising far from the walls. For this reason, in experiments on such setups the systems of parallel rolls sometimes make different angles with the walls, and their orientation changes in a random fashion from one experiment to another.[75]

4.3. Convective textures

Convection developing spontaneously from noise, as a rule, does not form a completely regular system of rolls: The regularity of the pattern is "spoiled" to a greater or lesser degree by structural defects of different types. Such complicated patterns, in which several ordered fragments can be identified, are called *textures*. We shall see that the presence of defects gives the system of rolls additional "degrees of freedom:" Wave-number restructuring of the rolls occurs most easily in the presence of suitable structural defects. Many observed defects are similar to defects of crystal lattices, so that the terminology employed to describe them is taken from the physics of crystals. Typical defects of roll structures are shown schematically in Fig. 10.

4.3.1. A dislocation (Fig. 10a) is a defect arising at a location where an "extra" pair of rolls, which is "wedged" into a regular roll structure (whose rolls near the dislocation are somewhat deformed), terminates. Both stationary and moving dislocations are observed. They move most often in a direction parallel to the rolls (*climbing*), though sometimes movement in a perpendicular direction (*gliding*), accompanied by topological restructuring near a dislocation, has also been observed.

4.3.2. Disclinations are defects associated with point singularities of the field of local wave vectors. Typical disclinations are shown in Fig. 10b. A *focus singularity*—a disclination arising at the center of an axisymmetric system of annular rolls or in fragments of a similar system, for example, near a sidewall of the reservoir—is studied especially often in papers investigating wave-number selection. In the process of restructuring of a convective structure containing foci, rolls often appear and disappear precisely at these points.

4.3.3. Grain boundaries[8)]—lines delimiting ordered fragments of texture within which the flow has the form of a regular system of rolls (Fig. 10c)—are a very characteristic defect. As will be explained in Sec. 6.5.3, the motion of grain boundaries can give rise to very effective wave-number restructuring of rolls over wide limits.

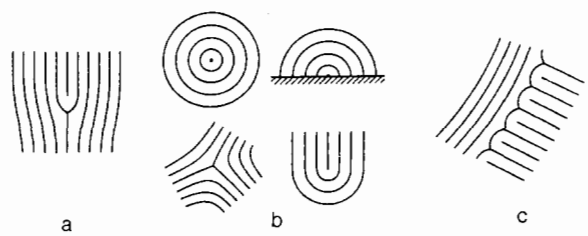

FIG. 10. Defects of roll structures. a) Dislocation, b) disclination (focus singularities are shown at the top). c) Grain boundary.

5. EXCHANGE OF CONVECTION REGIMES

Convection is manifested in diverse forms: cells can have different configuration and form more or less ordered spatial structures and the flow either can either attain a steady-state or undergo oscillations (also with a different degree of ordering) or it can be completely turbulent. The convection regime in a horizontal layer under standard conditions is determined, to a first approximation, by the numbers R and P. Transitions between regimes can be represented in the form of the diagram shown in Fig. 11. This diagram summarizes the experimental data of Krishnamurti[72,73,138] and a number of other authors. It was first constructed by Krishnamurti and modified by Busse.[22,23] The lines delimiting the regions of different regimes were drawn, to a certain extent, arbitrarily, since the results of different experiments do not always agree precisely with one another and, moreover, difficulties in determining the values of R corresponding to the transitions are possible, especially if as R changes in a step-like fashion the exchange of regimes is accompanied by hysteresis. As will become evident from what follows, the question of the transition from steady-state to non-steady-state convection is especially subtle.

The region where the liquid is in a stable motionless state lies below the line $I(R = R_c)$. The region of steady-state roll convection, conventionally speaking, two-dimensional (see Secs. 4.2 and 4.3), lies above this line. For high values of P it extends approximately up to $R \approx 13R_c \approx 2 \cdot 10^4$. Close to two-dimensional, but, generally speaking, not completely steady-state convection can be observed right up to supercritical Rayleigh numbers equal to several tens times R_c (see, for example, Ref. 139). The curve II is the threshold above which cross-roll instability (see Sec. 6.3) results in steady-state bimodal convection: The flow consists of a superposition of the primary rolls and secondary rolls, which are perpendicular to and narrower than the primary rolls and which extend vertically to less than the total thickness of the layer. It is interesting that for very large P ($= 8.6 \cdot 10^3$) the artificially induced bimodal convection (including its limiting form—square cells) can be stable even for $R \approx (2\text{–}8) \cdot 10^5$ and, moreover, it is unstable at $R \approx 10^5$.[140]

The transition to bimodal flow is observed only at quite large values of P. For small values of P, however, a transition to non-steady-state convection occurs immediately (curve

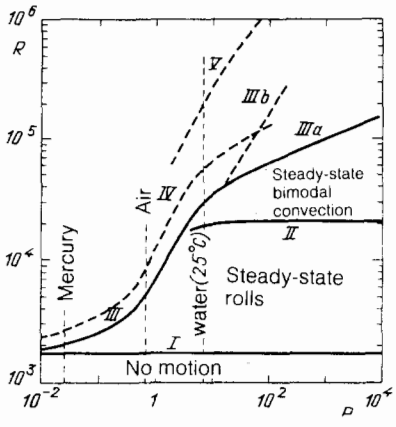

FIG. 11. Diagram of convection regimes (according to Refs. 72, 73, and 138 and other experimental works).

III). This transition is associated with oscillatory instability: Wave-like bends are observed to travel along the rolls. (It is now clear, however, that the last phrase pertains more to theoretical predictions, made for idealized models (see Sec. 6.3). In what follows it will become clear that for small values of P it is impossible to indicate universal threshold values of R for exchange of regimes in diverse experimental setups.) For some R bimodal convection also becomes of a non-steady-state nature. In addition, according to Krishnamurti, in the region $P \gtrsim 50$ this value of R is almost constant and is equal to $5.5 \cdot 10^4$, while subsequent experiments[17,140,141] give values which increase with P (see Fig. 11). The splitting of the curve III into two branches is connected with the fact that the appearance of oscillations depends strongly on the presence of nonuniformities in the pattern. Nonuniformities can engender oscillations in isolated sections for relatively small values of R (branch $IIIa$) and the very uniform bimodal convection pattern (created artificially in the experiment) demonstrates a transition to a non-steady-state at much larger values of R (Fig. $IIIb$).[17] For convection with $R \sim 10^5$–10^7 and moderate values of P there characteristically exist sharply non-steady-state fine-scale elements against a background of relatively non-steady-state large-scale cells (spoke-pattern convection;[17] see Sec. 6.3.1). The curve IV corresponds to the appearance of higher-order harmonics in the spectrum of oscillations (and, as in the case of other transitions also, to a change of the derivative of the heat flux with respect to R). For it the above remark concerning the characteristics of the exchange of regimes for small P is valid. Above the curve V there lies a region of completely turbulent convection.

The basic qualitative features of the diagram of regimes were reproduced by Vel'tishchev and Zhelnin by numerical modeling of convection.[142]

An important property of convection, which has been actively studied for more than several decades and which cannot be represented on diagrams of this type, is that the attainability of a steady state for small and moderate supercritical reduced Rayleigh numbers and small values of P depends on the aspect ratio and even on the shape of the reservoir.

Ahlers and Behringer[143,144] (see also the review of Ref. 145) performed experiments with normal (not superfluid) liquid helium-4 in circular reservoirs with different aspect ratios. They studied the behavior of the temperature difference ΔT as a function of time with a prescribed heat flux through the layer. For $\Gamma = 57$ and $P \approx 3$–4, nonperiodic oscillations with a very wide spectrum, whose maximum lies at zero frequency, were observed at a value of R practically equal to R_c (here R is the Rayleigh number corresponding to the average value of ΔT). At the same time, for $\Gamma \approx 2$–5 and $P \approx 0.8$ there is an interval of values of R, having a width of up to several multiples of R_c, in which steady-state convection is established; for higher values of R the steady-state convection either is immediately replaced by irregular oscillations (with higher values of Γ) or it is preceded by periodic and quasiperiodic oscillations (for smaller values of Γ). Analogous experiments, limited to small values of Γ, are described in Refs. 146 and 147. These investigations were also performed for mercury.[148]

Further experiments with liquid helium, performed in circular reservoirs with different Γ ($2.4 \leqslant \Gamma \leqslant 22$) with

$0.5 \lesssim P \lesssim 0.7$,[149] demonstrated steady states even for larger values of Γ, though, it is true, in the case of $\Gamma \gtrsim 15$, in a very narrow interval of R: $R_c \leqslant R \leqslant 1.09R_c$. In addition, the regime immediately following the steady-state regime, for $\Gamma \gtrsim 4$, is always periodic (though, generally speaking, far from harmonic oscillations). It is possible that this regime was not achieved in experiments with $\Gamma = 57$ because of the very long time required for it to become established.

It is noteworthy that experiments on liquid helium in rectangular reservoirs with horizontal dimensions of $13.4h \times 5.95h$ and $18.2h \times 8.12h$ show that a non-steady-state regime starts at appreciably higher supercritical Rayleigh numbers: $3.39R_c$ and $2.53R_c$, respectively.[150]

Low-frequency noise, observed in the behavior of $\Delta T(t)$ for small supercritical reduced Rayleigh numbers, began to be associated with a special type of turbulence. One of the names given to it was *turbulence at threshold* [*of the convective instability*]. Cryogenic experiments do not permit visualizing the flow. Further experiments performed with other liquids and with visualization of the flow showed that this turbulence looks like slow motion of rolls and defects of the roll structure. Since attempts are often made to describe such processes in terms of space-time changes of phase of the system of rolls, the phenomenon is often called (*weak, low-frequency*) *spatial* or *phase turbulence.*

The experimental work in Ref. 14 was undertaken precisely in order to study the behavior of the spatial structure of convection, both in the steady state and in the presence of phase turbulence. The working liquid consisted of water near 70 °C. For it $P = 2.5$, which falls in the range of values for liquid helium. A rectangular reservoir, having the horizontal dimensions $20h \times 30h$, was employed. It was found that for $R < 5R_c$ evolution to a steady state looks like gradual elimination of defects and transition to a comparatively simple picture of smoothly curved rolls, which near the sidewalls are oriented perpendicular to the walls (Fig. 8a). This process can continue for hundreds of hours, which is four orders of magnitude longer than τ_v and an order of magnitude longer than τ_h. Nonetheless this is not always sufficient for achieving a steady state. (We note that according to the estimate made in Ref. 53 the settling time for such processes is $\gtrsim \Gamma\tau_h$.) At $R \approx 5R_c$ much faster processes appear, settling does not occur, and a continuous recording of the flow velocity at a fixed point gives a pattern of wideband noise with a principal spectral maximum at zero frequency. Defects arise in the spatial pattern. These defects move, interact, and vanish. Necks are a characteristic feature of the rolls. For $R \gtrsim 9R_c$ the spectrum contains one other peak, which occurs near 0.05 Hz and is associated with oscillations of the rolls.

Different convection regimes were also studied in Ref. 151. The same working liquid and the same circular reservoir with $\Gamma = 14$ were employed. Automatic processing of the shadow images made it possible to investigate in detail the field $\mathbf{k}(\mathbf{x})$ of local wave vectors and the distribution function $f(k)$ of the wave numbers. Three types of regimes were found depending on the supercritical reduced Rayleigh number ε. If $\varepsilon < 0.2$, then aperiodic motion, connected with restructuring of defects, is observed at least for a time $50\tau_h$. *For* $0.2 < \varepsilon < 3.5$ *steady-state textures form after sufficient* time has passed. For $\varepsilon > 3.5$ the flow is once again of a non-steady-state nature from time to time the necks in the rolls engender new evolving defects. It is interesting that in the first and third cases, when settling does not occur, the distribution $f(k)$ exceeds the limits of the wave-number band, where, theoretically (see Sec. 6.3.1), uniform spatially periodic roll flows should be stable (Fig. 12). As regards regimes with very small values of ε, the authors do not exclude the possibility that a non-steady-state regime is determined by random external actions and imperfect experimental conditions. In a square reservoir, whose edge length is equal to the diameter of a circular reservoir, they observed settling over a time of $100\tau_h$. On the other hand, settling was not observed in an experiment, lasting for a time of the order of $200\tau_h$ (about one month), in a circular reservoir with $\varepsilon = 0.141$, $P = 5.7$, and $\Gamma = 15$.[152]

Experiments with argon at room temperature ($P = 0.7$) in a circular chamber with $\Gamma = 7.66$ (Refs. 131 and 153) also demonstrated that under conditions of non-steady-state convection topological changes occur in the roll structure, and in addition they revealed that the character of the exchange of regimes is very complicated. For $\varepsilon < 0.126$ steady-state patterns of slightly curved rolls with two focus singularities were observed (see Fig. 8b). For larger values of ε the flow is a non-steady-state one. Sometimes a neck forms in some rolls at the center. This neck engenders two dislocations, which separate and climb to the sidewalls, after which they glide to the foci and vanish. New rolls are generated at the foci, and the pattern is restored. For $0.126 < \varepsilon < 0.175$ the process is periodic, and in this interval five scenarios of the behavior of defects are observed depending on the value of ε. The general features follow the scheme described above. For $0.175 < \varepsilon < 0.346$ topologically diverse structures arise. Their behavior is chaotic—phase turbulence is observed.

In steady-state regimes the local wave numbers fill some interval of values (the maximum lies at the center of the vessel and the minimum lies near the outer wall) which expands as ε increases. It is interesting that the upper limit of this interval reaches the theoretical threshold of instability, found for a uniform system of rolls (see Sec. 6.3.1), precisely near the value of ε for which the steady-state regimes are succeeded by non-steady-state regimes—the results obtained in Refs. 131, 153, and 151 are similar to one another.

In the region $0.346 \lesssim \varepsilon \lesssim 1$ there are four additional transitions:[153] chaotic evolution with increasing ε is once again succeeded by a steady state flow, after which a periodic process is observed, which is again followed by a steady-state process and once again a chaotic process.

The settling time in these experiments reached $500\tau_h$.

In the experiments mentioned above,[150] when liquid helium filled a larger rectangular chamber, "fine structure" as a function of ε was also observed in the distribution of steady-state, periodic, and aperiodic regimes.

Experiments with air[154] showed that if the ratio of the horizontal dimensions of a rectangular chamber lies in the range from 0.5 to 1, then phase turbulence associated with gliding of dislocations is possible. This process arises for values of R which approximately correspond to the threshold of the skewed varicose instability (see Sec. 6.3.1), which plays an important role in the disordering of the pattern.

It is natural to suppose that the intricate and clearly nonvariational dynamics, observed in many cases for small and moderate values of P, is related to the presence of large-

scale flow (see Sec. 3.2.2). Manneville[155] attempted to model numerically the phase turbulence in a rectangular reservoir with horizontal dimensions of $15.9h \times 11.5h$, starting from Eqs. (3.21)–(3.23), which take into account the z-independent average drift (which corresponds to a layer with free horizontal boundaries). In his calculations the steady state was reached, but, if P was sufficiently small ($= 1.6$), a prolonged settling process, which can be interpreted as a process of transition to turbulence, was observed. The average flow creates local compression of the roll structure and necks appear; the necks engender dislocations, which in turn climb; and, the rolls become deformed. This sequence of events is reminiscent of the experimentally observed sequence and can be repeated many times. An important feature of the process is, in my opinion, that the average flow (whose structure depends on the overall geometry of the flow, in particular, on the shape and dimensions of the region of flow) is inconsistent with the local curvature of the rolls (and, therefore, with the phase diffusion velocity). The unbalanced nature of phase diffusion and transfer of the rolls by the average flow results in "dynamic breaking" (frustration)—topological changes—of the roll structure and, ultimately, it makes the dynamics nonrelaxational.

The results of numerical modeling of flows in a circular chamber[47] on the basis of the model (3.28) and (3.30)–(3.34) wuth $a = b = 0$ and $c = a$ correspond closely to the behavior of defects observed in the experiments of Refs. 131 and 153. The calculations revealed chaotic regimes for both circular and rectangular regions.

Pocheau[156] constructed an explicit analytical solution of the Cross–Newell equations (3.60)–(3.62) for the field of the phase and average flow in a circular region, using an expansion in the small parameter related to the curvature of the rolls. In the process, for $P = 0.7$ a steady-state pattern of curved rolls and instability of this pattern under supercritical conditions, when the highest local wave number lies outside the stability band for straight rolls, were reproduced. This occurs when the average flow, directed in the region of greatest curvature of the rolls (at the sidewalls) toward the foci, and from the foci toward the center of the reservoir (Fig. 8b), becomes sufficiently intense. In the process, in the central part the rolls become appreciably compressed.

It was later shown[157] both experimentally and theoretically (by solving the Cross–Newell equations) that flow stabilization is possible if the sidewalls of the chamber are permeable to the average flow. If the circular reservoir is surrounded by an annular region, where there exists a large-scale flow but there is no convection, then the average flow distributed over a larger area will no longer compress the rolls at the center of the reservoir as strongly. As a result, steady states become unattainable only for $\varepsilon = 1.2$ and phase turbulence is observed only for $\varepsilon = 1.5$. In the experiment convection in the outer annular region was suppressed by a thin horizontal annular plate, which divided the layer into two convectively stable sublayers.

We shall now summarize. For the cases of small and moderate values of P the character of convection cannot be determined by a universal method starting only from the numbers R and P. The corresponding part of the diagram in Fig. 11 illustrates only the roughest features of the exchange of regimes. The detailed description must be very specific—for a reservoir with given dimensions and shape.

The fact that the stability of convection depends on the overall geometry of the flow will also be clear from the discussion of the question of the wave numbers of convective rolls (Sec. 6.5). Threshold turbulence is associated with the motion of defects. The degree to which the flow can be rearranged and the possibility of achieving the optimal wave number depend on the presence of defects.

6. SELECTION OF WAVE NUMBERS OF CONVECTIVE ROLLS

Even if the formulation of the problem or the conditions of a proposed experiment make it possible to predict the relative planforms of convective cells, the question of the scale of the realized flow, which can be characterized by the width of a roll, the radius of a polygonal cell, etc., nonetheless remains open. In the literature this subject is referred to as *selection* of wave numbers (or wavelengths).

Here we shall discuss this problem for the simplest case—when rolls are the main form of the convective flow. Even in this variant the problem has by no means been solved, though in the last decade many papers have been devoted to it. Dissimilar and at first glance sometimes contradictory results have made the term "selection of wave numbers" itself less meaningful.

As a rule, spontaneously developing roll convection demonstrates some distribution $f(k)$ of the local wave numbers, which has a more or less wide peak for some value of k (Refs. 75, 151, and others), indicating the existence of a preferred optimal scale (see Fig. 12). The expression "selection of scales" is associated precisely with such a preferred scale.

As will become clear from the examples presented below, however, this scale preference can be manifested to a

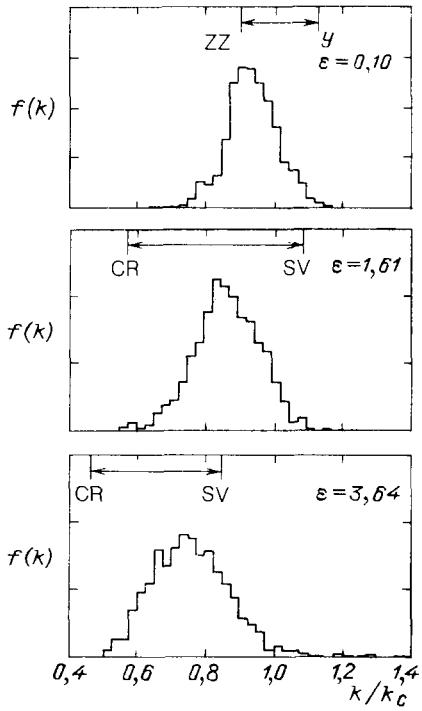

FIG. 12. Distribution functions of local wave numbers for different values of ε (experiment; $P = 2.5$ (Ref. 151)). The intervals of wave numbers in which uniform roll structures are stable according to the linear theory are designated and the types of instabilities arising at the boundaries of these intervals are indicated (see Sec. 6.3.1).

different degree. In particular, cases are possible when the function $f(k)$ is delta-function-like and there exists essentially only a single wave number. We shall call it the *final* (having in mind the final result of the temporal evolution) or *realized* wave number. Since the selection of this wave number appears to be completely unique, it is tempting to talk about selection precisely on the basis of data on such situations and to call them the "mechanisms of selection" and the realized wave number the "selected" wave number.

On the other hand, as we shall see, even for identical values of the parameters R and P of the regime, the single value of k that is realized depends on the history of the flow (and ultimately on the initial conditions), to say nothing of many other factors, which in the simplest cases reduce to boundary conditions. The discrepancy between the wave numbers which are achieved in different cases is often regarded as a basis for the assertion that not only does there not exist a universal principle of selection of wave numbers but there is also no universal principle for unique (for fixed R and P) selection of the spatial scale. There also arises the question of whether or not it is reasonable to term selection (or mechanism of selection) any act of realization of flow with a definite wave number, if the "separation" of this number is limited, possibly, to only the given case.

We shall adhere to a general viewpoint that makes it possible to represent the existing results in the form of a consistent integral picture of the phenomena.

We shall assume at the outset that there exists an *optimal* (*preferred*) wave number $k_p = k_p(R,P)$, which is an internal characteristic of roll convection in an infinite horizontal layer and to which definite dynamical *selective* factors tend to drive the flow. This tendency (which we shall term *selection*) can to a greater or lesser extent be suppressed by other (*antiselective*) factors, associated with the overall geometry of the flow, in particular, with the initial degree of ordering of the flow, the presence of sidewalls, etc. As a result the selection process stops at some particular stage of evolution from the initial state and the final (realized) wave number can to a greater or lesser degree differ from the preferred wave number. Artificially introduced ordering is capable of making the flow highly stable against the action of selective factors—as a result the difference between the realized and preferred wave numbers can be large. When convection develops from noisy initial disturbances there are usually no such powerful anti-selective factors, and the peak of the distribution $f(k)$ corresponds to k_p.

6.1. Wave numbers in experiments with random initial disturbances

We saw that for sufficiently large values of P stationary roll convection is observed right up to $R \approx 10R_c$. Roll flows which are not in a completely steady state can also be observed for larger supercritical Rayleigh numbers (for example, in Ref. 139 even with $P = 2.5$ the flow was primarily two-dimensional up to $40R_c$). In a quite wide range of values of the parameters flows with phase turbulence are quasi-steady state with respect to the characteristic turnover time of the liquid in the rolls. Defects destroy two-dimensionality only locally. The larger the value of R, the greater is the natural spread of the values of the local wave numbers, which is measured by the width of the peak of the distribution $f(k)$; see Fig. 12.

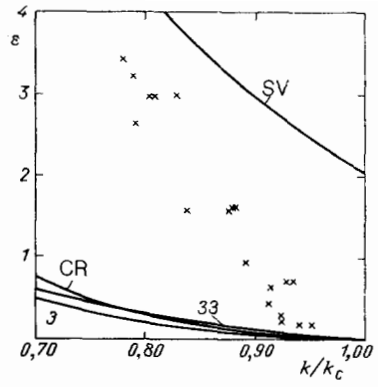

FIG. 13. The average values of the wave number of steady-state roll structures for different values of ε (experiment; $P = 2.5$ (Ref. 51)). The threshold curves for different types of instabilities are shown (see Sec. 6.3.1).

Numerous experiments have established that there is a general regularity in the behavior of the average wave number of roll convection. (Without distinguishing here between this average value of k and the position of the maximum of $f(k)$ close to it, we shall term both wave numbers the *observed preferred wave number* k_p.) This value of k_p decreases as R increases (Refs. 72, 74, 75, 139, 15, 131, 151, and others), and this is also true for experiments in which annular axisymmetric rolls have been observed (Refs. 158 and 137; see also the review of Ref. 159). An example of such behavior of k_p is presented in Fig. 13. Experiments performed with different liquids under similar conditions have shown that the degree to which k_p varies as a function of R decreases as P increases, and in addition for sufficiently large values of P the dependence $k_p(R)$ exhibits hysteresis.[72,74] In Ref. 139 ($P = 2.5$) it was noted that k_p was almost constant in the range $6 \lesssim \varepsilon \lesssim 40$ (for larger values of R the two-dimensionality was lost).

Attempts to describe theoretically the behavior of wave numbers of convection in an infinite layer have led, for a long time, to a result that contradicts experiment: k increased with R. This is also true for the value of k at which heat transfer through the layer is maximum (and which should be realized according to the so-called Malkus principle) and for the values of k which correspond to extrema of some other characteristics—see Sec. 6.2. The same effect has also been obtained in two-dimensional numerical modeling.[63] Relative agreement with experiment was achieved on the basis of a three-dimensional model. For this reason, the authors concluded that purely two-dimensional processes cannot lead to a preferred wave number. In their opinion, steady-state two-dimensional flow is formed after a three-dimensional transitional process, which affects the final wave number. It has also been stated that k_p decreases with increasing R because of secondary factors—the presence of side walls (in a bounded volume the condition of maximum heat transfer gives a qualitatively correct behavior of k;[160] the role of the side walls is further discussed in Sec. 6.5.1) or nonideal thermal conductivity of the plates bounding the layer at the top (according to Ref. 161, in this case k_c decreases; however, in experiments with plates having very good conductivity k_p nonetheless decreased with increasing R (Ref. 158)).

The question of the factors which affect the wave

numbers of two-dimensional rolls will be discussed in detail in subsequent sections. For the time being we note only that k decreasing with increasing R can be obtained in a purely two-dimensional numerical experiment, modeling the conditions of an infinite layer with boundaries having ideal thermal conductivity, if the condition of spatial periodicity of the flow, which is usually used in the practice of numerical modeling, is removed (Refs. 162 and 60; see Sec. 6.5.2).

6.2. Searches for universal selection criteria

The idea that there exist preferred forms and scales of convection is itself recent. Searches for a general principle that would make it possible to distinguish such forms and scales have apparently been conducted starting with the work of Malkus.[163] It makes sense to summarize everything done to implement this idea, which recently has been often undeservedly criticized.

Malkus' principle was suggested on an intuitive basis. According to this principle, flows for which convective heat transfer is maximum should be realized. Later, an attempt was made[21] to relate this principle to the stability of the steady-state solutions of the equations.

To this day, however, many cases have been found when predictions made based on Malkus' principle disagree with experiment or accurate theoretical investigations of stability. First of all, for two-dimensional roll flows the wave number for which heat transfer is maximum increases with increasing R (see, for example, Refs. 164 and 23) while the opposite behavior is observed experimentally. (It is true that Davis[160] indicated that in a bounded reservoir, in contrast to an infinite layer, the wave number selected according to Malkus' principle should still decrease with increasing R; in Sec. 6.5 we shall see that the decrease of k with increasing R is not necessarily caused by the effect of the side walls.) The fact that the realizability of a flow is not directly related with the condition of maximum heat transfer is indicated by numerical experiments.[165] Further, among the cells of several possible planforms, the greatest heat transfer is obtained with square cells,[21,103] which are unstable under the conditions of the standard problem. The motion of dislocations in the experiment demonstrates changes of the wave number such that the heat transfer decreases.[166] Finally, for a nonlinear temperature dependence $\rho(T)$ there exists an interval of Rayleigh numbers where the rolls are unstable, but they transfer more heat than stable hexagons.[22,94]

Busse[98] formulated an extremal principle, according to which for small supercritical reduced Rayleigh numbers, among the stationary solutions with different planforms and fixed $k = k_c$ the stable ones are those that minimize some functional. Under certain conditions this principle is equivalent to Malkus' principle, as well as the requirement that the kinetic energy of convection be maximum. (In this approach, however, there is no preferred wave number.)

The maximum kinetic energy as also the maximum heat transfer, generally speaking, also do not agree with the observed values of k_p.[23] This is also true for the maximum decrease of the potential energy in the layer of convecting liquid as compared with the static value,[23] the maximum of the rate of growth of disturbances which is found from the linear theory,[10] and for a number of other characteristics of convection.[167] The author of the last paper concluded that the k-dependence of the determinant of the second variation of the mean-square time derivative of the average temperature gives a much better result. The determinant is found by solving the so-called mean-field equations. We note that the method used to solve the problem has some flaws.

The thermodynamic approach based on the application of the principle of maximum production of entropy[168] makes it possible to investigate stability in concrete situations. The stability criterion obtained as a result does not, by itself, single out a unique preferred wave number within some interval of stability (see Sec. 6.3). But the stability functional ϕ has in this interval a single maximum, which shifts in the direction of smaller values of k as R increases.[167] This shift, however, is much more rapid than that of the experimentally observed value of k_p. In Ref. 167 the requirement

$$\frac{\partial^2}{\partial R^2}[\phi]_{k=k_p(R)} = 0 \tag{6.1}$$

is proposed on the basis of general considerations as a selection criterion. Together with an equation for ϕ it determines the dependence $k_p(R)$, if the initial conditions—the values of k_p and dk_p/dR at $R = R_c$—are given. It is understandable that $k_p(R_c) = k_c$. The author uses experimental data to determine $k_c'(R_c)$. The obtained dependences agree satisfactorily with the specific experiments for which the corresponding values of $k_p'(R_c)$ were found.

The possibility of finding a preferred wave number with the help of Lyapunov's functional for the equations describing convection will be discussed in Sec. 6.4 and subsequent sections.

6.3. Stability of two-dimensional roll flows

As noted in the introduction, a widely used approach to solving the selection problem involves the investigation of the stability of steady-state flows. The greatest attention has been focused on the question of the stability of two-dimensional spatially periodic systems of rolls.

6.3.1. Theoretical results. This direction was initiated by Schlüter, Lortz, and Busse[25] (see Sec. 3.2.1 and Sec. 4.1), whose work was based on the expansion of the undisturbed flow in terms of small amplitudes (supercritical reduced Rayleigh numbers) and investigation of the stability of the obtained solutions against small perturbations in the linear approximation. The authors showed that all three-dimensional flows are unstable (the problem is formulated in the standard manner). For two-dimensional flows, however, it was found that irrespective of the value of P and the boundary conditions on the horizontal surfaces, rolls with $k < k_c$ are unstable and rolls are stable in some interval $k_c < k < k_1(\varepsilon)$. The subsequently published stability diagrams (see Fig. 15 below) agree with the result for $k < k_c$ only for $P = \infty$. The reason for this disagreement became understandable after the role of the vertical component of vorticity for finite values of P was elucidated in Refs. 33 and 34 (see below). In Ref. 25 this component was eliminated by assumptions, introduced there, about the structure of the flow, and in later papers it was taken into account.

A detailed study of the linear stability of roll flows was performed for a wide range of supercritical Rayleigh numbers in a series of papers by Busse *et al.*[164,169-176] A steady-state unperturbed spatially periodic flow was calcu-

lated from the complete nonlinear equations Eqs. (2.9)–(2.11) by Galerkin's method and had the form

$$v_z = \sum_{\lambda,\nu} A_{\lambda\nu}\varphi_\nu(z)\cos\lambda kx \qquad (6.2)$$

with corresponding expressions for v_x and θ). Here $\varphi_\nu(z)$ ($\nu = 1, 2, \ldots$) form a complete system of orthonormalized functions, satisfying the boundary conditions for v_z. Small three-dimensional perturbations of the form

$$v_z' = \left[\sum_{\lambda,\nu} (B_{\lambda\nu}\cos\lambda kx + C_{\lambda\nu}\sin\lambda kx)\varphi_\nu(z)\right] e^{iax+iby+\sigma t} \qquad (6.3)$$

(with corresponding expressions for v_x', v_y', and θ') were superposed on this two-dimensional flow. Linearization of the starting equations with respect to the perturbations leads to an eigenvalue problem for the growth rate σ. A detailed description of the procedure of investigation is given in Ref. 170.

Some characteristic modes of instability of rolls have already been mentioned above. Some idea of these modes will be needed in what follows also. It makes sense to enumerate them with an indication of the range of Prandtl numbers where they can appear (we are now talking about a layer with rigid boundaries; a more detailed summary of the properties of these modes is given in Ref. 173).

1. *Zig-zag* (ZZ): $a = 0$, $\lambda + \nu$ is even, $B_{\lambda\nu} = 0$, and $P \gtrsim 2$. Results in sinusoidal curving of the rolls.

2) *Cross-roll* (CR): $a = 0$, $\lambda + \nu$ is odd, $C_{\lambda\nu} = 0$, and $P \gtrsim 1.1$. Forms a system of rolls perpendicular to the initial rolls.

3) *Skewed varicose* (SV): a/b is finite, $\lambda + \nu$ is even, $P \lesssim 30$. Roll deformation caused by it is shown schematically in Fig. 14.

4) *Knot* (K): a supplementary branch of the CR instability with maximum σ for relatively small b; $1.1 \lesssim P \lesssim 10$.

5) *Eckhaus* (E): $b = 0$, $\lambda + \nu$ is even, $C_{\lambda\nu} = 0$, and $P \lesssim 1$. This is the only mode that does not destroy the two-dimensionality of the flow; it leads to compression and extension, alternating along the x-axis, of groups of rolls.

6) (*Even*) *oscillatory* (EO): $a = 0$, $\lambda + \nu$ is even, $B_{\lambda\nu} = 0$, $P \lesssim 2.5$. It corresponds to sinusoidal wavy disturbances, traveling along the rolls.

7) (*Oscillatory*) *two-blob instability* (BO2): $a = 0$, $\lambda + \nu$ is odd, $C_{\lambda\nu} = 0$, and $2 \lesssim P \lesssim 8$. The transverse section of a roll contains two spots of high temperature, which are located in diametrically opposite parts of the cross section, and two spots with low temperature, which are located analogously.

8) (*Oscillatory*) *one-blob instability* (BE1): $a = 0$, $\lambda + \nu$ is even, $C_{\lambda\nu} = 0$, $7 \lesssim P \lesssim 12$. The transverse cross section of a roll contains one spot of high temperature and one spot of low temperature. They are located at diametrically opposite parts of the cross section.

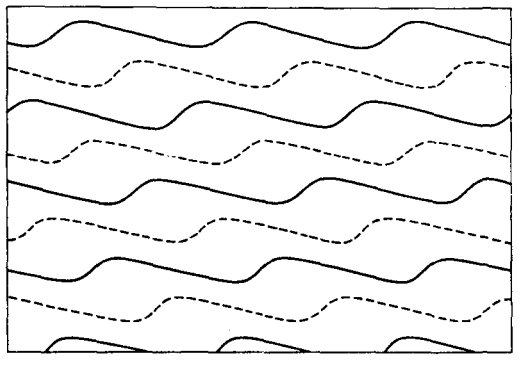

FIG. 14. Deformation of rolls as a result of the skewed varicose instability (solid and dashed lines correspond to the boundaries of the rolls along which upward and downward motions occur).

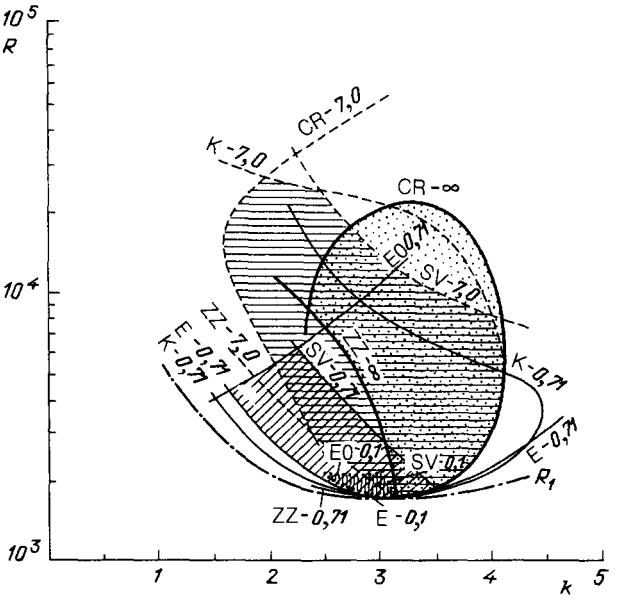

FIG. 15. Regions of stability of infinite spatially periodic systems of rolls (in the k, R plane)—"Busse balloons"—for $P = \infty$ (filled with dots),[164] $P = 7$ (horizontal hatching),[172] $P = 0.71$ (oblique hatching),[171] and $P = 0.1$ (vertical hatching).[171] The boundaries of the regions are formed by segments of the threshold curves of different types of instabilities, which are designated by letters with an indication of the values of P.

Some results of the investigation of stability for the case of rigid boundaries are summarized in Fig. 15. Curves are constructed in the (k, R) plane for each chosen value of the Prandtl number. Each curve corresponds to the threshold of instability ($\mathrm{Re}\,\sigma = 0$) of a definite mode; the region of stable flows (where all $\mathrm{Re}\,\sigma < 0$), sometimes called the "*Busse balloon*," delimited by such curves is shown.

The main forms of instability for large values of P and the important instabilities for moderate values of P are the ZZ instability, which results in an effective decrease of the characteristic scale of the flow and thus raises the long-wavelength boundary of the region of stability, and the CR instability, which can both increase and decrease the characteristic scale.[164,172] According to the experimental data of Ref. 111 (see below), for moderate values of R the development of the CR instability results in replacement of the starting rolls by new rolls, oriented in the transverse direction. If, however, $R \gtrsim 10R_c$, the cross rolls develop primarily in the temperature boundary layers, created by the main flow, and correspondingly have smaller horizontal dimensions. Ultimately a three-dimensional flow—a superposition of the main and cross rolls (*bimodal convection*)—is established. The stability of stationary bimodal convection against infinitesimal perturbations was investigated in Ref. 103.

For intermediate values of P the knot instability can come into play.[171,172] In Ref. 177 the behavior of established

rolls with secondary flow engendered by the knot mode and the characteristic oscillatory instabilities of such a superposition were investigated in detail by means of a numerical experiment. If R is sufficiently large, then the development of the knot mode results in the formation of concentrated ascending and descending flows. After this mode is completely developed it forms a characteristic oscillating *spoke pattern*, in which large polygonal cells are observed (the formation of such a structure, observed experimentally in Ref. 17, was initially termed a *collective* instability).

For moderate values of P the existence of a small segment of the boundary of the region of stability (in its top part, near the intersection of the neutral curves for CR and knot modes), which is governed by the action of the BE1 (for large values of P) or (and) BO2 (for small values of P) instability, is also characteristic.[173] In particular, both modes are present in the case $P = 7$; they are not designated in Fig. 15 only because the corresponding diagram was not given in the original paper.

For moderate and small values of P the short-wavelength boundary of the region of stability is determined by the SV mode,[171,172] which is observed experimentally[172] and increases the characteristic scale of the flow.

Finally, for $P \lesssim 1$ one boundary of the region of stability is the neutral curve of the EO mode.[170] We note that the analytical investigation of the stability of rolls in the limit $P \to 0$ for a layer with free boundaries[169] gives the threshold value of the Rayleigh number for the EO instability $R_i = R_c(1 + 0.31P^2)$ (it was calculated for $k = k_c$). This means that the interval of values of R where rolls are stable vanishes in this limit—in contrast to the case of rigid boundaries, when it is finite. The reason for this difference lies in the fact that the EO mode is related to the appearance of a vertical component of vorticity, absent in the unperturbed roll flow. In the case of free boundaries in the limit $b \to 0$ an undamped perturbation with uniform vertical vorticity along the layer (rotation of the layer as a whole) can exist. The critical Rayleigh number for the oscillations corresponds to such a perturbation. For rigid boundaries vertical vorticity which is constant as a function of z is forbidden by the boundary conditions, and the critical value of R is reached for a finite value of b. The oscillatory instability is further studied in Ref. 174.

The results, obtained up to 1980, of investigations of the stability of two-dimensional rolls are also reviewed by Busse.[22,23]

For the case of free boundaries the intervals of values of the parameters where stable roll flow is possible are appreciably narrower. An investigation, performed analytically for small supercritical reduced Rayleigh numbers[175] and numerically for a wide range of supercritical Rayleigh numbers,[176] showed that for $P < 1$ the band of wave numbers of stable rolls is very narrow (for example, for $P = 0.71$ it does not exceed 0.0065 for any value of R). The long-wavelength boundary of the region of stability is determined in this case by the *oscillatory skewed varicose* instability (which is not observed in the case of rigid boundaries) while the short-wavelength boundary is determined by the standard (monotonic) SV instability. For $P < P_c = 0.543$ stable flow is completely impossible. We note (this will be important in what follows) that the interval of wave numbers where the rolls are stable against the Eckhaus instability, is nonetheless quite wide for any value of P. For $P = \infty$ the boundaries of the Busse balloon, which are determined in this case by the CR instability, were found in Ref. 211.

Two important conclusions can be drawn from the results described here.

First, if the case just mentioned (free boundaries, $P < P_c$) is excluded, then in some range of Rayleigh numbers there always exists an interval of wave numbers which corresponds to stable two-dimensional roll flows. For not too small values of P, this interval is quite wide (and in addition, the shrinking of this interval as P decreases is always related to the three-dimensional instabilities). Thus all flows with wave numbers lying in the interval of stability appear to be equally realizable. From what follows it will become clear that this is not so.

Second, if the flow is artificially restructured, this restructuring is most often governed by three-dimensional processes, since k for the flow lies outside the region of stability. This engendered the widespread belief (supported by numerical experiments[63]) that two-dimensional deformations are an ineffective means for changing k (in particular, the experimentally observed decrease of k with increasing R). We shall demonstrate below the error of this point of view.

We now note some results of investigations of the stability of rolls by other methods.

In Ref. 44 such an investigation was undertaken on the basis of model equations in order to choose a model that would best reproduce the properties of stability that were found by solving the Boussinesq equations. The authors studied two classes of models—a generalization of the SH equation (3.28) and the Herzberg–Sivashinskiĭ equation Eq. (3.29). Since the vertical component of the vorticity plays a fundamental role in the development of some instabilities (in particular, the SV instability), the authors included in the equation a term which is governed by it and describes drift, and in a number of cases they also introduced a special filtering procedure which suppresses the short-wavelength instabilities (for example, the CR instability). The model (3.29) with $d = 3$, to which drift and filtering were added, gave the best qualitative agreement with a rigorous theory.

In the language of the theory of phase dynamics[29,41,49,52,53,210] (see Sec. 3.2.2) the Eckhaus instability corresponds to the case $D_{\parallel} < 0$, and the ZZ instability in the absence of average drift corresponds to the case $D_{\perp} < 0$. The average drift, of course, affects the stability of the rolls.[33,34,175,176,210] The ZZ instability is strongly suppressed by it for small values of P (in this case it occurs if $D_{\perp}^{\text{eff}} < 0$). Conversely, drift has a destabilizing effect on the SV mode. Analysis based on Eqs. (3.63) and (3.64) showed[210] that in the case when the SV instability develops the average drift creates positive feedback: Caused by deformation of the rolls, the drift intensifies the deformation, creates necks, and ultimately can cause reconnection of the lines of constant phase and creation of pairs of dislocations. For this reason, the SV instability plays an important role in the appearance of phase turbulence (see Sec. 5). The boundaries of the Busse balloon and the threshold boundaries for the Eckhaus, ZZ, and SV instabilities are reproduced very well with the help of the indicated equations,[210] and in addition explicit expressions can be obtained for the growth rates and the

form of the most dangerous disturbances.

It is by no means always possible to describe in terms of the theory of stability the results of numerical modeling of flows, though in the main theory and the model calculations do agree with one another. We note only that in two-dimensional calculations with conditions of periodicity on the side boundaries of the region of computation with both free[61] and rigid[62] horizontal boundaries the band of wave numbers of stable flows is very wide (as in the case of the Eckhaus mode) and almost fills the entire region of linear instability of the immobile liquid. If, however, the side walls are rigid, then the stability band shrinks[57] (see Sec. 6.5.1). Of the three-dimensional numerical experiments performed in order to investigate the stability of rolls, we call attention to Ref. 212 ($P = \infty$, free boundaries, small aspect ratios of the region of computation), where the results are compared with the results of Refs. 176 and 211.

6.3.2. Experimental results. The same question was studied experimentally—by observing the artifically created rolls with fixed width—in parallel with theoretical investigations of the stability of two-dimensional roll flows.

It is interesting that in the first investigation of this series, performed by Chen and Whitehead[16] almost simultaneously with Busse's calculations,[164] there were noted features of the phenomena which for a long time were not mentioned in discussions: The fact that these features could not be directly associated with the theoretical predictions of instabilities apparently played a role. Chen and Whitehead, using the technique of controlled initial conditions (see Sec. 3.1), investigated the behavior of rolls with different initial widths. Circular reservoirs with $\Gamma = 10$–16, liquids with $P \sim 10^3$ (silicone oils), and the method of shadow visualization were employed. It was found that in the range of Rayleigh numbers studied $R_c \leqslant R \leqslant 2.5R_c$ the region where the rolls are stable against three-dimensional perturbations is clearly delimited in the (k, R) plane, and in addition on the short-wavelength side it is bounded by the threshold of the CR instability while on the long-wavelength side it is bounded by the ZZ instability. In this sense the results agree with Ref. 164. But within this region the rolls by no means always remained unchanged. Their width, generally speaking, changed, approaching some optimal value close to 1.1h. The process of such restructuring is primarily two-dimensional and is possible because of the fact that at the side walls, near focus singularities (see Fig. 8b), new rolls appear or old rolls vanish. The characteristic restructuring time is equal to tens of hours, which is 100 times longer than τ_v and is comparable to τ_h. The interval of roll widths (or wave numbers) where significant changes of the rolls are not observed, is much narrower than the interval where the rolls are not subjected to three-dimensional restructurings. Conversely, in the regions of three-dimensional instability changes of the roll width are accompanied by development of three-dimensional modes.

Thus two-dimensional restructuring of the rolls in this case appears to be a more general property than the three-dimensional instability and a more universal mechanism for achieving an optimal scale.

Later experiments with controlled initial conditions were performed in order to check directly the theoretical results obtained by Busse and Clever (see Sec. 6.2.1). Rectangular reservoirs were employed. Experiments with silicone oil with $P \sim 10^2$ and $R_c < R < 6 \cdot 10^4 \approx 35R_c$ are described in Ref. 111. In Ref. 141 experiments with silicone oil with $P = 16$ and water at 70 °C ($P = 2.74$) as well as a wide range of Rayleigh numbers covering the region of existence of stable flows are described. Depending on R and the artificially set value of k, either stable regimes (without explicit restructuring of the roll structure) or development of instabilities of some particular type, which in most cases can be identified with the theoretically predicted instabilities, were observed. In Ref. 111 the distribution of points, representing the experimental regimes, in the (k, R) plane showed satisfactory agreement with the computed diagram of stability[164] for $P = \infty$ (see Fig. 15). In Ref. 141 the regions of stability were appreciably deformed and displaced toward smaller values of k compared with those calculated for the corresponding values of P (especially for $P = 2.74$). The authors attribute this discrepancy to the finite thermal conductivity of the top and bottom surfaces of the layer. The characteristic dimensions of the region of stability, even in the latter case, nonetheless do not differ very much from the theoretical dimensions, so that the theory can be considered to be qualitatively confirmed.

An important circumstance should, however, be kept in mind.[9)] In contrast to Ref. 16, in Refs. 111 and 141 the conclusion that the rolls are stable was based on the passage of a comparatively short period of time from the moment at which free evolution of the flow started (i.e., the "forcing" lamp was switched off). This time interval exceeded τ_v by only a factor of two or, at the most, by several fold, and it was vanishingly small compared with t_h. This means that in those cases when the authors thought the regime to be stable, generally speaking, the possibility of slow quasi-two-dimensional restructuring of the rolls along their width with a tendency toward some optimal final wave number—a process observed in Ref. 16—was not excluded. We shall see below (see Sec. 6.5.4) that under some conditions this process can proceed rapidly.

Busse and Clever[172] also performed an experiment with controlled initial conditions in order to check the conditions under which the knot and SV instabilities, predicted in the same work, arise. In Refs. 17, 141, and 140 the stability of an artificially generated bimodal flow was also investigated. Further experimental investigations of the stability of rolls in a reservoir with a moderate value of Γ are described in Ref. 179; these experiments agree qualitatively with the theory.

In Ref. 178 the reaction of a roll structure to artificially induced Eckhaus and ZZ disturbances was studied experimentally and compared with the theory of phase dynamics.

6.4. Lyapunov functional and selection

The fact that the dynamics of a convecting liquid, generally speaking, is nonvariational is already evident from the possibility of low-frequency turbulence, associated with the motion of defects (Sec. 5). In particular, the monotonic decrease of the potential is incompatible with the possible cyclical nature of the restructuring of the pattern.

There are situations when potential dynamics can nonetheless be expected. For a chamber of finite dimensions this happens, for example, if $P \to \infty$ or if the flow is two-dimensional, and the conditions of applicability of the NWS equations are satisfied.

For spatially periodic flows in an infinite region the integral representing the Lyapunov functional diverges. Sometimes a potential calculated for an integer number of spatial periods and rescaled to unit length in the direction x of the wave vector (and, of course, per unit length in the direction y) is studied. We shall call it the *specific potential*. In an infinite region, to an arbitrarily small change of the wave vector there corresponds a finite variation of the periodic function (flow velocity). For this reason it is obvious that there cannot be an analogy between variation of the functional of a finite system associated with a small variation of the velocity field and variation of the specific potential of an infinite system associated with a small change of the wave number.

According to the calculation of Pomeau and Manneville[41] for the SH model (3.26), the specific potential has a minimum at the edge of the band of wave numbers which corresponds to stable spatially periodic roll flows. The wave number k_F at which this minimum is reached and which the authors have termed optimal decreases slightly as ε increases, and in addition its departure from the critical wave number k_c is proportional to ε^2.

It is clear from what has been said above that the presence of such a minimum does not mean that the roll structure must necessarily be restructured from a nonoptimal to an optimal wave number, and it does not contradict the fact that flows with arbitrary wave numbers falling within the band mentioned are stable.

A completely analogous situation arises when determining the "optimal" value of the angle α made by the rolls and the normal to the side wall (Ref. 133; see Sec. 4.2). Although the minimum of the potential falls at $\alpha = \alpha_{opt} \neq 0$, a linear stability analysis of the rolls shows that they are stable at $\alpha = 0$. Since a semi-infinite region was studied, for an arbitrarily small change in α the variation of the function describing the roll structure at a quite large distance from the wall is found to be finite.

With accuracy up to corrections of highest order in ε the optimal value of k_F in the SH model corresponds to the value of k_{ZZ} at which the transverse diffusion coefficient D of the phase vanishes (see Sec. 3.2.2) or, in other words, it corresponds to the threshold of ZZ instability.[41]

In a number of cases (though not in all cases), which will be studied in the subsequent sections, the wave numbers realized in potential systems coincide with k_F.

In Ref. 46 an attempt was made to use the Lyapunov functional to investigate the comparative stability of different (not too complicated) textures.

The behavior of the Lyapunov functional, calculated from the formula (3.39) of the SH model for experimentally observed evolving textures, was studied.[151,180] More precisely, the calculations were performed using the formulas found in Ref. 46 for contributions made by different components of the texture to the functional. Although in this experiment the Prandtl number was comparatively small ($P = 2.5$), in the range of supercritical reduced Rayleigh numbers $0 < \varepsilon < 3$ the functional either decreased monotonically or exhibited small brief increases, associated primarily with the appearance of new defects, against the background of an overall decreasing trend. For larger values of ε the nonrelaxational character of the behavior became more obvious. For very small values of ε the temporal changes of the functional are very slow and they are difficult to study. In the established regimes the values of the Lyapunov functional have a spread of about 25%; this reflects the fact that the possible stationary textures in the case of sufficiently large aspect ratios are not unique.

6.5. Selection in a system of straight parallel rolls

We saw in Sec. 6.3 that spatially periodic two-dimensional roll flow in an infinite layer can be stable if its wave number k lies in a more or less wide interval of values. Within this interval each k can be realized with equal success, if only the corresponding spatial periodicity is prescribed initially. (Formally, following a widespread tendency (see the beginning of Sec. 6), any of these values of k can be said to be "selected," though the absurdity of this word usage is obvious.)

The situation is approximately the same in the experiments of Refs. 111 and 141 with controlled initial conditions, though there rolls with prescribed k filled only a region of finite size—the experimental chamber. At least this is the case if the possibility of restructuring over times longer than the time of the experiment (of the type which were observed in Ref. 16) is neglected.

Restructuring of rolls over their width without topological changes and significant breakdown of two-dimensionality, when they tend toward a preferred wave number, is termed *elastic relaxation*. Such relaxation has not been observed under the conditions mentioned. We shall now discuss some other situations.

6.5.1. Effect of the side walls. Cross *et al.*[27] investigated, with the help of the amplitude equations, the stationary regimes of two-dimensional convection with small supercritical Rayleigh number $\varepsilon = (R - R_c)/18\pi^2$ in a bounded chamber with free horizontal surfaces and large aspect ratio (here R_c is the value of R for an infinite layer). The purpose of the work was to analyze the possibility of flows with different wave numbers k (different $q = k - k_c$). In an infinite layer such flows can be represented by the "phase-winding" solutions

$$A(X) = (1 - Q^2)^{1/2} e^{iQX}, \quad |Q| \leq 1, \tag{6.4}$$

of the NWS equation (3.5) for the stationary case. According to Eq. (3.4) this means that $-\varepsilon^{1/2} \leqslant q \leqslant \varepsilon^{1/2}$. If, however, the region is bounded in the x direction (even if it is semi-infinite), then the phase-winding solutions are impossible under the condition $A = 0$ on the sidewalls (see Eq. (3.18)), but they are possible in the presence of boundary forcing, which gives near the wall a nonzero value of A of the order of the small quantity λ. It was found that far from the wall, where $A = O(1)$, the band of admissible values of q has a width of the order of $\lambda\varepsilon^{1/2}$.

In a more realistic case (side walls of finite thickness and thermal conductivity and thermally insulated on the outside) it follows from the amplitude equation (derived by the authors in the next order in $\varepsilon^{1/2}$ compared with the NWS equation) that $\lambda = \varepsilon^{1/2}$. This gives for a semi-infinite region (with one wall) a band of wave numbers $q_- \leqslant q \leqslant q_+$ of width $O(\varepsilon)$ and for the finite region $-L \leqslant x \leqslant L$ a discrete set of values of q, which lie in the same band (the number of these values is of the order of $\varepsilon L/\pi$). The quantities q_- and q_+ are proportional to ε, and in addition $q_- < 0$ always and

the sign of q_+ depends on P and the thermal conductivity of the walls.

Thus the contribution of the side walls will decrease the width of the band of wave numbers of possible steady-state solutions from $O(\varepsilon^{1/2})$ to $O(\varepsilon)$. Instabilities can make this band even narrower.

Analogous results were obtained in Ref. 43 from the model equations—the potential SH equation Eq. (3.26) and the nonpotential Eq. (3.27)—with the conditions $w = \partial_x w = 0$ on the boundaries of the region.

We note that the band $q_- \leqslant q \leqslant q_+$ does not depend on the size $2L$ of the system. In Ref. 27 the impossibility of passing in the limit directly to the case of an infinite layer is explained by the fact that as $L \to \infty$ the propagation time of the effect of the walls along the layer increases without bound. In such a case, however, it is not understandable why the admissible values of q in the case of a semi-infinite region are limited to the same band. We shall now present some arguments showing that in the presence of at least one wall steady-state solutions with q outside the indicated band are impossible.

The effect of shrinking of the band is interpreted by some authors in the sense that the side walls themselves create a selective factor. We shall interpret this effect differently on the basis of the idea of a preferred scale of convection.

We now compare the situations in an infinite layer and in a bounded region. In the first case the system of rolls cannot be smoothly restructured by means of expansion or compression, since a small change of the width of all rolls by the same amount cannot be obtained as a small perturbation of the flow. Such a system should become unstable only if the nonoptimality of the wave number, which will result in destruction of the pattern formed—appearance of new or disappearance of existing rolls, is sufficiently large. In the second case, adjustment to the optimal wave number does not necessarily require significant changes in the velocity field: As the authors themselves point out,[27] the boundary layers at the side walls can give rise to smooth adjustment. Even if it is impossible to approach the optimum without changing the number of rolls, the process of appearance or disappearance of rolls also occurs more easily in the boundary layers, where the flow velocity is low (this is proved by numerical integration of the equation of phase diffusion[51]). It is understandable that if the scale is not optimal, the rolls must become restructured even in the presence of one wall and the regime will be a non-steady-state one.

Thus spatial periodicity (high degree of ordering) of the flow emerges as a powerful antiselective factor. The side walls do not have a selective effect, but they give rise to a weaker antiselective effect than in the first case.

The role of boundary layers is evident, in particular, from the results of Ref. 181, where the formulation of the problem is analogous to that studied in Ref. 27, but (with more general boundary conditions) the values of the boundary-forcing parameter λ are not small and can reach $O(1)$ (in the notation of Ref. 181, $O(\varepsilon^{1/2})$). In the case of strong forcing the band of wave numbers is wider and its boundaries can reach the boundaries of the Eckhaus instability.

In connection with the proposed point of view, it is interesting that the numerical modeling of the evolution of disturbances in a long region, into which 50–80 rolls fit, performed on the basis of Eqs. (3.26) and (3.27) on long time intervals,[42] demonstrates in all cases that a single wave number is generated. For the potential model of Eq. (3.26) it minimizes the specific potential and, in addition, it coincides with the threshold of the zig-zag instability, determined by the condition $D_\perp = 0$ (see Sec. 3.2.2). For the nonpotential model of Eq. (3.27) the realized wave number falls in the region of instability with respect to zig-zag disturbances, where $D_\perp < 0$.

As mentioned above, the evolution of convective flows involves different characteristic times. Daniels,[50] extending the work performed in Ref. 27, investigated the stability of phase-winding solutions for a chamber $-L \leqslant x \leqslant L$ and he identified among a discrete set of admissible solutions with $q_- \leqslant q \leqslant q_+$ the stable and unstable solutions. He found that the final value of k is established by means of elastic relaxation over a time $O(\varepsilon^{-2})$ that is much longer than the time $O(\varepsilon^{-1})$ over which the amplitude is established. For sufficiently small values of P, k decreases appreciably with ε, i.e., qualitative agreement with experiment is achieved in spite of the two-dimensionality of the model.

The results of Refs. 27 and 50 were supplemented by numerical calculations of the evolution of rolls on the basis of the NWS equation.[182] As in Ref. 50, it was found that the stable regimes are not unique. This, by the way, does not eliminate the possibility of obtaining (as in Ref. 42 based on the model equations) a unique wave number with the help of an amplitude equation of a higher order approximation than the NWS equation.

In experiments with controlled initial conditions,[111,141,172] described in Sec. 6.2.2, one would expect good agreement with Ref. 27, which is not the case in reality. Aside from the fact that the duration of the experiment may not have been long enough, it was not excluded that the discrepancy is associated with the strong forcing at the wall: It is possible that in these experiments the thermal boundary conditions gave stable ascending flows at the side walls, which fix the position of the extreme rolls.

In Ref. 183, however, an experiment was performed in which the narrowing of the band of wave numbers associated with the presence of the side walls was observed. It is true that in this case the thermocapillary effect played a significant role. The experiments were performed in an annular channel, imitating an infinite layer; a radial barrier could be inserted into the channel in order to obtain the case of a finite reservoir.

This effect was also observed in two-dimensional numerical experiments based on the complete equations.[57] At the initial stage a different number of rolls was produced. Restructuring usually began near the side walls in the manner of the development of the Eckhaus instability. Over a time $< 12\tau_v$ the convection wave number was found to fall within the band of stability predicted in Ref. 173. The further evolution occurred over times several times longer and narrowed the band of values of k by a factor of three.

Thus in laboratory and numerical experiments only fast processes can be identified with the instabilities found theoretically for an infinite layer.

6.5.2. The case of great freedom of elastic relaxation. A pronounced tendency for a preferred wave number to be singled out can be observed in the absence of side walls.

Getling[162,184,60] performed, on the basis of the complete system of Boussinesq equations, numerical calculations of

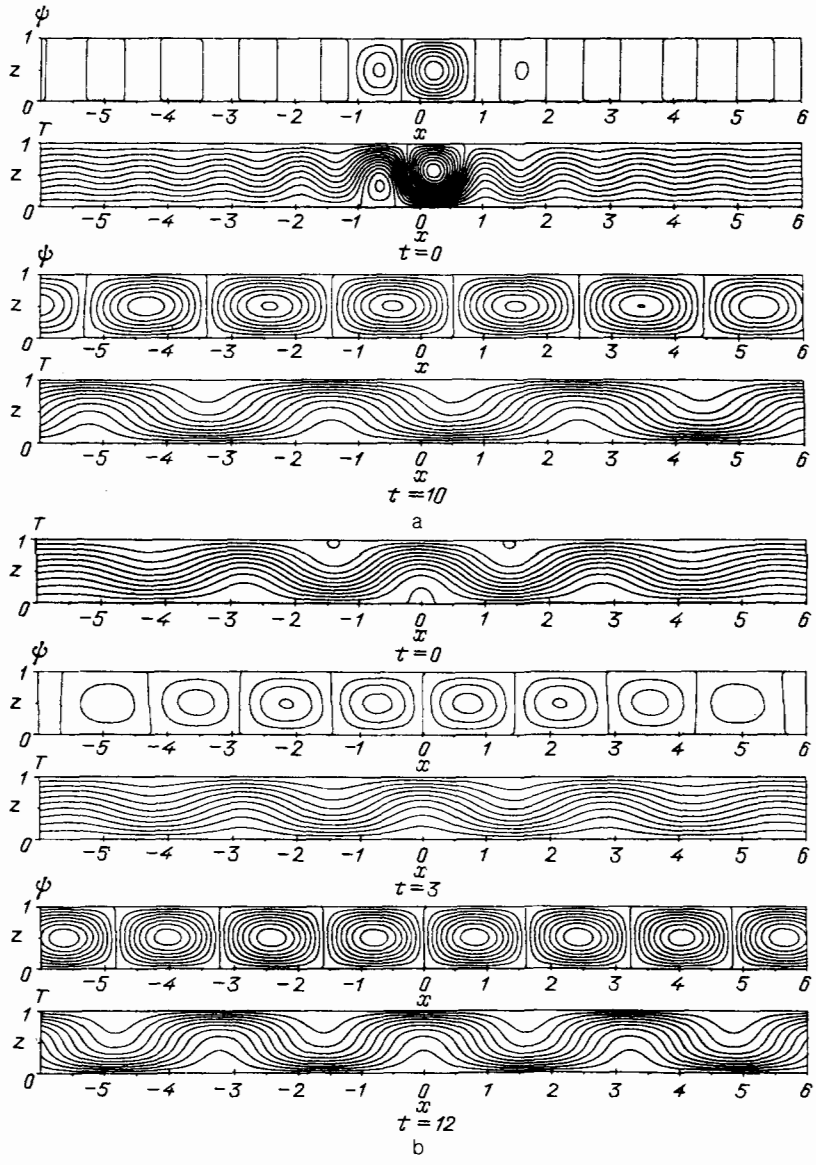

FIG. 16. The development of convection in an infinite layer from initial disturbances of the first (a) and second (b) type[60] (the side boundaries of the figures *are not* the boundaries of the region of computation). The streamlines (isolines of the stream function ψ) and the isotherms are shown. The time is expressed in units of τ_v (in contrast to the original paper of Ref. 60). $P = 0.1$, $R = 1.5R_c$.

the evolution of a two-dimensional roll flow in an infinite layer with free horizontal boundaries. The condition of spatial periodicity was not imposed, and the flow velocity and temperature were represented by Fourier integrals over x.

Two types of initial conditions were studied. The first type is illustrated at the top of Fig. 16a. In the process of evolution the convection encompasses an increasingly wider region, and in addition the rolls that are formed rapidly enter a steady-state regime (bottom of Fig. 16a), characterized by a definite value of the wave number—the *computed preferred wave number* k_p, determined by R and P. An initial condition of the second type corresponds to a temperature perturbation which at the very beginning of the evolution process generates a set of rolls of given width, which occupies some region of finite (along x) width (Fig. 16b). It is noteworthy that the wave number of these rolls, regardless of its value initially, tends to approach the wave number k_p which was obtained in the calculations with the initial conditions of the first type. Figure 16b illustrates this restructuring of the rolls. An important feature of this process is that the more rolls are produced at the initial stage the slower is the subsequent restructuring. This confirms the antiselective role of the ordered spatially periodic structures.

We also note that for sufficiently small values of P the computed value of k_p decreases with R. This corresponds qualitatively with the experimentally observed behavior (see Sec. 6.1). As in Ref. 50, the restructuring of the flow with respect to the wave number is possible within the framework of the purely two-dimensional geometry.

Thus if convection develops from localized disturbances, a preferred wave number can be "generated" very effectively by means of elastic relaxation of the rolls. Antiselective factors are even weaker than in the case when side walls are present.

6.5.3. Motion of grain boundaries. A finite set of x-rolls, which are bordered on both sides, forming two grain boundaries, by systems of transverse y-rolls (Fig. 17), clearly demonstrates elastic relaxation. If the x-rolls are not optimal with respect to the wave number, then the length of the y-rolls easily changes and the y-rolls do not present any significant resistance to restructuring of the x-rolls. Although such a flow pattern is, on the whole, three-dimensional, restructuring of the x-rolls is a substantially two-dimensional process and the systems of y-rolls play the role of mobile side

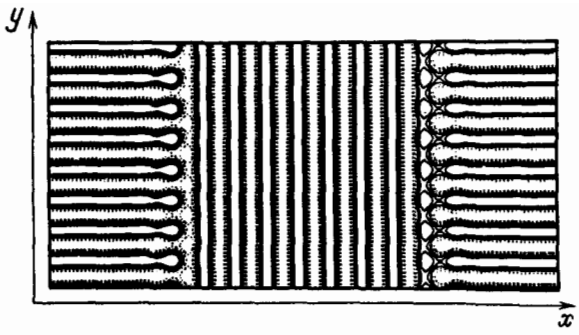

FIG. 17. Roll pattern with two grain boundaries (according to Ref. 69).

walls, adjusting to the optimal width of the system of x-rolls.

This situation was investigated in Ref. 69 by solving the model equations—the SH potential equation Eq. (3.26) and the nonpotential equation Eq. (3.29) with $d = 3$. The equations were integrated over time numerically; the condition of periodicity in x and y was imposed on the boundaries of the region of computation (Fig. 17). In addition, the apparatus of amplitude equations, which were derived from the starting model equations, was employed in order to find the steady states. These states are the same, with good accuracy, as the states to which the temporal evolution leads.

For both model equations it was found that to each ε there correspond unique values of the wave numbers of the x and y rolls $k_x = k_x^s$ and $k_y = k_y^s$, for which a steady state is possible. If initially $k_x > k_x^s$, then the x-rolls expand (and, correspondingly, the y-rolls become shorter), as a result of which a steady state is reached. For the initial wave number $k_y > k_y^s$ new x-rolls appear, i.e., the area occupied by the nonoptimal y-rolls decreases. If initially $k_x > k_x^s$ and $k_y > k_y^s$, a combination of both processes occurs. In all cases the final value $k_x = k_x^s$ is independent of both k_y and the initial value of k_x. For the potential model of Eq. (3.26) $k_x^s = k_y^s = k_F = k_{ZZ}$, where k_F is the value of the wave number that minimizes the specific Lyapunov functional and k_{ZZ} is the threshold wave number for the zig-zag instability. For the nonpotential model Eq. (3.29) ($d = 3$) $k_x^s \neq k_y^s$, and in addition both values are different from k_{ZZ}, found in Ref. 44.

Pocheau and Croquette[18,185] investigated experimentally the behavior of a system of rolls confined between two grain boundaries. The experiment was performed with silicone oil, for which $P = 70$, under controlled initial conditions. The initially induced x-rolls did not completely fill the reservoir, and near the side walls, parallel to these rolls, due to the cross-roll instability, there arose systems of short y-rolls, separated from the main system by grain boundaries (see Sec. 4.2). The flow was allowed to settle down for each value of R, which was changed in small steps. Study of the sequence of equilibrium stages gave a clear unique (hysteresis-free) dependence of the wave number of the main collection of rolls on R (see the crosses in Fig. 18). As one can see from the diagram, this wave number in some part of the range of values of R exhibits a systematic, though small, deviation from the value of k_{ZZ}. At the same time, it is practically identical to the value obtained in the same paper by studying the conditions of equilibrium of dislocations (see Sec. 6.7).

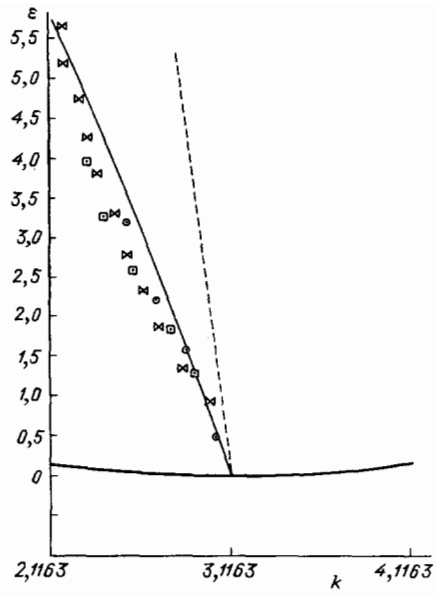

FIG. 18. The wave numbers in the experiments with grain boundaries and dislocations ($P = 70$).[18,185] The solid curve at the bottom is the neutral curve of stability of the motionless state. The crosses are the average values of the wave numbers of the central system of x-rolls in an experiment with grain boundaries; the circles are the wave numbers of structures with a steady-state dislocation; the squares are the wave numbers obtained by extrapolating the climb velocity (see Sec. 6.7); the solid straight line is the dependence $k_{ZZ}(\varepsilon)$ according to Refs. 48 and 49; and, the dashed line is the dependence $k_a(\varepsilon)$ according to Ref. 49 (see Sec. 6.6).

In the presence of only a single grain boundary, separating two semi-infinite systems of rolls with wave vectors oriented arbitrarily relative to this boundary, it was found,[186] at the level of analysis of the amplitude equations, that a steady state is possible for certain values of the wave numbers, which depend on the indicated angles and differ from k_c by an amount $O(\varepsilon)$ (if only these angles are not too close to one another). In this case the restructuring of the rolls of each system, generally speaking, is impeded as strongly as in a homogeneous infinite system. The possibility that the boundaries reach an equilibrium state is determined by the interaction of the rolls in the boundary region. (We note that the applicability of the apparatus of amplitude equations to the investigation of real grain boundaries is limited. For defects of this type sharp spatial transitions are characteristic; this contradicts the idea that the amplitude changes slowly.)

6.5.4. Elastic relaxation at a contact with disordered flow. The behavior of rolls, initially induced artificially in the central part of the reservoir, was also investigated in an experiment performed by Berdnikov, Getling, and Markov with ethyl alcohol ($P = 16$). Thin wires, along which an electric current was passed for several seconds at the beginning of each experiment, were stretched horizontally through the chamber. As soon as the induced rolls became clearly visible, the current was switched off.

In contrast to the experiments of Pocheau and Croquette,[18,185] these rolls occupied a comparatively small part of the reservoir, so that there was enough time for a much less ordered flow to form on both sides of the rolls even before the current was switched off. Since along the perimeter of the chamber there was a gap where the top surface of the liquid layer was free (see Fig. 3), the orientation of the spon-

taneously developing rolls could be arbitrary. By means of their effect on the induced rolls, they gradually destroyed the latter. For this reason, the induced rolls never settled down: only a single roll pattern can become established under these conditions at the later stage of evolution—generally speaking, after the induced rolls are demolished. It made sense to follow the change in their wave number only while they were still, on the whole, ordered.

Over this comparatively short time (a maximum of several minutes; compare with $\tau_v \approx 3$ min) very significant restructuring—elastic relaxation—of the induced rolls nonetheless occurred. Their average wave number, irrespective of the initial value, approached the value of k_p observed in experiments with random initial disturbances[75] (on the same apparatus and with the same working liquid). This process is basically two-dimensional. Since it occurs over times that are short compared with τ_h and the time τ_h/P of transmission of the disturbance along the layer due to viscosity, it is not significantly affected by the side walls (moreover, the effect of the side walls can be additionally suppressed by the above-mentioned buffer role of the gap where the surface of the liquid near the walls is free).

Thus the preferred wave number is manifested as an internal characteristic of convection for fixed values of R and P. (We note that it does not correspond to the threshold of stability with respect to zig-zag disturbances.)

It is interesting that in spite of the presence of disordered flows on both sides of induced (ordered) rolls, these rolls evolve approximately in the manner described in Refs. 184 and 60, where the liquid outside the zone of the initial disturbances was assumed to be completely still. Just as in Refs. 184, 60, 18, and 185, here three-dimensional processes are not necessary in order to achieve the optimal wave number of the rolls, which, as usual, decreases as the Rayleigh number increases.

Remarks for Secs. 6.1, 6.3 and 6.5.2–6.5.4. Comparing the above results shows that the wave numbers falling in the stability band of two-dimensional spatially periodic roll flows are by no means equivalent from the standpoint of realizability. First, experiments with uncontrolled initial conditions (Sec. 6.1) show that the average wave numbers of roll flows, according to their own laws, fall within the region of stability and fill its bounded part (Fig. 13; see also Fig. 9 in Ref. 72, Fig. 1 in Ref. 171, where the experimental data of Ref. 74 are employed, and Fig. 5 in Ref. 75). Second, the experiments described in Refs. 18, 185, and 11 (see Secs. 6.5.3 and 6.5.4) and the calculations of the evolution of flows in the absence of side walls with initial localization of the rolls in a bounded strip of the layer[184,60] (Sec. 6.5.2) show that the local wave number can change as a result of elastic relaxation, even if it initially lies in the region of stability. On the other hand, it follows from calculations based on model equations[47] that for some values of Γ steady states in which the wave numbers of the central rolls lie beyond the threshold of the skewed varicose instability are possible in some circular region. Hence there follows the important conclusion that the stability criteria found for an infinite layer cannot be applied locally to a fragment of the convective structure, starting from the local wave number of the rolls in this fragment. Whether or not the local value of k will change depends on the general geometry of the flow.

6.5.5. Spatial ramp of the parameters. Imagine that the thickness h of the layer and (or) the temperature difference ΔT between the surfaces of the layer varies along the x coordinate, so that the local Rayleigh number is also some function $R(x)$. In such cases it is said that there exists a (*spatial*) *ramp* of Rayleigh numbers and the parameters determining it. We shall be interested in ramps such that for some $x = x_c$ the function $R(x)$ passes through a critical value R_c. Assume for definiteness that everywhere $dR/dx \leqslant 0$, and in addition the conditions are supercritical in the region $x < x_c$ and subcritical in the region $x > x_c$. We shall also assume that the supercritical region to the left of some point $x_1 < x_c$ is uniform: $h = \text{const}$, $\Delta T = \text{const}$.

For a sufficiently small slope of the ramp $|dR/dx|$ it can be expected that the amplitude of the two-dimensional flow of the x-roll type, if such a flow exists in the supercritical region, will gradually decrease with the transition into the subcritical region. Such a ramp must operate as a "soft side wall"—in particular, it should give little resistance to elastic relaxation of the rolls. (Generally speaking, in a system with a ramp large-scale circulation of the liquid, encompassing the region with characteristic dimensions of the region of the ramp, can occur. In the particlar case when the vertical coordinates and the temperatures of the surfaces of the layer vary in unison, so that the undisturbed isotherms in the layer are everywhere horizontal, circulation does not occur.)

There arises the question of whether or not a regime with a preferred wave number will be established in a uniform supercritical region in the presence of a slow ramp? At first glance, the results of existing theoretical investigations by no means answer this question positively. We shall see that they nonetheless do not contradict the concept of an internal optimal scale.

Kramer *et al.*[187] (see also Ref. 188) studied a quite general problem, starting from the system of reaction-diffusion equations

$$\partial_t u_i = \sum_{j=1}^{n} D_{ij} \Delta u_j + f_i(u_1, \ldots, u_n), \quad i = 1, 2, \ldots, n, \qquad (6.5)$$

where the parameters α_l, on which D_{ij} and f_i depend, vary slowly as a function of x. As a result the system goes over in space from supercritical conditions (when the perturbations of the initial steady state can lead, as they develop, to the formation of periodic structures) to subcritical conditions (when the perturbations are damped). The authors introduced the slow coordinate X and the slow time T with the help of a small parameter, which characterizes the rate of change of α_l, and they performed an expansion of the equations analogous to the expansion employed in the derivation of the Cross–Newell equations (see Sec. 3.2.2). The obtained equation of phase diffusion (containing, generally speaking, drift of the entire structure as a whole owing to the nonuniformity of the conditions) gives in the steady-state case a first-order differential equation, determining the distribution of the local wave number $k(X)$, if it is given at some point. In order to choose such a unique dependence, the authors employed a device which has become standard for problems of this type, namely, they set $k = k_c$ at the critical point. (The justification of this assumption is a key element and will be discussed below.) It was found that all ramps which can be transformed into one another by a transformation of the spatial variable give the same dependence of k on

α_l. In potential systems all ramps lead to the same value of k in the uniform supercritical region, namely, to the value k_F that minimizes the specific potential of the uniform system.

The relation between the wave numbers of structures in systems in which there is a slow ramp of one parameter ε and the wave numbers that minimize the functional was demonstrated in Ref. 189. A differential equation relating $\varepsilon(x)$ and the local wave number $k(x)$ of the "adiabatic" solution of the starting equation was derived for a starting steady-state equation of the most general form. The explicit dependence of k on ε, found for a family of equations of the amplitude type, in the case of potential systems is identical to the dependence of k_F on ε. (An example of a system of reaction-diffusion equations, which was discussed in Ref. 187, was studied next; according to Refs. 188 and 190 the amplitude equation derived for it is incorrect.) An important point is that the transition from a smooth ramp to a steep ramp should, according to the considerations presented in Ref. 189, be manifested as a transition from a single wave number to a finite band of wave numbers.

Convection of a liquid with $P = \infty$ in the case when the top surface of the layer is an isothermal horizontal plane and the position and temperature of the bottom boundary depend on the slow coordinate X was studied in Ref. 191. The expansion of the system of Boussinesq equations, following the example of Ref. 187, gave an equation for $k(X)$, which for small supercritical values of ε and free boundaries greatly simplifies and in some cases can be solved analytically. Generally speaking, the system of rolls undergoes drift. When there is no drift (which does not necessarily mean that there is no large-scale flow), the local value of k can be expressed directly in terms of the local value of ε. The curves in the (k, ε) plane, representing such dependences and passing through the critical point (k_c, 0), can, depending on the structure of the ramp, have slopes of very different characteristic magnitude and of different sign also. An impression is created that the preferred wave number is in no way manifested.

The formulation of the problem in Ref. 192 differs from the preceding formulation in that the top and bottom boundaries of the layer are assumed to be rigid and the Prandtl number is finite. The layer is uniform over its thickness, and a ramp is present only in the distribution of ΔT. The equation for the phase of the rolls in the steady-state case (when a large-scale flow nonetheless exists, but convective transfer of phase is compensated by diffusion) relates the local value of k with the local value of R. The dependence $k(R)$ is found by numerical integration in a wide range of Rayleigh numbers for different values of P. The quantity P strongly affects the form of the integral curve, drawn through the point (k_c, R_c). In particular, for $P < 0.7$ the value of k increases as R increases; this is radically different from the behavior of the observed value of k_p in a uniform layer.

Few experimental investigations of convection in the presence of a ramp have been performed, and in addition in some of the existing investigations, for example, Ref. 193, the ramp is so steep that it cannot play the role of a "soft" side boundary. A slow ramp was reproduced in the experimental paper of Ref. 13, but in this paper the behavior of the wave number as a function of the coordinate x through the dependence $R(x)$ was not investigated.

We shall now discuss the physical interpretation of the basic results. The theoretical conclusions regarding the value of the realized wave number in a uniform supercritical region are drawn based on the key assumption that locally $k = k_c$ at locations where $R = R_c$. From the logical standpoint, this step is doubtful. The values of R_c and k_c were found for spatially periodic flows in a uniform layer, where the interaction of the convective rolls does not generate an average flow of energy along the layer. In systems with a ramp this is, generally speaking, not the case: The more energetic rolls, located in a region with high supercritical Rayleigh numbers, transfer their energy to less energetic rolls, existing under less supercritical conditions. Moreover, this energy flow cannot become zero at the point where the regime is critical, and energy will unavoidably flow into the subcritical region. This is shown by the fact that there exist solutions which describe systems of rolls extending into this region. This effect is analogous to the well-known phenomenon of penetrating convection (see, for example, Ref. 194): If the undisturbed temperature profile $T(z)$ is not linear and in some range of heights z convective instability occurs ($dT/dz > 0$), then convective motions penetrate into this stable region. In the case when a ramp is present, penetration into the region of stability should also occur but along the horizontal rather than the vertical direction. Since there exists a family of solutions, reflecting the effect of the horizontal penetration, it is at least in principle possible to generate artificially different distributions $k(R)$. Similarly to the fact that the criterion of stability of existing rolls cannot be applied locally (see the remark at the end of Sec. 6.5.4), there are also no grounds for applying locally the criterion of stability of a motionless liquid and moreover, for assuming that the local conditions also dictate the local value of the wave number.

Therefore the disagreement in the realized wave numbers between systems with different ramps or between the case of a ramp and other situations cannot serve as an argument against the existence of a preferred wave number. Moreover, it is interesting that in potential systems there is no such disagreement (the case studied in the next section is an exception).

6.5.6. Motion of the convection front. The situation[162,60] when a localized two-dimensional disturbance is created in a layer of motionless liquid located in an unstable (supercritical) state was studied in Sec. 6.5.2. The roll structure extends over an increasingly wider part of the layer. This process looks like motion of two convection fronts, moving in opposite directions away from the region of the initial disturbance.

The motion of the front separating the formed periodic structure from the undisturbed region is regarded as one of the "mechanisms of selection," since under certain conditions the wave number of the structure arising behind the front can be predicted.[195,196]

We shall now consider the simplest variant of the NWS equation

$$\partial_T A = \partial_X^2 A + A - A^3 \tag{6.6}$$

with a real function A—a particular case of a nonlinear diffusion equation. We are interested in solutions of this equation that have the form $A(X,T) = A_c(X - cT)$, where c is the constant velocity of the front, and which therefore satisfy the equation

$$A_c'' = -cA_c' - A_c + A_c^3, \tag{6.7}$$

and in addition

$$\lim_{X\to-\infty} A_c(X) = 1, \quad \lim_{X\to+\infty} A_c(X) = 0. \tag{6.8}$$

Obviously, Eq. (6.7) can be interpreted as the equation of motion of a material point of unit mass in the potential field $\Phi(A_c) = A_c^2/2 - A_c^4/4$, if A_c is the coordinate, X is the time, and c is the coefficient of friction. According to Eq. (6.8), the particle leaves with zero velocity the point of the maximum of the potential ($A_c = 1$) and moves toward the final state—to the point of minimum of the potential ($A_c = 0$). It is understandable that solutions of this problem exist for any $c > 0$. The larger is the value of c the more slowly does the particle move, i.e., the wider is the front.

There exists a class of initial conditions of the starting problem that leads to selection of a definite velocity of the front. This was shown in Ref. 197 in connection with problems in population genetics: All initial states of the system described by the functions $A(X, 0)$, which are confined to the strip $0 \leqslant A \leqslant 1$, where A does not vanish everywhere and decreases with X at least just as rapidly as e^{-X}, generate fronts moving (in the limit $T \to \infty$) with the velocity $c = 2$. This velocity is the minimum velocity for which $A(X, T)$ remains nonnegative everywhere (in the language of the analogy mentioned above $c = 2$ is the lowest value of the coefficient of friction for which a particle, having rolled into the potential well, does not pass through the point of the minimum of the potential with finite velocity).

The velocity $c = 2$ is distinguished in a different respect also—the solution A_2 exhibits marginal stability, understood in the following special sense. We employ a reference system moving with the front velocity c. If a weak localized disturbance, distorting the form of the function A_c, such that A_c does not increase or decrease at some *fixed* point of the moving reference system, is possible, we shall say that A_c exhibits *marginal stability*, even though the introduced disturbance generated a wave of increasing amplitude, moving away from the observation point.

If Eq. (6.6) for real A is interpreted to be an amplitude equation (for example, NWS or the amplitude equation of the same form for the SH model), then the roll structure behind the front has, in any case, the wave number k_c. With the help of a complex amplitude function whose phase depends on X it is possible to describe a structure with $k \neq k_c$. The amplitude equation for complex A has a class of solutions with a traveling front and a "winding" phase. In Ref. 196 there are presented arguments according to which the localized initial disturbance must nonetheless generate a regime with a traveling front, an amplitude function with almost constant phase (i.e., with $k = k_c$) and correspondingly front velocity $c = 2$.

The authors also applied the condition, but now as a hypothesis, that the "natural" front velocity must correspond to marginal stability to the case for which such a correspondence has not been proved, namely, to the description of the propagation of a spatially periodic structure on the basis of the SH equations. The values obtained in this manner $c = c^*$ and $k = k^*$ differ from the values found from the amplitude equation $c = 2$, $k = k_c$ by $O(\varepsilon^\alpha)$ corrections, where $\alpha > 0$, and in addition k increases with ε.

Further, this process was modeled numerically on the basis of the SH equation with a localized initial disturbance.[195,196] The values of c and k were found to agree well with the values that follow from the hypothesis of marginal stability.

The quantity k^* differs appreciably from the value k_F of the wave number minimizing the specific Lyapunov functional for the SH model.

The motion of a convective front in a layer with rigid boundaries was modeled, by solving numerically the two-dimensional Boussinesq equations, in Ref. 198 for $P = 1$. The process was initiated by briefly heating the side wall. The range of supercritical reduced Rayleigh numbers $0.01 \lesssim \varepsilon \lesssim 0.2$ was investigated. The obtained values of the velocity were found to be close to the values predicted in Refs. 195 and 196. The wave numbers of the structure behind the front agree well with the wave number $k_{max} = k_c(1 + 0.245\varepsilon)$, for which according to the linear theory the disturbances of the steady state grow at the maximum rate.[10]

In Ref. 199 the propagation of a front was investigated on the basis of the amplitude equation in the case when the starting (unstable) state is not undisturbed, and corresponds to a periodic structure with some wave vector lying outside the stability band. A new stable structure with a different wave number forms behind the front. Numerical modeling with initial conditions corresponding to an abrupt transition from a stable state to an unstable state at some point $x = x_0$ showed that the front velocity agrees with the hypothesis of marginal stability. On the level of our discussion, it is interesting that the final wave number generated behind the front depends on the starting wave number in front of the front. Moreover, some final values of k cannot be reached for any initial value of k.

In all cases studied above the front velocity c, rescaled to the standard physical time and length scales, which do not depend on the supercritical reduced Rayleigh number ε, is equal to

$$V = c\frac{\xi_0}{\tau_0}\varepsilon^{1/2}. \tag{6.9}$$

Therefore the front traverses a fixed distance in a time $O(\varepsilon^{-1/2})$. According to Eq. (2.22), convection develops from small disturbances over a time $O(\varepsilon^{-1})$. This shows that the motion of a convection front can be produced in a motionless unstable liquid only with very small supercritical reduced Rayleigh numbers. Otherwise convective structures will develop spontaneously before the front has advanced appreciably.

An experiment with water at 30.2 °C ($P = 5.373$) in the range $4\cdot10^{-4} < \varepsilon < 2.5\cdot10^{-1}$ is described in Ref. 200. A chamber whose length is equal to 27.3h and whose width is approximately four times shorter was employed. At the beginning of each experiment the layer of liquid was transferred, by increasing the heating from below, from a subcritical into a supercritical state and at the same time one of the short side walls was heated also. A front began to move away from this wall and left behind it a roll structure. The velocity of the front in the interval of values ε studied corresponds, with high accuracy, to Eq. (6.9) with $c = 2$. The wave number of the structure behind the front increases with ε.

Proceeding now to a discussion, we call attention to the

fact that on the basis of the hypothesis of marginal stability and the numerical experiment (except for Refs. 162 and 60) as well as on the basis of a full-scale experiment the wave number of the structure behind the front increases as the supercritical Rayleigh number increases. The discrepancy between this wave number and the values realized in other "mechanisms" as well as the minimum specific potential (in the SH model) is presented as an illustration of the fact that there is no universal selection criterion.

It is even possible to strengthen the thesis that the wave numbers "selected" in different situations are different. The motion of the front is apparently in itself capable of giving structures with different wave numbers. Even if the assertion that the selection of regimes with velocity $c = 2$ is of a universal character, it pertains only to the limit $t \to \infty$. Until settling is achieved the velocity of the front can vary over wide limits: The more slowly the initial disturbance decreases along x, the more rapidly, obviously, will the front move initially. Generally speaking, the wave numbers will also be different.

On the other hand, however, in the results presented here the elastic relaxation effect—wave number restructuring, noted in Ref. 60, of the roll structures formed behind the front—is completely absent in the results presented here. One would think that for small ε this process is unnoticeable, since the settling time of the position of the roll boundaries in a chamber of finite length is $O(\varepsilon^{-2})$.[50] But this is true for a reservoir that is already filled with rolls. If, however, the collection of rolls is confined between fronts behind which the liquid is almost motionless, then the velocity of the process depends strongly on the width of the collection and can be much higher.[60] Further, the faster the front moves, the faster the state of the system approaches the conditions of "close packing" of rolls in the reservoir and the more rapidly the elastic relaxation slows down. According to recent calculations performed by Getling[213] using the NWS equation, high velocities should "conserve" the wave number, even if the wave number is not optimal. It is interesting that the degree of supercriticality affects the rate of relaxation primarily through the velocity of the front, and the lower the supercritical Rayleigh number, the more rapidly the restructuring occurs.

If the motion of the front is described by the NWS amplitude equation, then the wave number of the structure formed, as we have seen, is equal to k_c. The wave number k_F that minimizes the specific potential and is manifested in the variational dynamics as the preferred wave number k_p is also equal to k_c for the NWS equation. In this case the realized wave number corresponds to the optimum wave number.

In the numerical experiments of Ref. 198 based on the complete Boussinesq equations and the full-scale experiment of Ref. 200 the relaxation of the rolls could have remained unnoticed owing to the short length of the region of flow and, correspondingly, the short observation time. In the numerical experiments of Refs. 195 and 196 based on the SH equation the distribution of the local wave numbers k along x has a minimum at the point of initiation of the process $x = 0$, where k is much closer to k_F than $k = k^*$ for rolls formed later ($k^* > k_F$). This could be a reflection of the elastic relaxation, with which k decreases, approaching $k_p = k_F$. (It is true that the authors assert that near $x = 0$, on the contrary, k increases. This is possible at a later stage when there are many rolls with $k = k^*$: They also tend to expand and in the process compress the rolls near $x = 0$.)

All this means that the existing results of investigations of the motion of fronts are in no way inconsistent with the possibility of the existence of a preferred wave number.

6.6. Wave numbers of axisymmetric flows

In the last two subsections of Sec. 6 we discuss the properties of two important classes of flows with qualitatively different geometry.

Pomeau and Manneville[201] studied a steady-state axisymmetric system of annular rolls in an infinite layer at large distances r from the symmetry axis. The general procedure of expanding the equations in powers of $1/r$ leads, to first order in this parameter, to a system of equations the condition of solvability of which determines a unique wave number k_a of the rolls. The authors concluded that this wave number is always equal to the threshold value k_{ZZ} for the zig-zag instability and ensures that the condition $D_\perp = 0$ is satisfied. It was later found that this criterion is applicable only under certain conditions.

Manneville and Piquemal[49] introduced an important refinement into this question. As shown in Sec. 3.2.2, these authors obtained[48,49] the effective value of $D_\perp$ for a layer with rigid boundaries, taking into account the large-scale drift flow, which has a vertical profile of the Poiseuille type and tends to eliminate the zig-zag deformation of the rolls. Such a flow is impossible in a system of concentric annular rolls, since it must be directed radially toward the symmetry axis and result in accumulation of matter at the center. For this reason, in an axisymmetric system the radial flow acquires, owing to pressure redistribution, a different vertical profile—with two nodes and zero total flux. If this flow is taken into account, then for large values of r and sufficiently small supercritical Rayleigh numbers the wave number k_a will be determined by the relation[49]

$$\frac{k_a - k_c}{k_c} = -\frac{N'(P)}{R_2(P)}\frac{R - R_c}{R_c}, \tag{6.10}$$

where $N'(P) = 0.166 + 1.426P^{-1} - 1.220P^{-2}$, and $R_2(P)$ has the same form as in Eq. (3.43). Comparing Eqs. (6.10) and (3.43) shows that k_a corresponds to the condition $D_\perp^{\text{eff}} = 0$ only in the limit $P \to \infty$, when $D_\perp^{\text{eff}} = D_\perp$, and if P is finite, then for $k = k_a$ $D_\perp^{\text{eff}} > 0$.

As Cross and Newell, analyzing the modified CN equation (3.60), write[53] regarding this fact, taking the average drift into account has no effect on the wave number of the axisymmetric pattern (since drift does not arise in this geometry), but changes the value of k_{ZZ}, stabilizing the transverse disturbances of the rolls.

In the case of free boundaries, as we have already said, diffusion relaxation of the zig-zag disturbances does not arise. The zig-zag mode is replaced by an oscillatory mode, and the coefficient $D_\perp^{\text{eff}}$ does not exist for finite values of P. The following expression was obtained in Ref. 49, using the same technique, for the wave number of axisymmetric convection:

$$\frac{k_a - k_c}{k_c} = \frac{1}{16P}\left(\frac{5}{P} - 3\right)\frac{R - R_c}{R_c}. \tag{6.11}$$

In the further development of this work the assumption

that the supercritical reduced Rayleigh number is small is not made.[202] A combined numerical method is used to find the value of k_a for which the equation obtained in first order in $1/r$ has a solution: The horizontal dependence of the variables describing the flow is represented by a Galerkin approximation and the vertical dependence is represented by a finite-difference approximation. The authors investigated a wide range of values of R and P.

The results of Refs. 49 and 202 have a characteristic feature that contrasts sharply with the experimentally known behavior of the wave number: according to Eq. (6.10), for $P < 0.784$ as well as for, roughly speaking, $P < 0.7$ according to calculations of Ref. 202 the wave number k_a increases as R increases (as was noted in Sec. 6.1, in experiments with uncontrolled initial conditions the fact that k decreases with increasing R is more evident precisely for small values of P).

Here it should be noted that, generally speaking, it can hardly be expected that the results presented here of the analysis of the "selection" of wave numbers in an axisymmetric system of rolls would agree with experiment. This analysis pertains to rolls with a large radius and at the same time it is not assumed that the reservoir has an external boundary. For this reason, in reality the radius of this boundary (of a cylindrical wall) should, in turn, be appreciably greater than the radii of the rolls studied, so that the effect of the boundary would not be significant. This means that the rolls will no longer form concentric rings, since it will hardly be possible to maintain such an axisymmetric pattern. There must arise either a unified system of almost straight and almost parallel rolls or a texture in which sections with such rolls play the main role. The wave numbers found will thus be of quite academic interest.

On the other hand, the equation of phase diffusion (3.63) makes it possible to obtain the exact value of the wave number of a steady-state axisymmetric pattern for any value of P.[210] Because of the absence of average drift in such a pattern $rkB = \text{const}$ and in order that this hold right up to the center of symmetry, the constant on the right side must be equal to zero in the leading order of the expansion. This means that k is equal to the value of k_B at which $B(k_B) = 0$ (compare the expression (3.67) for $D_\perp$; we note that in Ref. 210 $D_\perp$ does not include drift effects and the formulas (3.67) are always correct, but $k_{ZZ} = k_B$ only for $P = \infty$). The wave numbers of the rolls, measured in Ref. 151 (for $P = 2.5$ and three values of R; see Fig. 12) and in Ref. 204 ($P = 6.1$; see below) agree well with the values of k_B calculated for the corresponding values of P. (These experimental data are also close to the values of k_a found in Ref. 202 for large values of P.) In Ref. 210 it is shown that for $k < k_B$ ($k > k_B$) the focus of the roll pattern acts like a source (sink) of rolls.

The experimentally measured wave numbers of the annular rolls, as already mentioned in Sec. 6.1, decrease as R increases. As R increases, from time to time the "extra" annular roll vanishes at the center of the pattern (Refs. 136 and 137). The focus singularity thus plays an important role in wave-number restructuring processes; this role is accurately reflected by the result of Ref. 210.

Croquette and Pocheau[185] compared their experimental values of k for $\Gamma = 20$ and $P = 70$ and 14 (silicone oils) with the theoretical values of k_a and k_{ZZ} (according to Ref. 49). A significant discrepancy with the computed data was

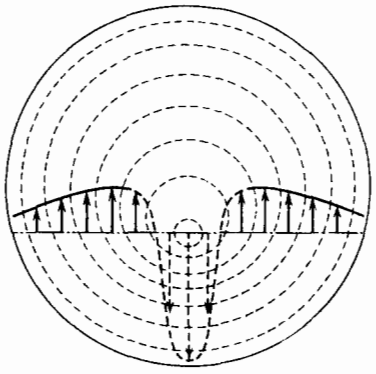

FIG. 19. Eccentric annular rolls and profile of large-scale flow in the experiment of Ref. 203. The solid curves and arrows are the actually measured velocities and the thick dashed curves are the hypothetical velocities.

obtained: for $P = 70$, at some value of R the value of k is appreciably less than both theoretical values (and from the standpoint of the theory it should fall into the region of instability), while for $P = 14$ it lies between these values (for $P = 70$ the theoretical dependences $k_{ZZ}(\varepsilon)$ and $k_a(\varepsilon)$ are shown in Fig. 18; for $p = 14$ the line $k_{ZZ}(\varepsilon)$ is inclined even more strongly to the left). The change of the number of rolls in the system, occurring due to the creation or annihilation of a roll at the focus of the system, as R changes is a discrete process. Understandably, when R alternately increases and decreases the changes of the wave number exhibit hysteresis. But the nonuniqueness associated with the hysteresis is appreciably smaller than the discrepancy between the measured value of k and k_a and k_{ZZ}.

Careful measurement of the observed pattern revealed a detail which the authors associated with the mentioned discrepancy and which is very interesting from the viewpoint of investigation of stability and flow geometry. The pattern was not strictly axisymmetric. It was found that the focus of the system of rolls is displaced relative to the center of the reservoir (by an amount of the order of 1 mm for a reservoir with a radius of 40 mm). The displacement was larger for $P = 14$ than for $P = 70$, and in trial experiments with methyl alcohol ($P = 7$) the displacement could even be seen with the naked eye. This indicates that the strictly axisymmetric pattern in which the radial pressure gradient suppresses the radial flow averaged over the height of the reservoir is unstable relative to small disruptions of the symmetry. The authors proposed that the asymmetry engenders general circulation of the double-vortex ("dipole") type (Fig. 19), which is what makes the formula (6.10) inapplicable.

In Ref. 203 a special experiment was performed in order to check this hypothesis. A photochromic material—benzothiazolinic spiropyran, which becomes colored when irradiated with UV radiation—was added to the working liquid (methanol, $P = 7$). Irradiating a selected diameter in the system of annular rolls, the experimenters marked in this manner part of the volume of the liquid and were then able to reveal the large-scale flow.

If R is gradually increased, then the asymmetry of the pattern appears to be strongest before the next central roll is annihilated and disappears after annihilation. For this reason, at almost the same value of R it is possible to observe both a symmetric and an asymmetric pattern. It was ob-

served that the diameter marker is not deformed in an axisymmetric pattern (although diffusion smears it), but is systematically transported by the average flow in an unsymmetric pattern, if it is oriented perpendicularly to the eccentric displacement of the focus.

This experiment thus demonstrates the existence of large-scale flow, which according to Refs. 33 and 34 is associated with the curvature of the rolls. The average drift in an eccentrically deformed system of annular rolls was calculated in Ref. 2 on the basis of the modified Cross–Newell equation (3.60) and also in Ref. 210: The *focus instability* resulting in such a deformation was obtained there by linear analysis of the stability of an axisymmetric flow on the basis of Eqs. (3.63) and (3.64). It is interesting that this instability can arise for R and $k = k_B$ lying inside the Busse balloon.

Another experiment in which eccentricity was observed (and wave numbers of axisymmetric convection were studied) was performed in Ref. 204 with $\Gamma = 7.5$ and $P = 6.1$ (water at 25 °C). For $\varepsilon > 0.16$ a system of annular rolls, generated at the beginning of the experiment by forcing at the walls, subsequently remained stable with virtually no such forcing (this is undoubtedly a consequence of the small aspect ratio). For $\varepsilon < 0.16$ over times much longer than τ_h a transition to a lower degree of ordering (textures) occurred. The eccentricity of the annular rings was noticeable starting at $\varepsilon \approx 2.5$ and changed with ε qualitatively just as in Ref. 203.

The measured wave numbers were found to be close to those obtained in Ref. 137 at $P \approx 500$–900 and were sharply different from k_a, calculated for $P = 6.8$ according to Ref. 49, though they are in good agreement with the values of k_B found for the same value of P in Ref. 210. Hysteresis was observed in the dependence of k on ε.

6.7. Motion and equilibrium of dislocations

The presence of defects in the convective structures makes the possible paths along which the system can arrive at the preferred wave numbers very diverse. The appearance and disappearance of rolls in the presence of focus singularities occur most easily precisely at these foci. We have already mentioned the role played by structural boundaries in the change of the wave numbers. We shall now study restructurings associated with the motion of dislocations. Such processes are, in principle, not two-dimensional, though the study of two-dimensional restructuring greatly aids in understanding what happens in this case.

Most investigations are concerned with the mechanism of climbing of dislocations. This mechanism could enable the system to adjust itself effectively to the optimal wave number.

Siggia and Zippelius[205] were probably the first to study theoretically the motion of dislocations. They studied the question both analytically (on the basis of the NWS equation) and numerically by integrating both the complete system of Boussinesq equations and the NWS equation. They studied a pair of dislocations which forms if a segment of an "extra" pair of rolls is "wedged" into the rolling system—such a configuration is obtained if Fig. 20 is supplemented by its mirror image with respect to the top edge. Since the authors employed the amplitude equation without taking into account the vertical component of the vorticity, the results based on it are valid only in the limit $P \to \infty$.

The analytic calculation was performed under the assumption that the undisturbed (no dislocations) system of rolls (filling an infinite layer) has the wave number $k = k_c + \delta k$, $\delta k \ll 1$ (only $\delta k > 0$ was studied, since for $\delta k < 0$ and $P \gg 1$ the initial roll system is unstable under slightly supercritical conditions). It was also assumed that $\delta k^{-1/2}$ is much less than the distance between dislocations (i.e., the length of the "wedged in" segment of the roll pair). For the indicated choice of wave number the dislocations come closer to one another, i.e., the "wedged in" pair is shortened. This means that the rolls compressed together when the dislocation is introduced tend to expand. An expression whose structure does not depend on the type of boundary conditions on the surfaces of the layer was derived for the velocity V of each dislocation (climb velocity):

$$V = 1{,}47\frac{\xi_0^2 \delta k^{3/2}}{\sqrt{2} k_c^{1/2} \tau_0}, \tag{6.12}$$

where ξ_0 and τ_0 are given by the formulas (2.24)–(2.26). Thus in the approximation used by the authors the wave number k_d of the undisturbed structure in which the introduced dislocation turns out to be stationary is equal to k_c (i.e., for the NWS equation to k_F also).

The numerical experiments were performed by the pseudospectral method with periodic boundary conditions along x and y. This means that if the size of the region along x is equal to L_x and the undisturbed system of n pairs of rolls has, correspondingly, the wave number $2\pi n/L_x$, then in the part of the roll pattern (bounded along y) that is disturbed by the presence of a defect (at the top of Fig. 20) the wave number is equal to $2\pi(n+1)/L_x$.

The authors were mainly concerned with determining the velocity of the dislocation. They found that the values of this velocity obtained on the basis of the complete equations and from the amplitude equation do not always agree well with one another, even with $P = \infty$. In many cases the evolution of flow is complicated by instabilities and the results are difficult to analyze. If the overall structure remains for a sufficiently long time, then the velocity of the dislocations settles down quite rapidly and subsequently changes very little. The relation between the velocity and the wave numbers was not studied systematically. It was found that as n and L_x increase with the wave number of the unperturbed pattern remaining fixed and equal to k_c, the velocity of dislocations approaches zero (it is difficult to expect a different result, since in this limit the perturbed wave number approaches the unperturbed wave number).

The force determining the climbing of dislocations in

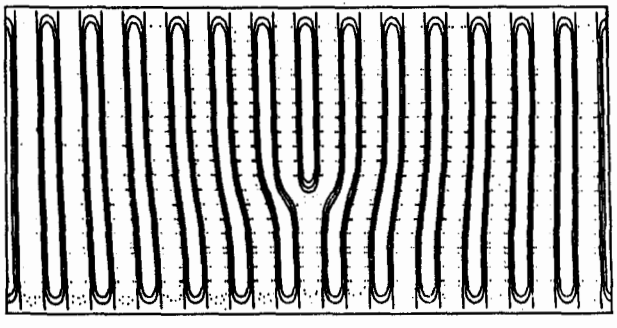

FIG. 20. Roll structure with a dislocation (according to Ref. 68).

the crystal structure is called the *Peach–Koehler* (PK) *force*.[206] If the additional layer wedged into the structure and terminating in a dislocation is squeezed by the surrounding layers, the PK force strives to expel this layer and eliminate the dislocation. If, however, the pressure of the surrounding layers is negative, the PK force pushes the additional layer in deeper. In the theory of convective structures an analog of this force is studied. In the case of potential dynamics the change of the Lyapunov functional, associated with the displacement (climb) of a dislocation over some distance, is interpreted as the work performed by the PK force. We shall calculate this force following Ref. 68.

We assume that the main parameter of a roll system containing a dislocation is the wave number k obtained by averaging the local wave numbers over the region being studied. Assume the dislocation is located at the point $(0, y_d)$ inside the strip $-L<x<L$, whose boundaries $x=\pm L$ fix the position of the extreme x-rolls. Then the change δF_L of the Lyapunov functional F_L accompanying a displacement δy_d of the dislocation will be determined only by the fact that in a rectangle with area $2L\delta y_d$ rolls with the wave number $k_+ = k|_{y\to+\infty}$ will be replaced by rolls with the wave number $k_- = k|_{y\to-\infty}$. Thus

$$\delta F_L = -(F(k_+) - F(k_-)\cdot 2L\delta y_d = -\frac{dF}{dk}\Big|_{k=\bar{k}}\cdot 2L(k_+ - k_-)\delta y_d$$
$$= -\frac{dF}{dk}\Big|_{k=\bar{k}}\cdot 2\pi\delta y_d, \quad (6.13)$$

where $F(k)$ is the specific potential for a uniform pattern characterized by the wave number k, and the final difference is replaced by a differential under the assumption that L is large and $\bar{k} = (k_+ + k_-)/2$. Thus the PK force is equal to

$$f_{PK} = -\frac{dF_L}{dy_d} = -2\pi\frac{dF}{dk}\Big|_{k=\bar{k}}. \quad (6.14)$$

Obviously, the dislocation is stationary when $f_{PK}=0$, i.e., $\bar{k}$ is equal to the wave number k_F that minimizes F and therefore, in addition, it corresponds to the boundary of stability with respect to zig-zag disturbances:

$$k_d = k_F = k_{ZZ}. \quad (6.15)$$

In Ref. 207 the relation between the velocity of a dislocation with the wave number of the roll structure was investigated for two problems: the problem of convection in a layer bounded by plates through which weak heat conduction occurs (this problem admits a variational formulation; see Sec. 3.2.2) and the problem of convection in a layer of a porous material. As in the analytical part of Ref. 205, here a structure transforming at large distances from the dislocation into a regular roll structure with wave number k is studied. The apparatus of amplitude equations is employed. In the steady-state case the condition of solvability of the equation for the complex amplitude determines the value of k_d and in the non-steady-state case with prescribed k it determines the climb velocity V.

In the first problem it was found that

$$V \propto (k - k_d)^{3/2}, \quad (6.16)$$

and in addition $k_d = k_F = k_{ZZ}$. A relation was also obtained between this velocity and the diffusion coefficients $D_\perp$ and $D_\parallel$ of the phases. The second problem, which is nonvariational in the approximation studied, leads to a value of k_d that is different from k_{ZZ}.

Gliding of dislocations, i.e., motion in a direction perpendicular to the rolls, was also studied in Ref. 207. It was found that under conditions of the variational dynamics gliding is impossible in a system of uniformly curved rolls: The potential of the system does not change in the presence of gliding and there is nothing to compensate the energy losses due to viscosity.

In Ref. 68 the behavior of dislocations was studied analytically and numerically on the basis of the model equations—the SH potential equation (3.26) and the nonpotential equation (3.29) with $d=3$. A modification of these models, which includes large-scale drift, was also studied in Eqs. (3.30)–(3.32).

The velocity of a dislocation in the potential models is proportional to $(\bar{k}-k_d)^{3/2}$ (compare with the formula (6.12) derived in Ref. 205). For nonpotential models k_d is different from the other distinguished wave numbers k_{ZZ} and k_a. For small $\bar{k}-k_d$ the climbing velocity increases linearly with this quantity.

Thus the basic characteristics of the motion of dislocations do not depend on the details of the formulation of the problem and can be easily interpreted based on the idea of a preferred wave number. Climbing tends to make the roll structure approach k_p, while a dislocation is in equilibrium when the wave number of the undisturbed system is equal to k_p. For potential systems $k_p = k_F$.

Experiments designed specifically for studying dislocations were apparently first undertaken by Busse and Whitehead[111,166] (the first paper contains only qualitative results, the word *dislocation* is not employed yet, and the process of displacing a dislocation is called the *pinching mechanism*; its role as a possible mechanism of change of the wave number is noted). A chain of dislocations, which arises on the line of contact between two systems of rolls, joining at their ends, was studied with the help of the technique of controlled initial conditions, and in addition the wave numbers of the systems are in the ratio 2:3. The values of the wave numbers were such that the narrower rolls were displaced by the wider rolls. The speed of the dislocations increased nearly linearly with increasing R and it decreased with increasing P.[166]

Pocheau and Croquette made a detailed experimental study of the behavior of an isolated dislocation.[18,185] The dislocation was produced, when the initial flow was generated, by illuminating the layer through an appropriately shaped mask. Special measures were taken to prevent the cross-roll instability from developing near the sidewalls of the chamber, as was done in the experiment with grain boundaries described in the same work. Thin copper wires, glued to the bottom of the reservoir near the sidewalls, created, due to their thermal contact with the bottom, upward flows, which fix the position of the extreme rolls. Silicone oil with $P=70$ was employed.

The motion of the dislocation was, as a rule, almost uniform—only near a wall it sometimes slowed down and even stopped (the authors write about this effect as trapping of the dislocation by the wall). The basic results of measurements of the optimal wave numbers k_d, which correspond to the stationary position of a dislocation not trapped by the wall (i.e., in the central part of the reservoir), are presented

in Fig. 18. In those cases when a stationary situation was achieved by adjusting the value of R, k_d was determined as the arithmetic mean of the two wave numbers present in the pattern—undisturbed and disturbed. These values are designated in the figure by cross marks. A different method for determining k_d was based on applying the $(k - k_d)^{3/2}$ law (see Eqs. (6.12) and (6.16)) to the climb velocities, measured for different values of k and a fixed value of R (here k is also the half-sum of two values). The corresponding values of k_d in the figure are designated by squares.

It is obvious that the measured wave numbers agree fairly well with k_{zz} right up to $\varepsilon \approx 1.5$. The authors regard this agreement as being good in the entire investigated range of supercritical Rayleigh numbers, extrapolating to this range the linear dependence of k_{zz} on ε, obtained in Refs. 48 and 49 for small values of ε. It seems that there are still not sufficient grounds for arriving at this conclusion (and correspondingly for the conclusion about the variational character of the dynamics for all ε). But it is all the more interesting that the data provided by the authors demonstrate right up to $\varepsilon \approx 4$ excellent agreement between the optimal wave numbers found in the experiment with dislocations and in the experiment with the motion of grain boundaries (see Sec. 6.5.3). This supports the existence of a single preferred wave number, irrespective of the potentiality of the system. In the case of the motion both of dislocations and of grain boundaries the flow geometry does not create strong antiselective factors, and the system arrives at a wave number very close to the preferred wave number.

The role of climbing of dislocations in the restructuring of the wave number of the roll structure has also been investigated in experiments with air;[154] it was also found that gliding can lead to the appearance of phase turbulence.

Finally, Whitehead[208,209] performed some interesting investigations of dislocations in bimodal convection. Such dislocations can also exhibit gliding[209] and play an important role in the transition to chaotic motion.[208]

7. CONCLUSIONS

The material examined above convincingly shows that the realizability of a flow is not identical with stability of the flow. The realized state in turn is not necessarily optimal. It is the result of the combined action of selective and antiselective factors and depends on the overall flow geometry, determined by the initial and boundary conditions. Correspondingly, the stability cannot be judged on the basis of only the local structure of the flow.

In the case of systems of two-dimensional rolls, there does not exist even one fact that would contradict the concept of the existence of a preferred wave number or an internal optimal scale of such flows, in spite of the difference between the wave numbers realized in different concrete situations. In those cases when the convection dynamics can be described by relaxational models, such an optimum corresponds to a minimum of the specific potential.

The presence of structural nonuniformities (defects) or at least boundary layers at the side walls gives rise to antiselective factors and gives the structure additional degrees of freedom. For this reason, the more defects—"margins" for restructuring to the optimum—there are in the evolving structure the closer the final wave number (at least, on the average over the spatial pattern) is to the preferred wave number. In spontaneously arising structures, which pass through a stage of complex textures and gradual elimination of defects, the preferred wave number is thus the most likely wave number.

Complete understanding of the conditions of equilibrium of textures is a matter for future work. From what has been said above it is clear only that the more complicated is the structure the more stringent must be the conditions under which it is a steady-state one. For this reason, different parts of the texture can depart by different amounts from the optimum and they can have different degrees of stability; some fragments can be optimized at the expense of deoptimization of other fragments. Under some conditions, together with vanishing of defects, new defects can constantly arise, the texture does not become a steady-state one, and phase turbulence is observed.

Slow processes must be studied more carefully. It has not been excluded that in many cases, when the optimum seems to be unattainable, antiselective factors still can be overcome over long periods of time.

Finally, the character of the approach to the optimal scale and the appearance of antiselective factors under conditions when three-dimensional forms of flow are preferred still have not been investigated. It can be expected that the general laws observed in two-dimensional flows will also be manifested in one form or another in three-dimensional flows.

I wish to thank all my colleagues who sent me material on the subject of this review and L. M. Alekseev for a detailed discussion of the content and text of this review.

[1)] It is occasionally called Bénard–Rayleigh convection as well as Bénard convection or Rayleigh convection. It is pointless to omit the name of either of these two pioneers of the systematic investigation of convection—an experimenter and a theoretician. Chronologically, it would be more accurate to mention, in spite of tradition, Bénard's name first. With respect to the physics of the phenomena, however, combining both names in one term reflects the long-standing confusion, which has still not been eliminated, in the understanding of the mechanism of convection: Bénard observed the phenomenon in which instability associated with the temperature dependence of the surface tension played an appreciable role while Rayleigh studied convection caused by a different instability—owing to the temperature (and density) nonuniformity of the layer of liquid. The difference between these two mechanisms is manifested in the different structure of the flows; this will be discussed in Sec. 4.1. Convection owing to the Rayleigh mechanism is almost exclusively studied in this review. The term *Rayleigh–Bénard convection* usually refers precisely to this type of convection, and the term *Bénard–Marangoni convection* refers to thermocapillary convection.

[2)] The word *cell* is recently often employed in the literature in a different sense—as a synonym for the term *reservoir*, *chamber*, or *cavity* (the working volume of the experimental setup). These two usages should not be confused.

[3)] The aspect ratio is sometimes defined as the reciprocal of the quantity indicated here.

[4)] It is understandable that the setup for a cryogenic experiment is structurally very different from the setup described here.

[5)] It is often noted that there is an analogy between the equations of two-dimensional models of convection and the Ginzburg–Landau equation of the theory of superconductivity. This is the origin of the terminology.

[6)] For incomprehensible reasons, in the literature published in the USSR the latinized word (geksagony) is often used instead of the common Russian equivalent (shestingol'niki).

[7)] It is obvious that in this situation (and in all analogous situations that will be encountered more than once) hysteresis is possible accompanying the transitions (motionless state) $\leftrightarrows$ (hexagonal cells) in the region of finite-amplitude subcritical instability of the motionless state and the transitions (hexagonal cells) $\leftrightarrows$ (rolls) in the region where both types of motions are stable.

[8)] The corresponding English term *grain boundary* in the literature on the physics of crystals, whence it is taken, is often translated as the *boundary of grains*. In the hydrodynamic context a different Russian equivalent of

this term seems to be better—*structural boundary*, especially since structure is one of the meanings of the word grain. The term domain *wall* is also employed to designate defects of this type.

[9)] I am grateful to E. L. Koshmider for bringing this fact to my attention.

[1] L. D. Landau and E. M. Lifshitz, *Fluid Mechanics*, Pergamon Press, N.Y., 1959, p. 102 [Russ. original, Nauka, M., 1986, 3rd edition].
[2] A. C. Newell, *Propagation in Systems Far from Equilibrium*, edited by J. E. Wesfreid *et al.*, Springer-Verlag, Berlin, 1988, p. 122.
[3] Lord Rayleigh, Phil. Mag. **32**, 529 (1916).
[4] A. Pellew and R. V. Wouthwell, Proc. R. Soc. London A **176**, 312 (1940).
[5] S. Chandrasekhar, *Hydrodynamic and Hydromagnetic Stability*, Clarendon Press, Oxford, 1961.
[6] R. Perez Cordon and M. G. Velarde, J. Phys. (Paris) **36**, 591 (1975).
[7] G. Velarde and R. Perez Cordon, J. Phys. (Paris) **37**, 177 (1976).
[8] G. Z. Gershuni and E. M. Zhukhovitskiĭ, *Convective Stability of Incompressible Liquids* [in Russian], Nauka, M., 1972.
[9] J. Wesfreid, Y. Pomeau, M. Dubois, C. Normand, and P. Berge, J. Phys. (Paris) **39**, 725 (1978).
[10] M. A. Dominguez-Lerma, G. Ahlers, and D. S. Cannell, Phys. Fluids **27**, 856 (1984).
[11] V. S. Berdnikov, A. V. Getling, and V. A. Markov, Preprint No. 165–88, (In Russian), Institute of Thermal Physics of the Siberian Branch of the USSR Academy of Sciences, Novosibirsk, 1988; Exp. Heat Transfer **3**, 269 (1990).
[12] S. S. Kutateladze, A. G. Kirdyashkin, and V. S. Berdnikov, Izv. Akad. Nauk SSSR, Fiz. Atmos. i Okeana **10**, 137 (1974). [Izv. Acad. Sci. USSR Atmos. Oceanic Phys. **10**, 82 (1974)].
[13] I. Rehberg, E. Bodenschatz, B. Winkler, and F. H. Busse, Phys. Rev. Lett. **59**, 282 (1987). I. Rehberg and F. H. Busse in Ref. 2, p. 225.
[14] J. P. Gollub, A. R. McCarriar, and J. F. Steinman, J. Fluid Mech. **125**, 259 (1982).
[15] B. Martinet, P. Haldenwang, G. Labrosse, J.-C. Payan, and R. Payan, C. R. Acad. Sci. Ser. II **299**, 755 (1984); *Cellular Structures in Instabilities*, (Eds.) J. E. Wesfreid and S. Zaleski, Springer-Verlag, Berlin, 1984, p. 33.
[16] M. M. Chen and J. A. Whitehead, J. Fluid Mech. **31**, 1 (1968).
[17] F. H. Busse and J. A. Whitehead, J. Fluid Mech. **66**, 67 (1974).
[18] A. Pocheau and V. Croquette, J. Phys. (Paris) **45**, 35 (1984).
[19] D. B. White, J. Fluid Mech. **191**, 247 (1988).
[20] L. P. Gor'kov, Zh. Eksp. Teor. Fiz. **33**, 402 (1957) [Sov. Phys. JETP **6**, 311 (1958).
[21] W. V. R. Malkus and G. Veronis, J. Fluid Mech. **4**, 225 (1958).
[22] F. H. Busse, Rep. Prog. Phys. **41**, 1929 (1978).
[23] F. H. Busse, *Hydrodynamic Instabilities and the Transition to Turbulence*, (Eds.) H. L. Swinney and J. P. Gollub, Springer-Verlag, Berlin, 1981.
[24] H. L. Kuo, J. Fluid Mech. **10**, 611 (1961).
[25] A. Schluter, D. Lortz, and F. H. Busse, J. Fluid Mech. **23**, 129 (1965).
[26] A. C. Newell and J. A. Whitehead, J. Fluid Mech. **38**, 279 (1969).
[27] M. C. Cross, P. G. Daniels, P. C. Hohenberg, and E. D. Siggia, Phys. Rev. Lett. **45**, 898 (1980); J. Fluid Mech. **127**, 155 (1983).
[28] L. A. Segel, J. Fluid Mech. **38**, 203 (1969).
[29] M. S. Cross, Phys. Rev. A **27**, 490 (1983).
[30] S. N. Brown and K. Stewartson, Proc. R. Soc. London A **360**, 455 (1978).
[31] M. C. Cross, Phys. Fluids **23**, 1727 (1980).
[32] E. A. Kuznetsov and M. D. Spektor, Zh. Prikl. Mekh. Tekh. Fiz., No. 2, 76 (1980). [J. Appl. Mech. Tech. Phys. (USSR) (1980)].
[33] E. D. Siggia and A. Zippelius, Phys. Rev. Lett. **47**, 835 (1981).
[34] A. Zippelius and E. D. Siggia, Phys. Fluids **26**, 2905 (1983).
[35] P. G. Daniels, Proc. R. Soc. London A **358**, 173 (1977).
[36] S. N. Brown and K. Stewartson, Stud. Appl. Math. **57**, 187 (1977).
[37] M. C. Cross, Phys. Fluids **25**, 936 (1982).
[38] P. Manneville, J. Phys. (Paris) **44**, 759 (1983).
[39] J. Swift and P. C. Hohenberg, Phys. Rev. A **15**, 319 (1977).
[40] G. Ahlers, M. C. Cross, P. C. Hohenberg, and S. Safran, J. Fluid Mech. **110**, 297 (1981).
[41] Y. Pomeau and P. Manneville, J. Phys. (Paris) Lett. **40**, 609 (1979).
[42] Y. Pomeau and P. Manneville, Phys. Lett. A **75**, 296 (1980).
[43] Y. Pomeau and S. Zaleski, J. Phys. (Paris) **42**, 515 (1981).
[44] H. S. Greenside and M. C. Cross, Phys. Rev. A **31**, 2492 (1985).
[45] V. L. Gertsberg and G. I. Sivashinsky, Prog. Theor. Phys. **66**, 1219 (1981).
[46] M. C. Cross, Phys. Rev. A **25**, 1065 (1982).
[47] H. S. Greenside, M. C. Cross, and W. M. Coughran, Phys. Rev. Lett. **60**, 2269 (1988).
[48] P. Manneville and J. M. Piquemal, J. Phys. (Paris) Lett. **43**, 253 (1982).
[49] P. Manneville and J. M. Piquemal, Phys. Rev. A **28**, 1774 (1983).
[50] P. G. Daniels, Proc. R. Soc. London A **387**, 539 (1981).
[51] P. G. Daniels, J. Fluid Mech. **143**, 125 (1984).
[52] A. C. Newell, *Nonlinear Partial Differential Equations in Applied Science*, edited by H. Fujita, North-Holland, Amsterdam, 1983, p. 205.
[53] M. C. Cross and A. C. Newell, Physica D **10**, 299 (1984).
[54] G. B. Whitham, J. Fluid Mech. **44**, 373 (1970).
[55] B. M. Berkovskiĭ and V. K. Polevikov, *Numerical Experiments in Convection* [in Russian], Universitetskoe Izd., Minsk, 1988.
[56] S. A. Orszag, Stud. Appl. Math. **50**, 293 (1971); J. Fluid Mech. **49**, 75 (1971).
[57] W. Arter, A. Bernoff, and A. C. Newell, Phys. Fluids **30**, 3840 (1987).
[58] W. Arter and A. C. Newell, Phys. Fluids **31**, 2474 (1988).
[59] A. V. Getling, Dokl. Akad. Nauk SSSR **233**, 308 (1977) [Sov. Phys. Dokl. **22**(3), 120 (1977)].
[60] A. V. Getling, J. Fluid Mech. **130**, 165 (1983).
[61] Y. Ogura, J. Atmos. Sci. **28**, 709 (1971).
[62] V. G. Vasin and M. P. Vlasyuk, Preprint No. 84, (In Russian) Institute of Applied Mechanics of the Academy of Sciences of the USSR, M., 1974.
[63] F. B. Lipps and R. C. J. Somerville, Phys. Fluids **14**, 759 (1971).
[64] N. F. Velitshchev and A. A. Zelnin, J. Fluid Mech. **68**, 353 (1975).
[65] H. S. Greenside, W. M. Coughran, and N. L. Schryer, Phys. Rev. Lett. **49**, 726 (1982).
[66] H. S. Greenside and W. M. Coughran, Phys. Rev. A **30**, 398 (1984).
[67] P. Manneville, J. Phys. (Paris) **44**, 563 (1983).
[68] G. Tesauro and M. C. Cross, Phys. Rev. A **34**, 1363 (1986).
[69] G. Tesauro and M. C. Cross, Philos. Mag. A **56**, 703 (1987).
[70] M. C. Cross, G. Tesauro, and H. S. Greenside, Physica D **23**, 12 (1986).
[71] H. Bénard, Rev. Gen. Sci. Pures Appl. **11**, 1261, 1309 (1900).
[72] R. Krishnamurti, J. Fluid Mech. **42**, 295 (1970).
[73] R. Krishnamurti, J. Fluid Mech. **42**, 309 (1970).
[74] G. E. Willis, J. W. Deardorff, and R. C. J. Somerville, J. Fluid Mech. **54**, 351 (1972).
[75] V. S. Berdnikov and A. G. Kirdyashkin, Izv. Akad. Nauk SSSR, Fiz. Atmos. i Okeana **15**, 812 (1979). [Izv. Acad. Sci. USSR Atmos. Oceanic Phys. **15**, 813 (1979)].
[76] M. J. Block, Nature **178**, 650 (1956).
[77] E. L. Koschmieder, Adv. Chem. Phys. **32**, 109 (1975).
[78] C. Normand and Y. Pomeau, Rev. Mod. Phys. **49**, 581 (1977).
[79] E. L. Koschmieder and M. I. Biggerstaff, J. Fluid Mech. **167**, 49 (1986).
[80] E. L. Koschmieder, J. Fluid Mech. **30**, 9 (1967).
[81] E. L. Koschmieder, *On Turbulence: Proceedings of the 5th EPS Liquid State Conference*, Moscow, October 16–21, 1989, Inst. Prob. Mech. USSR Academy of Sciences, Moscow, 1989, p. 10; Europ. J. Mech. B/Fluids Suppl. **10**(2), 232 (1991).
[82] C. Perez-Garcia, P. Cerister, and R. Occelli in Ref. 2, p. 232.
[83] P. G. Grodzka and T. C. Bannister, Science **176**, 506 (1972); **187**, 165 (1975).
[84] J. R. A. Pearson, J. Fluid Mech. **4**, 489 (1958).
[85] D. A. Nield, J. Fluid Mech. **19**, 341 (1964).
[86] J. W Scanlon and L. A. Segel, *ibid.* **30**, 149 (1967).
[87] J. R. Kraska and R. L. Sani, Int. J. Heat Mass Transfer **22**, 535 (1979).
[88] A. Cloot and G. Lebon, J. Fluid Mech. **145**, 447 (1984).
[89] A. Graham, Phil. Trans. R. Soc. London A **232**, 285 (1933).
[90] H. von Tippelskirch, Beitr. Phys. Atmosph. **29**, 37 (1956).
[91] E. Palm, J. Fluid Mech. **8**, 183 (1960).
[92] L. A. Segel and J. T. Stuart, J. Fluid Mech. **13**, 289 (1962).
[93] E. Palm and H. Piann, J. Fluid Mech. **19**, 353 (1964).
[94] L. A. Segel, J. Fluid Mech. **21**, 359 (1965).
[95] S. H. Davis and L. A. Segel, Phys. Fluids **11**, 470 (1968).
[96] E. Palm, T. Ellingsen, and B. Gjevik, J. Fluid Mech. **30**, 651 (1967).
[97] F. H. Busse, *Das Stabilitatsverhalten der Zellularkonvektion bei endlicher Amplitude*, Munich, 1962.
[98] F. H. Busse, J. Fluid Mech. **30**, 625 (1967).
[99] C. Hoard, C. Robertson, and A. Acrivos, Int. J. Heat Mass Transfer **13**, 849 (1970).
[100] F. M. Richter, J. Fluid Mech. **89**, 553 (1978).
[101] K. S. Stengel, D. S. Oliver, and J. R. Booker, J. Fluid Mech. **120**, 411 (1982).
[102] D. S. Oliver and J. R. Booker, Geophys. Astrophys. Fluid Dyn. **27**, 73 (1983).
[103] H. Frick, F H. Busse, and R. M. Clever, J. Fluid Mech. **127**, 141 (1983).
[104] F. H. Busse and H. Frick, J. Fluid Mech. **150**, 451 (1985).
[105] D. R. Jenkins, J. Fluid Mech. **178**, 491 (1987).
[106] J. T. Stuart, J. Fluid Mech. **18**, 481 (1964).
[107] D. R. Jenkins, J. Fluid Mech. **190**, 451 (1988).
[108] E. F. C. Somerscales and T. S. Dougherty, J. Fluid Mech. **42**, 755 (1970).
[109] M. Dubois, P. Berge, and J. Wesfreid, J. Phys. (Paris) **39**, 1253 (1978).
[110] R. W. Walden and G. Ahlers, J. Fluid Mech. **109**, 89 (1981).

[111] F. H. Busse and J. A. Whitehead, J. Fluid Mech. **47**, 305 (1971).
[112] F. H. Busse and N. Riahi, J. Fluid Mech. **96**, 243 (1980).
[113] M. R. E. Proctor, J. Fluid Mech. **113**, 469 (1981).
[114] D. R. Jenkins and M. R. E. Proctor, J. Fluid Mech. **139**, 461 (1984).
[115] N. Riahi, J. Fluid Mech. **152**, 113 (1985).
[116] P. le Gal, A. Pocheau, and V. Croquette, Phys. Rev. Lett. **54**, 2501 (1985).
[117] P. le Gal and V. Croquette, Phys. Fluids **31**, 3440 (1988).
[118] R. Krishnamurti, J. Fluid Mech. **33**, 445 (1968).
[119] R. Krishnamurti, J. Fluid Mech. **33**, 457 (1968).
[120] A. A. Zhelnin, Meteorol. Gidrol., No. 11, 29 (1974). [Sov. Meteor. Hydrol. (1974)].
[121] M. N. Roppo, S. H. Davis, and S. Rosenblat, Phys. Fluids **27**, 796 (1984).
[122] P. C. Hohenberg and J. B. Swift, Phys. Fluids **30**, 603 (1987); Phys. Rev. A **35**, 3855 (1987).
[123] C. W. Meyer, D. S. Cannell, G. Ahlers, J. B. Swift, and P. C. Hohenberg, Phys. Rev. Lett. **61**, 947 (1988).
[124] S. H. Davis, J. Fluid Mech. **30**, 465 (1967).
[125] K. Stork and U. Muller, J. Fluid Mech. **54**, 599 (1972).
[126] B. F. Edwards, J. Fluid Mech. **191**, 583 (1988).
[127] R. P. Davies-Jones, J. Fluid Mech. **44**, 695 (1970).
[128] M. S. Chana and P. G. Daniels, J. Fluid Mech. **199**, 257 (1989).
[129] H. Ozoe, H. Sayama, and S. W. Churchill, Int. J. Heat Mass Transfer **17**, 401 (1974).
[130] K. Stork and U. Muller, J. Fluid Mech. **71**, 231 (1975).
[131] A. Pocheau, V. Croquette, and P. le Gal, Phys. Rev. Lett. **55**, 1904 (1985). V. Croquette, P. le Gal, and A. Pocheau, Phys. Ser. **T13**, 135 (1986).
[132] V. Croquette, M. Mory, and F. Schosseler, J. Phys. (Paris) **44**, 293 (1983).
[133] S. Zaleski, Y. Pomeau, and A. Pumir, Phys. Rev. A **29**, 366 (1984).
[134] P. le Gal, Thesis, Paris (1986).
[135] C. W. Meyer, G. Ahlers, and D. S. Cannell, Phys. Rev. Lett. **59**, 1577 (1987).
[136] E. L. Koschmieder, Beitr. Phys. Atmosph. **39**, 1 (1966).
[137] E. L. Koschmieder and S. G. Pallas, Int. J. Heat Mass Transfer **17**, 991 (1974).
[138] R. Krishnamurti, J. Fluid Mech. **60**, 285 (1973).
[139] J. P. Gollub and A. R. McCarriar, Phys. Rev. A **26**, 3470 (1982).
[140] J. A. Whitehead and B. Parsons, Geophys. Astrophys. Fluid Dyn. **9**, 201 (1978).
[141] J. A. Whitehead and G. L. Chan, Dyn. Atmosph. Oceans **1**, 33 (1976).
[142] N. F. Vel'tishchev and A. A. Zhelnin, Izv. Akad. Nauk SSSR, Mekh. zhidkosti i gaza, No. 6, 17 (1977). [Fluid Dyn. (1977)].
[143] G. Ahlers and R. P. Behringer, Phys. Rev. Lett. **40**, 712 (1978).
[144] G. Ahlers and R. P. Behringer, Prog. Theor. Phys. Suppl., No. 64, 186 (1978).
[145] R. P. Behringer, Rev. Mod. Phys. **57**, 657 (1985).
[146] A. Libchaber and J. Maurer, J. Phys. (Paris) Lett. **39**, 369 (1978).
[147] G. Ahlers and R. W. Walden, Phys. Rev. Lett. **44**, 445 (1980).
[148] S. Fauve, C. Laroche, A. Libchaber, and B. Perrin, *Cellular Structures in Instabilities*, (Eds.) J. E. Wesfreid and S. Zaleski, Springer-Verlag, Berlin, 1984, p. 278.
[149] R. P. Behringer, H. Gao, and J. N. Shaumeyer, Phys. Rev. Lett. **50**, 1199 (1983).
[150] R. W. Motsay, K. E. Anderson, and R. P. Behringer, J. Fluid Mech. **189**, 263 (1988).
[151] M. S. Heutmaker and J. P. Gollub, Phys. Rev. A **35**, 242 (1987).
[152] G. Ahlers, D. S. Cannell, and V. Steinberg, Phys. Rev. Lett. **54**, 1373 (1985).
[153] A. Pocheau, J. Phys. (Paris) **50**, 2059 (1989).
[154] J. R. Leith, Physica D **37**, 334 (1989).
[155] P. Manneville, J. Phys. (Paris) Lett. **44**, 903 (1983).
[156] A. Pocheau, J. Phys. (Paris) **49**, 1127 (1988).
[157] F. Daviaud and A. Pocheau, Europhys. Lett. **9**, 675 (1989).
[158] E. L. Koschmieder, J. Fluid Mech. **35**, 537 (1969).
[159] E. L. Koschmieder, Adv. Chem. Phys. **26**, 177 (1974).
[160] S. H. Davis, J. Fluid Mech. **32**, 619 (1968).
[161] D. A. Nield, J. Fluid Mech. **32**, 393 (1968).
[162] A. V. Getling, Dokl. Akad. Nauk SSSR **250**, 826 (1980) [Sov. Phys. Dokl. **25**(2), 89 (1989)].
[163] W. V. R. Malkus, Proc. R. Soc. London A **225**, 196 (1954).
[164] F. H. Busse, J. Math. Phys. **46**, 140 (1967).
[165] T. D. Foster, J. Fluid Mech. **37**, 81 (1969).
[166] J. A. Whitehead, J. Fluid Mech. **75**, 715 (1976).
[167] I. Catton, J. Heat Transfer **110**, 1154 (1988).
[168] P. Glansdorff and I. Prigogine, *Thermodynamic Theory of Structure, Stability and Fluctuations*, Wiley-Interscience, N.Y., 1971. [Russ. Transl., Mir, M., 1973].
[169] F. H. Busse, J. Fluid Mech. **52**, 97 (1972).
[170] R. M. Clever and F. H. Busse, J. Fluid Mech. **65**, 625 (1974).
[171] R. M. Clever and F. H. Busse, Z. Angew. Math. Phys. **29**, 711 (1978).
[172] F. H. Busse and R. M. Clever, J. Fluid Mech. **91**, 319 (1979).
[173] E. W. Bolton, F. H. Busse, and R. M. Clever, J. Fluid Mech. **164**, 469 (1986).
[174] R. M. Clever and F. H. Busse, J. Fluid Mech. **176**, 403 (1987).
[175] F. H. Busse and E. W. Bolton, J. Fluid Mech. **146**, 115 (1984).
[176] E. W. Bolton and F. H. Busse, J. Fluid Mech. **150**, 487 (1985).
[177] R. M. Clever and F. H. Busse, J. Fluid Mech. **198**, 345 (1989).
[178] V. Croquette and F. Schosseler, J. Phys. (Paris) **43**, 1183 (1982).
[179] P. Kolodner, R. W. Walden, A. Passner, and C. M. Surko, J. Fluid Mech. **163**, 195 (1986).
[180] M. S. Heutmaker, P. N. Fraenkel, and J. P. Gollub, Phys. Rev. Lett. **54**, 1369 (1985).
[181] S. Zaleski in: Ref. 148, p. 84; J. Fluid Mech. **149**, 101 (1984).
[182] M. C. Cross, P. C. Hohenberg, and S. A. Safran, Physica D **5**, 75 (1982).
[183] D. Bensimon, Phys. Rev. A **37**, 200 (1988).
[184] A. V. Getling, Dokl. Akad. Nauk SSSR **257**, 1081 (1981) [Sov. Phys. Dokl. **26**(4), 377 (1981)].
[185] V. Croquette and A. Pocheau in Ref. 148, p. 104.
[186] A. A. Nepomnyashchiĭ, Preprint, (In Russian), Defects in convective structures, Ural Division of the Academy of Sciences of the USSR, Sverdlovsk (1988).
[187] L. Kramer, E. Ben-Jacob, H. Brand, and M. C. Cross, Phys. Rev. Lett. **49**, 1891 (1982).
[188] P. C. Hohenberg, L. Kramer, and H. Riecke, Physica D **15**, 402 (1985).
[189] Y. Pomeau and S. Zaleski, J. Phys. (Paris) Lett. **44**, 135 (1983).
[190] L. Kramer and P. C. Hohenberg in Ref. 148, p. 63.
[191] L. Kramer and H. Riecke, Z. Phys. B **59**, 245 (1985).
[192] J. C. Buell and I. Catton, J. Fluid Mech. **171**, 477 (1986).
[193] E. L. Koschmieder, Beitr. Phys. Atmosph. **39**, 208 (1966).
[194] G. Veronis, Astrophys. J. **137**, 641 (1963).
[195] G. Dee and J. S. Langer, Phys. Rev. Lett. **50**, 383 (1983).
[196] E. Ben-Jacob, H. Brand, G. Dee, L. Kramer, and J. S. Langer, Physica D **14**, 348 (1985).
[197] D. G. Aronson and N. F. Weinberger, Adv. Math. **30**, 33 (1978).
[198] M. Lucke, M. Mihelcic, and B. Kowalski, Phys. Rev. A **35**, 4001 (1987).
[199] G. Dee, Physica D **15**, 295 (1985).
[200] J. Fineberg and V. Steinberg, Phys. Rev. Lett. **58**, 1332 (1987).
[201] Y. Pomeau and P. Manneville, J. Phys. (Paris) **42**, 1067 (1981).
[202] J. C. Buell and I. Catton, Phys. Fluids **29**, 23 (1986).
[203] V. Croquette, P. le Gal, A. Pocheau, and R. Guglielmetti, Europhys. Lett. **1**, 393 (1986).
[204] V. Steinberg, G. Ahlers and D. S. Cannell, Phys. Scr. **32**, 534 (1985).
[205] E. D. Siggia and A. Zippelius, Phys. Rev. A **24**, 1036 (1981).
[206] J. Friedel, Dislocations, Pergamon Press, Oxford, 1964. [Russ. Transl., Mir, M., 1967].
[207] G. Pomeau, S. Zaleski, and P. Manneville, Phys. Rev. A **27**, 2710 (1983).
[208] J. A. Whitehead, Phys. Fluids **26**, 2899 (1983).
[209] J. A. Whitehead, Phys. Fluids **27**, 2389 (1984).
[210] A. C. Newell, T. Passot, and M. Souli, J. Fluid Mech. **220**, 187 (1990).
[211] M. Schnaubelt and F. H. Busse, Z. Angew. Math. Phys. **40**, 153 (1989).
[212] B. Travis, P. Olson, and G. Schubert, J. Fluid Mech. **216**, 71 (1990).
[213] A. V. Getling, Physica D (1992) (in press).

Translated by M. E. Alferieff